UNIVERSITÀ
DEGLI STUDI
FIRENZE

DOTTORATO DI RICERCA IN SCIENZE BIOMEDICHE

CICLO XXVI

COORDINATORE Prof. Dello Sbarba Persio

Antibodies against plasma membrane molecular targets: tools for cancer immunotherapy

Settore Scientifico Disciplinare MED/04

Dottorando
Dott.ssa Crescioli Silvia

Tutore
Prof.ssa Arcangeli Annarosa

Coordinatore
Prof. Dello Sbarba Persio

Anni 2011/2013

INTRODUCTION

1. CANCER IMMUNOTHERAPY

Cancer is the second leading cause of death in economically developed countries and the third in developing countries, in 2008 worldwide cancer victims were 7.6 million (Siegel et al. 2012). Despite during the past decades huge progresses have been made regarding cancer traditional therapies (chemotherapy, ionising radiation and surgery), this harmful disease is still difficult to eradicate and prevent. As a consequence, novel methods for anti-cancer therapy are continuously developed. In the past few decades immunotherapy of cancer became an attractive alternative approach for cancer prevention and treatment.

1.1 IMMUNE SURVEILLANCE

At the begin of 20th century the Nobel prize Paul Ehrlich introduced the concept of immune surveillance, supporting the hypothesis that the immune system is able to detect and eradicate nascent transformed cells, which continuously arise, before they are clinically detected (Ehrlich 1909). 50 years later, Burnet and Thomas postulated that the control of nascent transformed cells may represent an ancient immune system, which played a critical role in surveillance against malignant transformation. The idea that tumours could be repressed by the immune system was supported by experimental evidence from tumour transplantation models (Burnet 1957). Although these evidences, immune surveillance has remained a controversial topic until 1990s when experimental animal models using knock-out mice validated the existence of cancer immune surveillance in both chemically induced and spontaneous tumours (Dunn et al. 2005).

1.2 IMMUNOEDITING

Host and tumour cells interaction was described proposing three essential phases: elimination, equilibrium and escape (Dunn et al. 2002). Cancer immunoediting has been proposed in terms of the dual functions of host immunity: on one side elimination of single tumour cells, on the other side shaping malignant disease during the period of equilibrium between the tumour and host. During tumour growth, immune selection produces tumour cell variants that have low immunogenicity and are resistant to immune attack, the equilibrium phase proceed even though the elimination phase continues through immune selection pressure. The release of tumour-derived soluble factors which facilitate the escape from immune attack, allows tumour progression and metastasis (Kim et al. 2007).

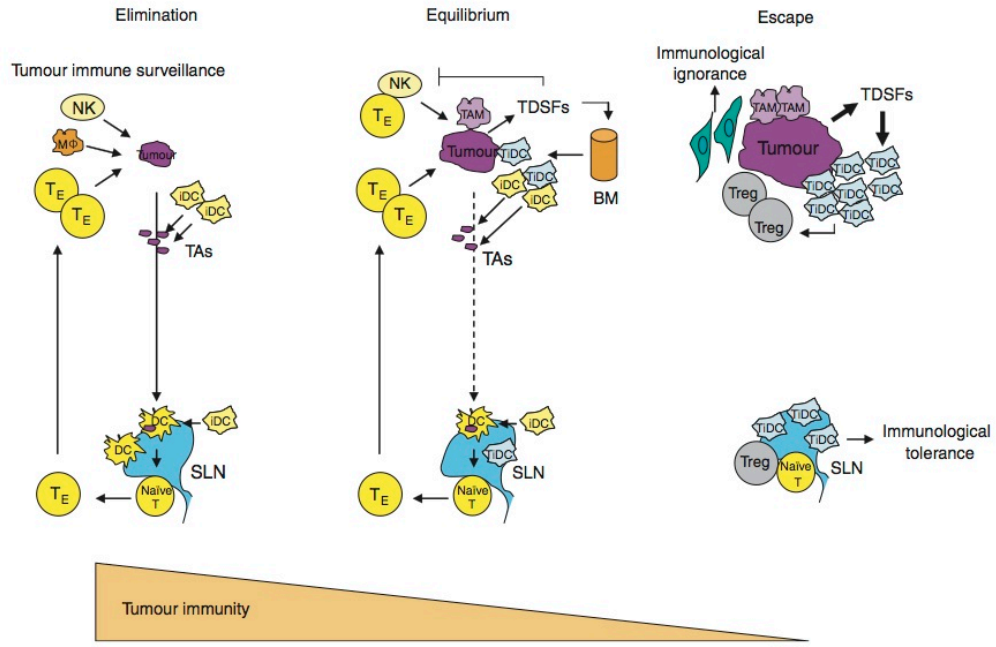

Figure 1. Cancer immunoediting from immune surveillance to escape. Picture from *Cancer immunoediting from immune surveillance to immune escape* (Kim et al. 2007).

1.3 TYPES OF CANCER IMMUNOTHERAPY

Immunotherapy of cancer uses the immune system to fight cancer and can be active or passive.

- Active immunotherapy stimulate patient's own immune system to fight the disease.

- Passive immunotherapy employs exogenous immune system components such as monoclonal antibodies (mAbs) and small molecules to destroy cancer cells.

Immunotherapy is sometimes used by itself to treat cancer, but it is most often used along with or after another type of treatment to boost its effects.

1.4 PASSIVE IMMUNOTHERAPY

As regard passive immunotherapy, activation of antitumour immune responses by using molecular targeting drugs may provide remarkable enhancement of chemotherapeutic effects in cancer therapy.

1.4.1 ANTIBODIES

Antibodies are serum glycoproteins that belong to the immunoglobulin (Ig) superfamily and are produced by the immune system B cells in response to an antigen. The main characteristic of these proteins is the ability to bind a specific structure on the antigen responsible for their production termed epitope.

Antibodies are composed by four polypeptide chains: two identical heavy chains (about 440-550 amino acids) and two identical light chains (about 220 amino acids) held together by non-covalent interaction and covalent disulfide bond (Figure 2).

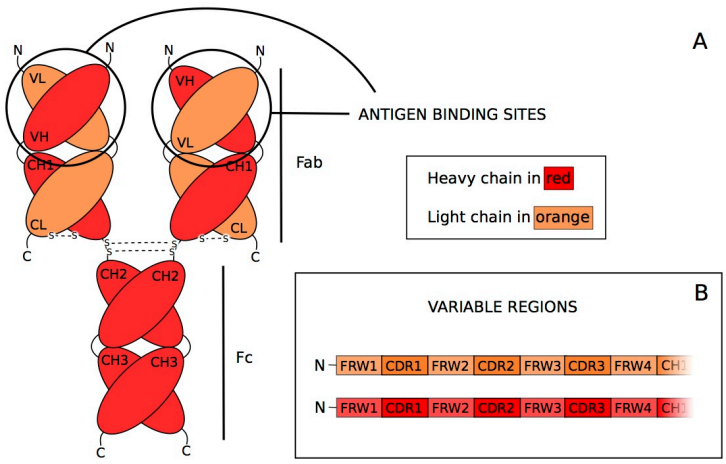

Figure 2. Cartoon with a schematic representation of the structure of an IgG antibody (A), and of its heavy (VH) and light chain (VL) variable domains (B).

Immunoglobulins are grouped into five classes (IgA, IgD, IgE, IgG, IgM) depending on the sequence of their heavy chain (α, δ, ε, γ, μ respectively). Heavy and light chains are composed by repeated motifs of about 110 amino acid called immunoglobulin (Ig) domains. Each Ig domain folds independently thanks to an intrachain disulfide bond. Light chains are composed by one variable domain (VL) and one constant domain (CL), while heavy chains are composed by one variable domain (VH) and three (CH1, CH2, CH3) or four constant domains. Variable domains of antibodies are located to the N-terminal of each chain and are composed by 3 hypervariable regions (also called Complementary Determining Regions, CDR) separated and flanked by relatively constant regions named framework regions (Figure 2). Light chain (VL and CL) pairs with VH and CH1 regions of heavy chain, and the hypervariable loop of each chain are clustered together to form the antigen binding site. The remaining constant domains of heavy chains form the Fc region, which determines the biological properties of the antibody. Changing in the length and amino acid sequence of hypervariable regions are the basis for the generation of an enormous diversity of antigen binding sites (Alberts et al. 2002).

The specificity of antibodies and small molecules derived by antibody engineering make them suitable to be used as molecular targeting drugs.

1.4.2 MONOCLONAL ANTIBODIES (mAbs)

Monoclonal antibodies (mAbs) are monospecific antibodies produced by cells that are all clones of a unique parental cell, and thus they are identical to each other and bind the same epitope. These antibodies are usually made through hybridoma technology, developed in 1975 by George Köhler and César Milstein (Kohler and Milstein 1975) (Nobel Prize in Physiology or Medicine, 1984). Hybridomas are cells derived by fusing, through polyethylene glycol (PEG) method (Galfre and Milstein 1981), not-producing-antibody myeloma cells with spleen cells from an animal (typically a mouse) that has been immunised with the antigen of interest. Hybridomas are immortal (thanks to myeloma characteristics) and have the ability to produce antibodies (thanks to B lymphocyte characteristics).

1.4.3 ANTIBODIES AND CANCER IMMUNOTHERAPY

Two kinds of monoclonal antibodies are used in cancer treatments:

- naked antibodies: are antibodies without any drug or radioactive material attached to them
- conjugated antibodies: are antibodies conjugated to chemotherapic drugs, toxins or radioactive particles.

Naked antibodies can succeed to kill tumour cells in different ways: by direct action of the antibody (through receptor blockade or agonist activity leading to apoptosis) (Figure 3, a); by immune-mediated mechanisms (complement-dependent cytotoxicity (CDC), antibody-dependent cellular cytotoxicity (ADCC) and regulation of T-cell function (Figure 3, b)); by vascular and stromal cell ablation (e.g. through vasculature receptor antagonism) (Figure 3, c) (Scott et al. 2012). Conjugated antibodies act through payload delivery of drugs, cytotoxic agents or radioactive particles on tumour cells and their microenvironment (Figure 3, a, c).

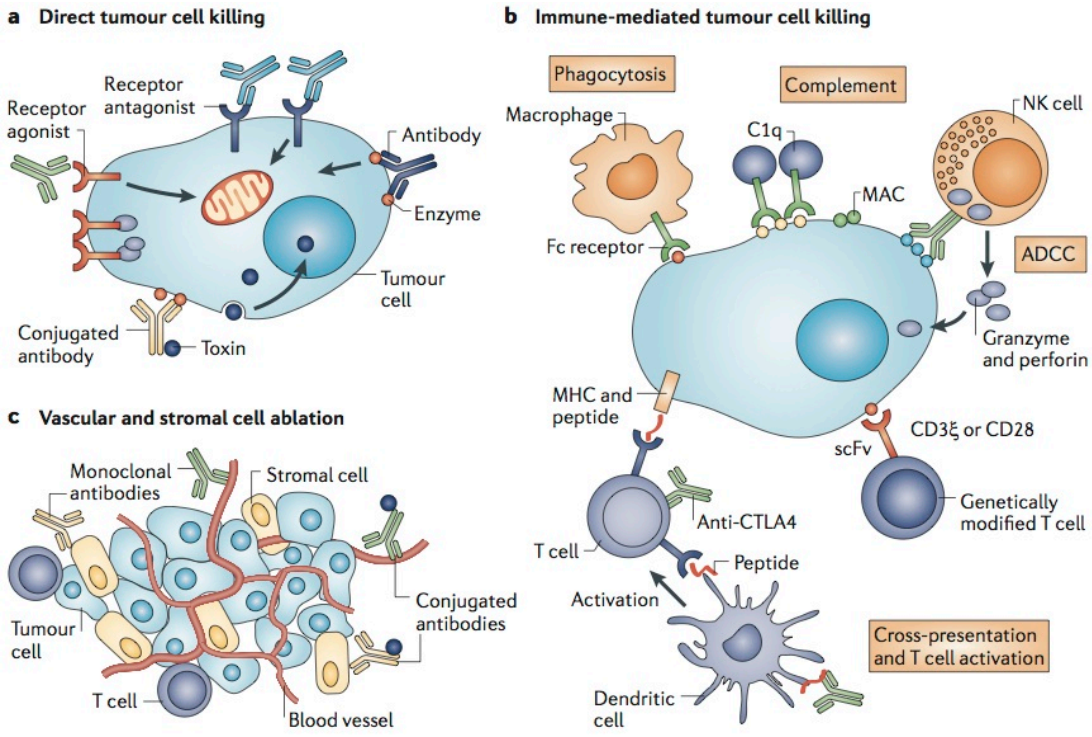

Figure 3. Mechanism of tumour cell killing by antibodies. Picture from *Antibody therapy of cancer* (Scott et al. 2012).

In the past decades several immunotherapeutic methods against cancer have been used successfully in the clinic. The first therapeutic monoclonal antibody (mAb), rituximab was approved in 1997 by the US FDA for the treatment of B-cell non-Hodgkin's lymphoma by targeting CD20 present on B cell surfaces (Grillo-Lopez et al. 2002). By 2012, twelve mAbs have been approved by the US FDA for cancer treatment (Table 1) (Scott et al. 2012).

For these reasons many studies aim to find new molecular targets on the surface of plasma membrane of tumour cells in order to develop antibodies able to inhibit tumour progression.

Antibody	Target	FDA-approved indication	Approval in Europe*	Mechanisms of action
Naked antibodies: solid malignancies				
Trastuzumab (Herceptin; Genentech): humanized IgG1	ERBB2	ERBB2-positive breast cancer, as a single agent or in combination with chemotherapy for adjuvant or palliative treatment	Similar	Inhibition of ERBB2 signalling and ADCC
		ERBB2-positive gastric or gastro-oesophageal junction carcinoma as first-line treatment in combination with cisplatin and capecitabine or 5-fluorouracil		
Bevacizumab (Avastin; Genentech/Roche): humanized IgG1	VEGF	For first-line and second-line treatment of metastatic colon cancer, in conjunction with 5-fluorouracil-based chemotherapy; for first-line treatment of advanced NSCLC, in combination with carboplatin and paclitaxel, in patients who have not yet received chemotherapy; as a single agent in adult patients with glioblastoma whose tumour has progressed after initial treatment; and in conjunction with IFNα to treat metastatic kidney cancer	Similar	Inhibition of VEGF signalling
Cetuximab (Erbitux; Bristol-Myers Squibb)‡: chimeric human–murine IgG1	EGFR	In combination with radiation therapy for the initial treatment of locally or regionally advanced SCCHN; as a single agent for patients with SCCHN for whom prior platinum-based therapy has failed; and palliative treatment of pretreated metastatic EGFR-positive colorectal cancer	Similar	Inhibition of EGFR signalling and ADCC
Panitumumab (Vectibix; Amgen)‡: human IgG2	EGFR	As a single agent for the treatment of pretreated EGFR-expressing, metastatic colorectal carcinoma	Similar	Inhibition of EGFR signalling
Ipilimumab (Yervoy; Bristol-Myers Squibb): IgG1	CTLA4	For the treatment of unresectable or metastatic melanoma	Similar	Inhibition of CTLA4 signalling
Naked antibodies: haematological malignancies				
Rituximab (Mabthera; Roche): chimeric human–murine IgG1	CD20	For the treatment of CD20-positive B cell NHL and CLL, and for maintenance therapy for untreated follicular CD20-positive NHL	Similar	ADCC, direct induction of apoptosis and CDC
Alemtuzumab (Campath; Genzyme): humanized IgG1	CD52	As a single agent for the treatment of B cell chronic lymphocytic leukaemia	Similar	Direct induction of apoptosis and CDC
Ofatumumab (Arzerra; Genmab): human IgG1	CD20	Treatment of patients with CLL refractory to fludarabine and alemtuzumab	Similar	ADCC and CDC
Conjugated antibodies: haematological malignancies				
Gemtuzumab ozogamicin (Mylotarg; Wyeth): humanized IgG4	CD33	For the treatment of patients with CD33-positive acute myeloid leukaemia in first relapse who are 60 years of age or older and who are not considered candidates for other cytotoxic chemotherapy; withdrawn from use in June 2010	Not approved in the European Union	Delivery of toxic payload, calicheamicin toxin
Brentuximab vedotin (Adcetris; Seattle Genetics): chimeric IgG1	CD30	For the treatment of relapsed or refractory Hodgkin's lymphoma and systemic anaplastic lymphoma	Not approved in the European Union	Delivery of toxic payload, auristatin toxin
^{90}Y-labelled ibritumomab tiuxetan (Zevalin; IDEC Pharmaceuticals): murine IgG1	CD20	Treatment of relapsed or refractory, low-grade or follicular B cell NHL	Similar	Delivery of the radioisotope ^{90}Y
		Previously untreated follicular NHL in patients who achieve a partial or complete response to first-line chemotherapy		
^{131}I-labelled tositumomab (Bexxar; GlaxoSmithKline): murine IgG2	CD20	Treatment of patients with CD20 antigen-expressing relapsed or refractory, low-grade, follicular or transformed NHL	Granted orphan status drug in 2003 in the European Union	Delivery of the radioisotope ^{131}I, ADCC and direct induction of apoptosis

ADCC, antibody-dependent cellular cytotoxicity; CDC, complement-dependent cytotoxicity; CLL, chronic lymphocytic leukaemia; CTLA4, cytotoxic T lymphocyte-associated antigen 4; EGFR, epidermal growth factor receptor; FDA, US Food and Drug Administration; IgG, immunoglobulin G; INFα; interferon-α; NHL, non-Hodgkin's lymphoma; NSCLC, non-small-cell lung cancer; SCCHN, squamous cell carcinoma of the head and neck; VEGF, vascular endothelial growth factor.
*Based on information from the European Medicines Agency. ‡Not recommended for patients with colorectal cancer whose tumours express mutated KRAS.

Table 1. Monoclonal antibodies currently FDA approved in oncology and their mechanisms of action. Table from *Antibody therapy of cancer* (Scott et al. 2012).

1.4.4 ANTIBODY ENGINEERING

Murine monoclonal antibodies produced through hybridoma technology have unfortunately many disadvantages (such as immunogenicity and poor tissue penetration). Advances in antibody selections and antibody engineering techniques provided tools to reduce immunogenicity, improve pharmacokinetic and localisation in tumour, increase affinity, and enhance effector functions (Sanz et al. 2005).

The Fc portion of antibodies contains species-specific sites that may be recognised by human immune system. For this reason, in the most of cases, the first dose of murine antibodies raises in patients an immunological response that produces the so called Human Anti Murine Antibodies (HAMA) (Tjandra et al. 1990), with the consequent destruction of the following murine antibody doses. To address this problem, advances in antibody engineering provided flexible platforms for the development of chimeric antibodies (created by fusing murine variable domains with human constant domain); humanised antibodies (created by CDR grafting of murine hypervariable regions into human antibodies) and fully human monoclonal antibodies (using human hybridomas or transgenic mice created by replacing the entire mouse IgG repertoire with a human repertoire).

Thanks to antibody engineering techniques, antibodies have been dissected to their basic elements (VH and VL), and then rearranged to produce a variety of both smaller and larger formats not found in nature that display new properties. In solid tumour immunotherapy, a cause for a lack of therapeutic response may be a poor tissue penetration due to the huge molecular size of antibodies IgG (145 kDa) and IgM (900 kDa, five 190 kDa monomers). To improve antibody tissue penetration and concentration in tumour, antibody engineering approaches have been used to develop smallest molecules such as nanobodies of about 15 kDa, single chain variable fragments (scFvs) of about 30 kDa, diabodies, single-chain diabodies (scDbs) of about 60 kDa. Diabodies (Db) could be bivalent or bispecific recombinant antibodies, formed by the dimerisation of two VH-linker-VL or VL-linker-VH fragments. In these fragments, the linker sequence is too short to allow VH-VL pairing, forcing the variable

domains to interact with the variable domains of another chain and create two antigen binding sites (Holliger et al. 1993). Bispecific diabodies are produced by heterodimerisation of two fragments each formed by a variable domain of the antibody 1 and a variable domain of the andibody 2: VH1-linker-VL2 and VH2-linker-VL1. Single chain bispecific diabodies are recombinant protein composed by the variable domains (VH and VL) of two antibodies connected by three peptide linkers (A, M and B): VH1-A-VL2-M-VH2-B-VL1.

These engineered molecules are easy to produce in bacterial or yeast systems, furthermore extravasate more efficiently and have a higher tissue penetration ability than full length Ig; the only limit of these molecules is the short half-life due to their small size. Many strategies has been developed to improve pharmacokinetic such as multimerization of scFv (shortening their linker sequence) to form tribodies (of about 90 kDa) and tetrabodies (of about 120 kDa), or conjugation of antibodies to big molecules such as polyethylene glycol (PEG) (Natarajan et al. 2005) or human serum albumin (HSA).

Diabodies and scDbs are also the most effective way to generate bispecific antibody fragments, able to bind two different antigen and thus useful to crosslink cells (e.g. retargeting immune system effector cells); to recruit effector molecules (like toxins, drugs, cytokines, radioisotopes, or complement system), to retarget carrier system (such as viral vectors for gene therapy) (Kontermann 2005); to target and inhibit macromolecular complexes involved in tumour progression.

Antibody engineering provided also methods to increase avidity (e.g antibody fragments multimerisation); affinity (e.g. mutation in the variable regions of whole Ig or antibody fragments); and enhance effector functions (e.g. mutation in the constant regions of whole Ig or conjugation of antibody fragments with recombinant Fc, toxin, drugs, cytokines, death ligands, radioisotopes, nanoparticles or complement system molecules).

2. GLYCOLIPIDS

Glycolipids are amphiphilic cell membrane components characterised by an hydrophilic polar sugar head and an hydrophobic apolar lipid moiety which anchors the molecule in the membrane. These molecules constitute about 3% of the outer monolayer of the plasma membrane (Alberts et al. 2002) and basing on the type of lipid component can be divided in three main groups: glycoglycerolipids, glycosylphosphatidylinositols and glycosphingolipids (GSL). The latter are widely upregulated in cancer so they are important targets for tumour immunotherapy (Durrant et al. 2012).

2.1 SYNTHESIS AND STRUCTURE OF GSL

GLS are built up upon ceramides (a sphingosine in amide linkage to a fatty acid) by the stepwise addition of individual sugars from their nucleotide activated precursors. Ceramide structure vary in length, hydroxylation, and saturation of both the sphingosine and fatty acid moieties which may contain carbon chain lengths from C_{14} to C_{24} and vary in degree of unsaturation and/or hydroxylation, resulting in lipid structural diversity that impacts the presentation of the attached glycan at membrane surfaces. Ceramide is synthesised on the cytoplasmic face of the endoplasmic reticulum (ER) and it could be added with a galactose or a glucose depending on the cell compartment.

On the luminal face of endoplasmic reticulum, the enzyme ceramide galactosyltransferase (CGT) catalyses the transfer of galactose from UDP-galactose to ceramide forming the sulfatide (SM4) precursor galactosylceramide (van der Bijl et al. 1996). Galactosylceramide is then transported to Golgi apparatus together with other glycolipids where the enzyme galactose-3-O-sulfotransferase 1 catalyses the transfer of the sulfate group from 3'-phosphoadenosine-5'-phosphosulfate (PAPS) forming sulfatides series: SM4, SM3 (McKhann and Ho 1967), SM2a, SM1a, SB1b.

On the cytoplasmic face of the ER and early Golgi apparatus, the enzyme glucosylceramide synthase (GCS) catalyses the transfer of glucose from UDP-glucose to ceramide forming lactosylceramide precursor glucosylceramide

(Coste et al. 1986). Then glucosylceramide flips to the Golgi lumen where it is typically elongated by a series of glycosyltransferases, first of all galactosyltranferase which adds a galactose forming lactosylceramide. Lactosylceramide is the acceptor for various transferases that generate three major classes of GSLs.

LacCer provides the basis of all glycosphingolipids, which are elongated with the addition of further sugars including fucose, glucuronic acid, and sialic acid, and blood group structures that are similar to those of O- and N-glycans, modifications such as 9−O-acetylation, N-deacetylation of sialic acids, or O-sulfation and O-acylation of galactose residues may also be present.

2.2 BIOLOGICAL FUNCTION: GLYCOSYNAPSES

GSLs, primarily expressed in the outer leaflet of plasma membrane, are able to form clusters with functional membrane proteins such as integrins, growth factor receptors, tetraspanins, and non-receptor cytoplasmic protein kinases (e.g., Src family kinases, small G-proteins). These microdomains, involved in carbohydrate-dependent cell adhesion inducing cell activation, growth, and motility, are termed “glycosynapses” (Hakomori 2002). Currently three types of glycosynapses have been described.

Glycosynapse 1: cell-to-cell adhesion mediated by the glucidic mojety of GSLs through head-to-head (trans) interaction (GSL-GSL or GSL-binding protein), in which GSLs are clustered with signal transducers.

Glycosynapse 2: cell to cell adhesion based on O-linked mucin-type glycoproteins that are recognized by carbohydrate binding proteins associated with signal transducers.

Glycosynapse 3: refers to the adhesion of a cell to the extracellular membrane (ECM), which is mediated by N-glycosylated adhesion receptors (e.g. integrin receptor) complexed with tetraspanins and GSLs, as typically seen with the integrin-tetraspanin-ganglioside complex (Regina Todeschini and Hakomori 2008).

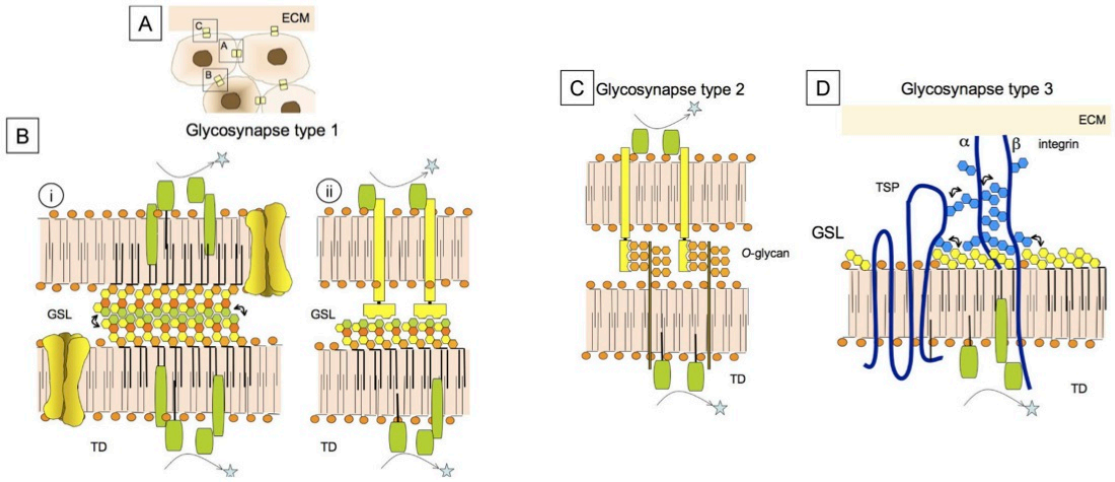

Figure 4. Cartoon representing the three type of glycosinapses. Picture from *Functional role of glycosphingolipids and gangliosides in control of cell adhesion, motility, and growth, through glycosynaptic microdomains* (Regina Todeschini and Hakomori 2008).

2.3 ALTERED GLYCOSILATION IN CANCER

GSLs are involved in many pathways of cellular physiology and a lot of studies have reported aberrant glycosylation and over-expression of glycolipids in tumour compared to normal tissue (Durrant et al. 2012).

Incomplete synthesis

In some cancers, pre-transcriptional gene regulation lead to the silencing of the transferases involved in the complete synthesis of some carbohydrate determinants. For example, the incomplete synthesis of sialyl- 6-sulpho Lewis x and disialyl Lewis a dramatically increase sialyl Lewis x and sialyl Lewis a levels (Kannagi 2003), promoting cell adhesion and motility resulting in increased metastasis (Wei et al. 2010).

Neo-synthesis

Tumour cells can express aberrant glycans through neo-synthesis, an enhanced transcription of glycosyltransferases was reported in the hypoxic regions of solid tumours (Koike et al. 2004).

Abnormal fucosilation

In cancer cells an up-regulation of enzymes involved in the addition of fucose residues produces abnormal fucosilated glycoproteins (Miyoshi et al. 2008). Fucosilated α-fetoprotein (AFP) was found over-expressed in hepatocarcinomas compared to chronic hepatitis and liver diseases, and in 2005 it was approved as hepatocarcinoma tumour marker by the Food and Drug Administration (FDA) (Moriwaki and Miyoshi 2010).

Over-expression

Different types of glycolipids are over-expressed in cancer compared to normal tissue: gangliosides are over-expressed in malignant melanoma and tumours from neuroectodermal origin (Tsuchida et al. 1987),(Hamilton et al. 1993); sulfatides are over-expressed in colorectal (Morichika et al. 1996) and ovarian carcinoma (Makhlouf et al. 2004); sialyl Lewis a is over-expressed in a range of cancers, including colorectal (Yamada et al. 1997), breast (Jeschke et al. 2005) and ovarian (Charpin et al. 1982) cancer.

Abnormal sialylation

Sialic acid is expressed in mammalian cells in two most common forms: N-acetlyneuraminic acid (NeuAc) and N-glycolylneuraminic acid (NeuGc). The latter is synthesised by the enzyme cytidine monophosphate (CMP)-NeuAc-hydroxylase, which hydrolyses CMP-NeuAc into NeuGc. Humans have a deletion in the gene that code for CMP-NeuAc-hydroxylase and thus are not able to express the functional protein (Irie et al. 1998). However, it was found that some cancers express NeuGc variant (Oliva et al. 2006), which make it ideal as tumour associated antigen.

Changes in their sugar head would also result in changes in the antigenicity (ability to bind antibody) and immunogenicity (ability to induce immune response) of the cells expressing them, conferring advantages to cancer cells (Hakomori and Zhang 1997). For these reasons glycolipids may be good targets for monoclonal antibody (mAbs) based cancer immunotherapy.

A large number of mAbs was developed against tumour associated glycolipid antigens (such as Lewis antigens, GM2, GD2, GD3, NeuGc GM3) and many of them gave promising results inducing direct cell killing through oncosis, inducing apoptosis, CDC and ADCC, and many of them have been entering clinical trial (Durrant et al. 2012).

3. INTEGRINS

Integrins are a family of 24 heterodimeric (α- and β-subunits) transmembrane receptors involved in mediating cell-cell and extracellular matrix (ECM)-cell interactions (Hynes 2002), transducing signals bidirectionally across the cell membrane.

3.1 INTEGRIN STRUCTURE

Each subunit is composed by a large extracellular domain, a single spanning transmembrane domain and a small cytoplasmic tail.

The extracellular domain of α-subunits is formed by a seven bladed β-propeller, which constitutes a head region, hold on a leg composed by three immunoglobulin-like β-sandwich domains (termed thigh, calf-1 and calf-2). Among the 18 α-subunit types, nine have an additional domain (about 200 amino acids organised in five β-sheets surrounded by seven α helices) within the β-propeller, named α-I domain (Campbell and Humphries 2011).

The extracellular domain of β-subunits is formed by the β-I domain (homologous of the α-I domain), which forms a head region hold on a flexible leg formed by a hybrid domain inserted in a plexin-semaphorin-integrin (PSI) domain, followed by four cysteine-rich epidermal growth factor (EGF) modules and a β-tail domain (Xiong et al. 2009).

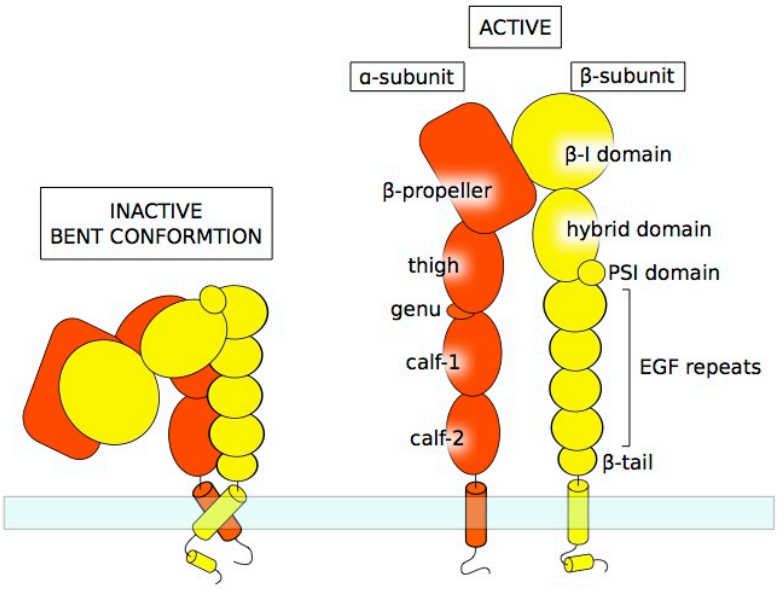

Figure 5. Cartoon with a schematic representation of integrin structure, in active and inactive conformation.

Both α and β subunits have a single spanned transmembrane α-helix domain. The current view is that association of integrin α and β transmembrane (TM) segments, results in an inactive resting receptor (Wegener and Campbell 2008).

The extended and flexible cytoplasmic tails are able to interact with a number of cytoskeletal and signalling proteins (Wegener et al. 2007). β-tails has two conserved NPXY motifs recognised by PTB domains on cytoplasmic proteins (e.g. talin and kindlin are important for activation of integrins from inside the cell).

3.2 INTEGRIN ACTIVATION

As integrins lack enzymatic activity, signalling is instead induced by the assembly of signalling complexes on the cytoplasmic face of the plasma membrane. Formation of these complexes is achieved in two ways; first, by receptor clustering, which increases the avidity of molecular interactions thereby increasing the on-rate of binding of effector molecules, and second, by induction of conformational changes in receptors that creates or exposes effector binding sites.

Current evidence suggests that conformational regulation is the primary mode of affinity regulation of integrins.

Current models of integrin activation describe inactive integrin in a bent conformation (Xiong et al. 2001),(Zhu et al. 2008). During the activation integrin assumes an extended form with a closed headpiece and then a fully extended form with an open headpiece (Takagi et al. 2002), in which the integrin subunit leg regions are separated to enable intracellular molecules binding and subsequent signalling.

3.3 INTEGRIN SIGNALLING

Integrins are able to integrate signals in two directions: “inside–out” and “outside-in” signalling.

During the “inside-out” signalling, an intracellular activator, such as talin or kindlin, binds to the β-subunit tail, inducing conformational changes that result in increased affinity for extracellular ligands, and allowing integrin to transmit forces required for cell adhesion, migration and ECM remodelling (Wegener and Campbell 2008).

During “outside-in” signalling, integrin binding to extracellular ligands induces conformational changes that enhance integrin clustering and downstream signalling. Signals from these adhesion receptors are integrated with those originating from growth factor receptors in order to organise the cytoskeleton, stimulate cell proliferation and rescue cells from matrix detachment and induced programmed cell death (Legate et al. 2009). The key element of all the integrin-mediated signalling pathways is the activation of the Focal Adhesion Kinase (FAK). Integrin clustering and talin binding to the β-subunit tail results in FAK oligomerization and consequent activation through autophosphorylation (residue Tyr397). Activated FAK can interact with and activate a number of proteins which in turn elicit a cascade of events that lead to cell proliferation, migration or survival. Together with FAK activation the other immediate effects of integrin activation is the up-regulation of lipid kinase activity that increases the concentrations of the phosphoinositide second messengers Phosphatidylinositol 4,5-bisphosphate (PIP2) and Phosphatidylinositol(3,4,5)-trisphosphate (PIP3), which in turn activate downstream signalling through

Diacylclycerol/inositol(1,4,5)-trisphosphate (DAG/IP3) and AKT pathways, respectively (Legate et al. 2009).

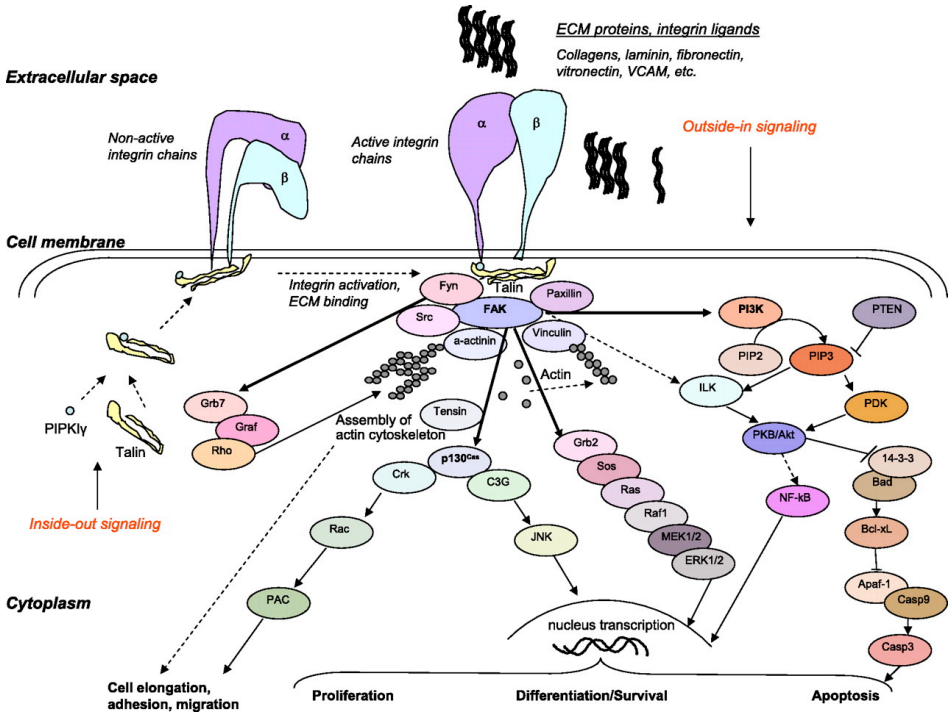

Figure 6: Schematic representation of the main integrin-related inside-out and outside-in signalling pathways. From *Role of integrins in fibrosing liver diseases* (Patsenker and Stickel 2011).

3.4 INTEGRIN AND CANCER

Recent evidence suggests ion channels as new integrin partners in macromolecular complexes on the surface of plasma membrane of cancer cells (Arcangeli and Becchetti 2006), (Millard et al. 2011).

4. POTASSIUM CHANNEL hERG1

The human ether-a-go-go-related gene (*hERG*, or *KCNH2*), located in the region q36.1 of chromosome 7, codes for the α-subunit of the voltage gated potassium channel hERG1 (also named Kv11.1).

4.1 hERG1 STRUCTURE

The pore region of hERG1 channel is delimited by four α-subunits (Figure 7, A), each composed by 6 transmembrane domains (S1-S6) (Figure 7, B).

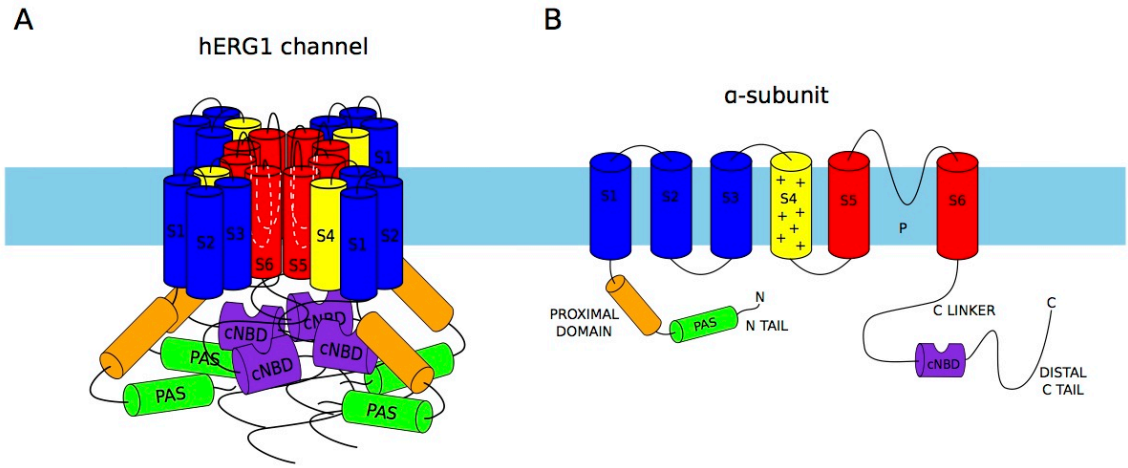

Figure 7. Cartoon with a schematic representation of hERG1 channel (A) and hERG1 single α-subunit (B).

S1-S4 segments constitute the voltage sensor domain: S4 is rich in basic amino acids (2 lysines (K) and 4 arginines (R)) and is linked by salt bridges with S2 and S3. The positive charges on the side chains of K and R move in response to change of transmembrane voltage, regulating channel opening. A study reports that neutralising one of the outer three positive charges in S4 segment (e.g. K525C mutation) causes a prominent hyperpolarising shift in the activation curve and induces channel opening at negative holding voltage, stabilising the open state, whereas neutralising one of the three inner three positive charges (e.g. R531C mutation) causes a depolarising shift in the activation curve, stabilising the closed states (Zhang et al. 2004).

S5, P-loop, and S6 domains of each subunit contribute to form the pore of the channel, determining potassium selectivity. In the large P loop (residues 573-637) there are 2 consensus site for N-glycosylation: N598 and N629; although it was demonstrated that only N596 is effectively glycosilated. N-glycosylation begins as a co-translational event in the endoplasmic reticulum, once the core-glycosylated protein is corrected folded, is transferred to the Golgi apparatus where it undergoes complete glycosylation. Conversely to previous studies (Petrecca et al. 1999), it was demonstrated that abolishing glycosylation does not prevent trafficking to the cell membrane, but it decreases the stability of hERG protein at the plasma membrane (Gong et al. 2002).

In addition to the transmembrane segments, each subunit has large cytoplasmic N-terminal and C-terminal regions. The N-terminal region contains: the N-tail

(residues 1-25), the Per-Arnt-Sim (PAS) domain (residues 26-135) that defines the *ether-a-go-go* subfamily of VGK channels (678), and the proximal N-tail (residues 136-376). The C-terminal region is composed by: the C-linker (residues 666-748), the cyclic nucleotide binding domain (cNBD) (residues 749-872) and the distal C-tail (residues 873-1159).

4.2 hERG1 EXPRESSION AND FUNCTION

hERG1 channel is expressed in the heart, various brain regions, smooth muscle cells, endocrine cells, and a wide range of tumour and tumour cell lines ((Arcangeli et al. 2009),(Jehle et al. 2011)).

The main biological function of hERG1 channel is to determine the rapid component of the delayed rectifier potassium current, I_{Kr}, which terminates the plateau phase and regulates repolarisation of the cardiac action potential. Reduction of hERG currents causes lengthening of the cardiac action potential. Mutations in KCNH2 gene or Kv11.1 blockade are associated to chromosome-7-linked congenital long QT syndrome (LQTS-2) and acquired long QT syndrome, respectively, both characterised by delayed cardiac repolarisation, prolonged electrocardiographic QT intervals, and a risk for the development of ventricular “torsade de pointes” arrhythmias and sudden death.

4.3 hERG1 AND CANCER

KCNH2 mRNA has been detected in several cancer cell lines (Bianchi et al. 1998) and its promoter region was found to harbour multiple binding sites for oncoproteins (Lin et al. 2007). Kv11.1 was found over expressed in colorectal cancer ((Lastraioli et al. 2004), (Lastraioli et al. 2012), (Crociani et al. 2013)), oesophagus adenocarcinoma (Lastraioli et al. 2006), gastric cancer ((Shao et al. 2005), Lastraioli 2005, (Crociani et al. 2014)), glioblastoma multiforme (Masi et al. 2005), endometrial adenocarcinoma (Cherubini et al. 2000), neuroblastoma (Arcangeli et al. 1993), melanoma ((Afrasiabi et al. 2010), (Arcangeli et al. 2013)) and both Acute Myeloid and Acute Lymphoblastic Leukaemia (AML and ALL) ((Pillozzi et al. 2007), (Pillozzi and Arcangeli 2010)). hERG1 channel can thus be considered a marker for malignant transition and

its expression usually correlates to poor prognosis ((Lastraioli et al. 2004), (Pillozzi et al. 2007), (Ding et al. 2010), (Lastraioli et al. 2012), (Arcangeli et al. 2013)).

hERG1 channel was found implicated in many aspect of tumour progression: enhanced cell proliferation, cell survival, invasiveness, angiogenesis, lymph node dissemination and metastasis (Arcangeli et al. 2009).

In slowly proliferating or non-proliferative cells resting membrane potential varies from -70mV to -90mV, while in highly proliferative cells varies from -40 mV to -55 mV; hERG1 channels are closed at membrane potentials below a threshold of -60 mV. Jehle et al. (2011) hypothesised that Kv11.1 over expression leads to a shift of the resting membrane potential of cancerous cells toward more depolarised values and repolarise them at the end of G1 phase, facilitating cell cycle progression and thus leading to cell proliferation. This idea is supported by several experiments which show cell cycle arrest in response to hERG1 blockers in various cancer cell lines (Jehle et al. 2011).

hERG1 channel plays a role in the development of new vasculature necessary for solid tumours growth. It has been shown that its gating is modulated by hypoxic conditions (Fontana et al. 2001), and the channel was also found correlated to tumour induced angiogenesis through vascular endothelial growth factor (VEGF) secretion ((Masi et al. 2005), (Pillozzi et al. 2007), (Crociani et al. 2013), (Crociani et al. 2014)).

Many studies report the effect of specific hERG1 blockers on tumour progression. In various leukaemia cell lines, treatment with the hERG1 blocker E-4031 reduces their proliferation rate (Smith et al. 2002). hERG1 channel blocking with E-4031 and silencing using specific siRNA prevent proliferation and cell migration in melanoma cell line MDA-MB-435S (Afrasiabi et al. 2010).

For these reasons many studies are addressed to find new selective and non-cardiotoxic hERG1 blockers for cancer treatment.

Kv11.1 blockers have shown proapoptotic effects on cancer cell lines and on reconstituted systems like transfected HEK293, a phenomenon probably due to

the inhibition of hERG1-related signalling pathways. hERG1 channel acts not only changing Vm potential but was found to trigger many intracellular signalling pathways. The channel was indeed found in macromolecular complexes on the surface of plasma membrane of cancer cells, together with integrin subunits ((Arcangeli et al. 1993), (Hofmann et al. 2001), (Cherubini et al. 2005), (Pillozzi et al. 2007), (Crociani et al. 2013)), growth factors receptors (e.g. vascular endothelial growth factor receptor-1 (FLT-1) (Pillozzi et al. 2007)) or chemokines receptors (e.g. chemokine CXC receptor-4 (CXCR-4) (Pillozzi et al. 2011)).

5. hERG1-β1INTEGRIN COMPLEX IN CANCER

Interaction between hERG1 channels and integrins, in particular the β1 subunits of integrin receptors was described in many types of cancer: neuroblastoma (Arcangeli et al. 1993), colon cancer (Crociani et al. 2013), leukaemia cells ((Hofmann et al. 2001), (Pillozzi et al. 2007), (Pillozzi et al. 2011)) and in reconstituted models of transfected HEK293 (Cherubini et al. 2005). This interaction has a twofold characteristic: integrin activates hERG1 channel (Arcangeli et al. 1993), and hERG1 channel modulate integrin downstream signalling ((Cherubini et al. 2005), (Arcangeli and Becchetti 2006), (Pillozzi et al. 2007), (Pillozzi et al. 2011), (Crociani et al. 2013)).

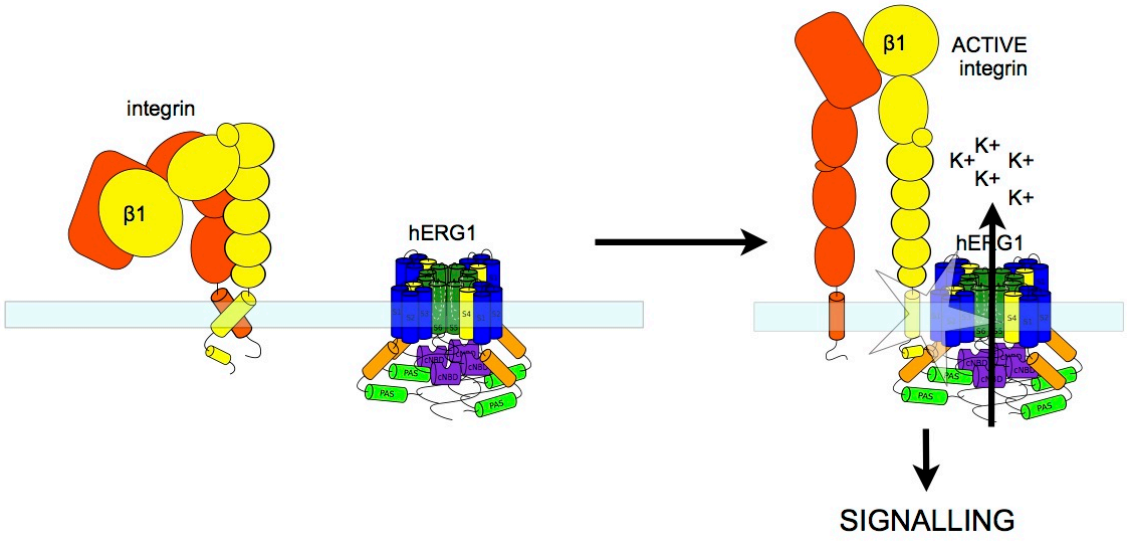

Figure 8. Cartoon with a schematic representation of β1 integrin and hERG1 channel interaction.

Selective hERG1 blockers inhibit FLT1-β1integrin-hERG1 complex related effects: FLT-1 signalling and migration in AML cells (Pillozzi et al. 2007), and CXCR4-β1integrin-hERG1 complex related effects in ALL cells (Pillozzi et al. 2011). In subcutaneous tumour models of colorectal cancer, selective hERG1 blockers disrupt β1integrin-hERG1 complex related signalling, resulting in the inhibition of cell growth, angiogenesis and metastatic spread (Crociani et al. 2013).

For these reasons, targeting hERG1 channel in specific macromolecular complexes selectively expressed on cancer cells, such as hERG1/β1integrin complex could be a valid strategy for cancer therapy.

AIM OF THE THESIS

The work presented in this thesis aims to characterise molecular targets on the surface of plasma membrane of cancer cell and to develop antibodies suitable for cancer immunotherapy.
The project focuses towards two molecular targets: glycosphingolipids and the potassium channel hERG1-β1 integrin macromolecular complex; and has three main goals:

1. Development and characterisation of monoclonal antibodies against glycolipid antigens
2. Study of the molecular mechanisms involved in hERG1-β1 integrin complex formation
3. Development of engineered antibodies able to target hERG1-β1 oncogenic unit, disrupting the complex and preventing downstream signalling

MATERIALS AND METHODS

1. DEVELOPMENT AND CHARACTERISATION OF ANTIBODIES AGAINST GLYCOSPHINGOLIPID ANTIGENS

1.1 HYBRIDOMAS DEVELOPMENT

1.1.1 IMMUNISATION

Hybridomas were produced according to Köhler and Milstein (1975) standard method. The immunisation was performed in collaboration with prof. Nativi's group (Department of Organic Chemistry, University of Florence) who provided the antigen: a stable mimetic of GM3 lactone (Arcangeli et al. 2010).

mimGM3, conjugated to two different carriers $Pam_3CysSer$ and Ovalbumin. mimGM3-$Pam_3CysSer$ and mimGM3-OVA were used to perform two parallel protocols of immunisation in Balb/c mice as reported in Table I.

Day	mimGM3-OVALBUMIN	mimGM3-$Pam_3CysSer$
1	100 µl (400 µg) INTRAVENOUS	500 µg + 100 µl Complete Freund's Adjuvant INTRAPERITONEAL
14	90 µl (360 µg) + 10 µl H_2O INTRAVENOUS	60 µl (100 µg) + 40 µl H_2O + 100 µl Incomplete Freund's Adjuvant INTRAPERITONEAL
28	90 µl (360 µg) + 10 µl H_2O INTRAVENOUS	60 µl (100 µg) + 40 µl H_2O + 100 µl Incomplete Freund's Adjuvant INTRAPERITONEAL
42	90 µl (360 µg) + 10 µl H_2O INTRAVENOUS	60 µl (100 µg) + 40 µl H_2O + 100 µl Incomplete Freund's Adjuvant INTRAPERITONEAL
56	125 µl (500 µg) INTRAVENOUS	100 µl (500 µg) INTRAVENOUS

Table 1. Immunisation of Balb/c mice performed at two weeks intervals.

1.1.2 CELL FUSION

Three days after the last injection, the mice were euthanised by cervical dislocation and spleens were harvested. To obtain spleen cells suspension, each spleen was minced in a sterile Petri dish with a surgical scalpel blade and gently homogenised in a minimal amount of DMEM using a glass tissue homogeniser. Cell fusion was performed using spleen cells and aminopterine sensitive myeloma cells (NS0) by the polyethylene glycol (PEG) (Sigma) method (Galfrè and Milstein 1981).

NS0 myeloma cells are Hypoxanthine-Guanine PhosphoRibosyl Transferase (HGPRT) defective cells. HGPRT is an enzyme that catalyses conversion of hypoxanthine to inosine monophosphate and guanine to guanosine monophosphate, transferring the 5-phosphoribosyl group from 5-phosphoribosyl 1-pyrophosphate (PRPP) to the purine, and plays a central role in the generation of purine nucleotides through the purine salvage pathway. Cells lacking this enzyme can produce purine nucleotide only through the *de novo* pathway. The *de novo* pathway is blocked by aminopterine, for this reason HGPRT- cells are aminopterine sensitive.

NS0 cells were maintained in logarithmic phase growth at least for 4-5 days before cell fusion. An equal number (10^8 cells) of spleen cells and NS0 were mixed together in 30 ml of DMEM + 4 mM L-Gln and centrifuged at 700 g for 5 min. Supernatant was discarded and the tube with cell pellet was placed in a Becker with 37°C water. We followed cell fusion protocol reported below.

A) Add 1 ml of 37°C preheated PEG in 1 minutes, stirring
B) Stir for 2 minutes
C) Add 1 ml of 37°C preheated DMEM + 4mM L-Gln in 1 minutes, stirring
D) Repeat C
E) Add 1 ml of 37°C preheated DMEM + 4mM L-Gln in 30 sec, stirring
F) Repeat E
G) Add 6 ml of 37°C preheated DMEM + 4mM L-Gln in 2 minutes, stirring.
H) Add 12 ml of 37°C preheated DMEM + 4mM L-Gln drop to drop, stirring.
I) Centrifuge at 800 g for 5 minutes and discard supernatant

Each fusion product was resuspended in DMEM + 4mM L-Gln supplemented with 20% FetalClone I (Hyclone) and HAT (Hypoxanthine, Aminopterine, Timidine) (Sigma) in order to select B-cell/NS0 hybrids. We prepared 1:2, 1:4, 1:8 and 1:8 cell fusion dilutions in 48 ml of selective medium and we aliquoted each in a 24-well multiwell plate, 2 ml for well; the plates were placed at 37°C, 5% CO2 for hybridomas selection. After two weeks the selected hybridomas formed visible colony-like clusters.

Hybridoma supernatants were analysed by enzyme-linked immunosorbent assay (ELISA) in order to select the most suitable population to be cloned.

1.2 SOFT AGAR CLONING

For monoclonal antibody production, clonal isolation of hybridomas was achieved after two subsequent cloning processes: manual colony picking and soft agar cloning.

First of all we picked up the single colonies grew after HAT selection in 24-well multiwell plates and we transfer each one into a new well. The supernatant of those clones was assayed by ELISA in order to chose the best hybridomas for soft agar cloning.

Hybridomas were plated (10000, 5000, 2500, 1250 cells per 60mm dishes) in a soft agar to allow single cell colonies formation. Soft agar plates were composed by a Base Layer (0.5% low melting point agarose in DMEM added with 4 mM L-Gln, 20% FBS and 1x HAT) and a Top Layer (cells in 0.25% low melting point agarose in DMEM added with 4 mM L-Gln, 20% FBS and 1x HAT). After about 15 days, the clones were picked up, seeded in a 24-well multiwell plate, amplified and adapted to grow in an aminopterine free medium. Aminopterine remains inside the cells even if HAT is removed from culture medium, continuing to exploit its inhibitory effect on the novo synthesis of nucleotide bases. For this reason aminopterine was diluted from the culture by several passages of the cells in hypoxanthine-thymidine (HT) supplemented medium (approximately 2-3 weeks) before transfer into normal hybridoma growth medium DMEM High Glucose without Sodium Piruvate added with 4 mM L-Gln and 10% FetalClone I (Hyclone).

1.3 LARGE SCALE ANTIBODY PRODUCTION

For large scale antibody production we cultured hybridoma clone C2 into CELLine CL1000 Bioreactor (INTEGRA Biosciences), harvesting and splitting the cell culture (1:5) every two weeks.

1.4 ISOTYPE TEST

Isotype test was performed using IsoQuick for Mouse Monoclonal Isotyping (Sigma) following manufacturer's instructions.

1.5 IgM ANTIBODY PURIFICATION

For purification of the IgM OVA-C2 mAb we used HiTrap IgM purification HP (GE Healthcare) according to manufacturer's instructions. The purified antibody was then dialysed against PBS at 8°C overnight, using Slide-A-Lyzer dialysis cassette 7K 0.5-3 ml (Thermo Scientific). To calculate purified antibody's concentration, an aliquot of the sample was analysed by SDS-PAGE and Coomassie Staining alongside different amounts of a standard antibody, whose concentration is known. Sample concentration was calculated comparing its 25 kDa band (light chain) with the one of the standards.

1.6 COOMASSIE STAINING

After SDS-PAGE, the separated proteins were stained on the gel with Coomassie Brilliant Blue method. The gel was incubated for 30 minutes at room temperature with Coomassie Staining Solution (Brilliant Blue R-250 0.05%, methanol 50%, acetic acid 10%, H_2O 40%) and then with Destaining Solution (methanol 40%, acetic acid 10%, H_2O 50%). After destaining, the protein bands will appear as blue bands.

1.7 GSL INDIRECT Enzyme-Linked Immunosorbent Assay (ELISA)

For indirect ELISA a 96-multiwell (U bottom, for ELISA assay) was coated with GM3 or sulfatide in 100 µl of ethanol and left overnight at room temperature. The non-specific binding sites were then saturated with PBS-2.5% Skim Milk (2.5% SM-PBS) for 1 hour at room temperature. The primary antibody (100 µl of

hybridomas supernatant) was incubated for 2 hours at room temperature, followed by washing three times in PBS. The wells were stained with the secondary antibody goat anti-mouse IgM-peroxidase (Sigma) for 1 hour at room temperature and then washed three time in PBS. The plate was then incubated with 100 µl of peroxidase substrate TMB for 5-10 minutes, then the reaction was stopped adding 100 µl of HCl 0.05 M, the plate was thus red at 450 nm.

1.8 GSL IMMUNOFLUORESCENCE

Cells were grown on glass coverslips and fixed with 4% methanol-free formaldehyde (Thermo Scientific) in PBS. Nonspecific sites were blocked with 2.5% SM-PBS for 2 hours. Primary antibody (hybridomas supernatant or anti-GM3 mAb M2590 (CosmoBio)) of was incubated overnight at 4°C. Glass coverslips were washed 3 times in PBS and the secondary antibody (anti-mouse IgM-FITC, Invitrogen) was incubated for 1 hour at room temperature in the dark. Glass coverslips were washed as above and then mounted on slides using ProLong Gold Antifade Reagent (Life Technologies) following manufacturer's instructions.

1.9 GSL IMMUNOHYSTOCHEMISTRY

Formalin fixed and paraffin embedded pancreatic tissue was cut in 7 µm-thin slices and used for immunohystochemistry assay. The slices were de-waxed in Histoclear and hydrated through graded ethanol solution to H_2O. The endogenous peroxidase were inactivated with H_2O_2 1% in PBS for 20 minutes, room temperature. After two washes in PBS, 5 minutes, room temperature, the non-specific sites were blocked with 5% SM-PBS for 45 minutes, room temperature, then the samples were washed as previously described. We used two OVA C2 mAb dilution (1:10 and 1:100) and a negative control without the primary antibody. We stained the samples overnight at 4°C. The day after we washed twice as previously described and we revealed the antigen bound to the primary antibody using PicTure-MAX Polymer Detection Kit according to manufacturer's instructions.

1.10 INSULIN IMMUNOHYSTOCHEMISTRY

Formalin fixed and paraffin embedded pancreatic tissue was cut in 7 µm-thin slices and used for immunohystochemistry assay. The slices were de-waxed in Histoclear and hydrated through graded ethanol solution to H_2O. The endogenous peroxidase were inactivated with H_2O_2 1% in PBS for 20 minutes, room temperature. After two washes in PBS, 5 minutes, room temperature, the non-specific sites were blocked with 5% SM-PBS for 45 minutes, room temperature, then the samples were washed as previously described. We used anti-insulin (Dako) mAb 1:150 in PBS and a negative control without the primary antibody. We stained the samples overnight at 4°C. The day after we washed twice as previously described and we revealed the antigen bound to the primary antibody using PicTure-MAX Polymer Detection Kit according to manufacturer's instructions.

2. LIPID ANALYSIS

2.1 CELL CULTURES

All cell lines was routinely cultured in an humidified incubator at 37°C with 5% CO_2.

Hybridomas were grown in Dulbecco's Modified Eagle Medium (DMEM) High Glucose (Euroclone) supplemented with 4 mM L-Gln and 10% FBS FetalClonel (HyClone). B16-F1, MCF-7, MDA-MB-23 were grown in Dulbecco's Modified Eagle Medium (DMEM) High Glucose (Euroclone) supplemented with 4 mM L-Gln and 10% FBS EU approved (Euroclone). MiaPaCa-2, BxPc3 were cultured in RPMI added with 2 mM L-Gln and 10% FBS Defined (Euroclone). Panc-1 was cultured in DMEM High Glucose supplemented with 4 mM L-Gln and 10% FBS Defined. RIN-5F cells were cultured in RPMI added with 2 mM L-Gln and 10% FBS EU approved, with or without 12 mM glucose.

2.2 LIPID EXTRACTION AND GANGLIOSIDES PURIFICATION

Adherent cells cultures for lipids analysis were amplified and grown until they are 90% confluent, then they were washed in cold PBS and harvested scraping them from culture plates in cold PBS. Cells was counted using Burker's chamber cell count method (for each extract we used 20-30 x 10^6 cells) and an aliquot (1/30) of cell suspension was harvested for protein extraction. Cell suspension was centrifuged at 1100 g and 4°C for 10 minutes and the pellet was resuspended in cold PBS and sonicated. Lipids were extracted with chloroform-methanol 2:1 to a final volume 20 times the volume following Folch's method (Folch et al. 1957). The extract was filtered using Watman paper into a cylinder to adjust the volume, added with 0.2% of its volume of CaCl2 and mixed thoroughly. The mixture was then allowed to separate into two phases. The lower chloroformic phase (which contains lipids) was dryed and resuspended in chloroform:methanol 19:1 in order to be fractionated in neutral and polar glycolipids by ionic exchange chromatography, according to Siakotos et al., (1965). The chromatography was performed with a column packed with Sephadex G25 (stationary phase) in a methanol:H_2O 1:1 solution (moving phase). The column was first washed allowing the methanol:H_2O 1:1 used for packing the column to pass through the resin bed at a flow rate of 1 ml/min followed by adding 100 ml Solution 1 (chloroform:methanol 19:1 solution saturated in water, 5 ml H_2O per litre), 100 ml of Solution 2 (chloroform:methanol 19:1 added with 16.7% acetic acid saturated with H_2O) and methanol:H_2O 1:1. These wash cycles was repeated another time and finally the column was equilibrated with Solution 1, in order to create an hydrophobic ambient outside the beads. We loaded the sample and then we loaded the chloroform:methanol 19:1 solution saturated with H_2O, so that the hydrophobic lipids (neutral glycolipids) can stay in the moving phase and be eluted (Fraction 1, neutral glycolipids), whereas the most polar lipids, such as gangliosides, interact with the beads of Sephadex G25 and remain in the column bed. Gangliosides were than eluted with a chloroform:methanol 19:1 added with 16.7% acetic acid saturated with H_2O: the acetic acid interact with the negative charges of sialic acid of gangliosides so that they result less polar, they pass in the moving phase and can be eluted (Fraction 2, polar glycolipids).

2.3 GANGLIOSIDE Thin Layer Chromatography (TLC)

The ganglioside fraction (Fraction 2) was dried with N_2, resuspended in chloroform and loaded on a TLC plate (0.25 mm 10x10 HPTLC, Merck). The plate is then placed in a closed glass container with the running solution (chloroform:methanol:0.02%$CaCl_2$ (50:45:10)). Gangliosides are than revealed using the colorimetric resorcinol method according to Svennerholm (1957). The TLC plate was dried and sprayed with resorcinol reactive (10 ml resorcinol 2%, 0.25 ml 0,1 M $CuSO_4$,80 ml HCl + H_2O to 100 ml) and then heated at 110°C for 15 minutes. Resorcinol reacts with sialic acid and form a brown-purple band corresponding to each ganglioside band.

2.4 GM3 LACTONISATION

GM3 lactonisation was performed according to Zhu et al (1999), 50 µg of purified GM3 in methanol (Santa Cruz Biotechnology) was dried with N_2, resuspended in 40 µl of Glacial Acetic Acid and kept at room temperature, in the dark for 1 week.

2.5 SULFATIDES TLC

Neutral lipids fraction (Fraction 1) was dried with N_2, resuspended in chloroform and loaded on a TLC plate (0.25 mm 10x10 HPTLC, Merck). The plate is then placed in a closed glass container with the running solution (chloroform:methanol:H_2O (65:25:4)). The TLC plate was dried and sprayed with Azure A reactive (Azure A 2% in 1 mM H_2SO_4) and then destained in 40 mM H_2SO_4:methanol (3:1) for 1 hour. Azure A reacts with sulphate groups and form a dark blue band corresponding to each sulfatides band.

2.6 TLC IMMUNOSTAINING

Fraction 1 or Fraction 2 was dried with N_2, resuspended in chloroform and loaded on an aluminium baked TLC plate (Merck). The plate was then placed in a closed glass container with the opportune running solution as described above. TLC immunostaining was performed without fixation of the plates according to Muller-Loennies et al. (2006). The TLC plate was then dried and

non-specific binding sites were saturated with 2.5% SM-PBS for 1.5 hour. TLC plate was then incubated overnight with the primary antibody (OVA C2 mAb 1:2 or mAb M2590 (Cosmo Bio) 1:50 in 2.5% SM-PBS). The day after TLC plate was washed 5 times, for 5 minutes in PBS and then incubated for 1 hour with the secondary antibody (goat anti-mouse IgM-peroxidase, Sigma) followed by 5 washes as described above. Antibody binding was revealed incubating 10 minutes with TMB and then stopping the reaction with H_2O for 5 minutes. All the incubation was performed at room temperature with a gently rocking.

2.7 GLS DOT BLOT ASSAY

We performed a Dot Blot assay using pre-casted strips with spotted glycolipids: sulfatides, GQ1b, GT1b, GT1a, GD3, GD1b, GD1a, GM3, GM2, GM1 (DOTZEN Ganglio Profile Ab, Zentech). We performed the assay following the protocol provided with the kit except for the secondary antibody. Since we were testing murine IgM antibodies, we revealed them using Anti-Mouse IgM (μ-chain specific)-Peroxidase (A8786, Sigma) 1:1500 in PBS. We used as positive control a murine antibody against GM3, M2590 (Cosmo Bio).

3. STUDY OF THE MOLECULAR MECHANISMS INVOLVED IN hERG1-β1 INTEGRIN COMPLEX FORMATION

3.1 CELL CULTURES

All cell lines was routinely cultured in an humidified incubator at 37°C with 5% CO_2.

HEK293 and GD25 were cultured in DMEM High Glucose supplemented with 4 mM L-glutamine and 10% FBS EU approved (Euroclone).

Transfected HEK293 were cultured in DMEM High Glucose supplemented with 4 mM L-glutamine and 10% FBS EU approved added with the selective agent G418 (1 mg/ml final concentration).

3.2 GST-PULL DOWN ASSAY

GST-fusion proteins were expressed in E. Coli and purified by affinity chromatography using a column packed with Glutatione-Sepharose 4B resin. Purified proteins were eluted with glutatione and gel filtrated. GST-β1Ct was cut with thrombin and β1Ct was recovered by gel filtration.

hERG1 cytoplasmatic domain fusion proteins (GST-N135, GST-P138, GST-C54) were incubated with β1Ct and 20 µl of Glutatione-Sepharose 4B resin in a total volume of 500 µl of PBS, overnight on a rocking platform, at 8°C. We performed also, control samples with GST or β1Ct alone with the resin. Each sample was then centrifuged at 500 g, 5', at 4°C, and the resin was washed 3 times with PBS. The samples with pulled down proteins were boiled (5 minute at 95°C) in Laemmli buffer 1x (total volume 25 µl) and analysed by SDS-PAGE and Coomassie staining.

3.3 GST "FISHING" ASSAY

GST-β1Ct was used as a molecular bait for "fishing" in a total protein cell lysate. HEK-293-hERG1 and HEK293 wild type total protein lysate (0.5 mg) were pre-cleared with 20 µl of Glutatione-Sepharose 4B resin, for 1 hour, on a rocking platform, at 8°C. Meanwhile, GST-β1Ct was allowed to bind to 20 µl of Glutatione-Sepharose 4B resin, for 1 hour, on a rocking platform, at 8°C. Pre-cleared protein lysate was added to the resin bound to GST-β1Ct, and incubated overnight on a rocking platform, at 8°C. Each sample was then centrifuged at 500 g, 5', at 4°C. The supernatant was harvested for further analysis and the resin was washed 3 times with PBS. The resin with pulled down proteins, and the supernatant containing the proteins which were not pulled down, were boiled (5 minute at 95°C) in Laemmli buffer 1x (total volume 25 µl) and analysed by SDS-PAGE and Western Blotting using anti-hERG1 C54 antibody.

3.4 CELL TRANSFECTION

Cell transfection was performed using Lipofectamine 2000 (Invitrogen).

For transient transfection, we used healthy log-phase HEK293 cells grown in 10-cm petri dishes. One day before transfection we plated the cells in order to have 90-95% of confluence at the time of transfection. For each plate we used 24 µg of pure ($A_{260}/A_{280} \simeq 1.8$) expression vector containing the gene of interest and 60 µl of Lipofectamine 2000. We prepared two tubes: the first with DNA diluted in 1.5 ml of Opti-MEM medium (Gibco) and the second with Lipofectamine 2000 diluted in 1.5 ml of Opti-MEM; we incubated for 5 minutes at room temperature. We combined then the diluted DNA and the diluted Lipofectamine 2000, mixing gently, and we incubated for 20 minutes at room temperature, to allow DNA-Lipofectamine 2000 complexes formation. In the meantime we changed cell medium with 15 ml Opti-MEM. After 20 minutes of incubation we added the complexes to the plate and we left the cells in the incubator over-night. After about 16 hours we removed the complexes changing cell medium with their ordinary medium. We used the cells 24 hours after removing the complexes.

For stable transfection, we used healthy log-phase HEK293 cells grown in 3.5-cm petri dishes. One day before transfection we plated the cells in order to have 90-95% of confluence at the time of transfection. For each plate we used 6 µg of pure ($A_{260}/A_{280} \simeq 1.8$) expression vector containing the gene of interest and 10 µl of Lipofectamine 2000. We prepared two tubes: the first with DNA diluted in 250 µl of Opti-MEM medium (Gibco) and the second with Lipofectamine 2000 diluted in 250 µl of Opti-MEM; we incubated for 5 minutes at room temperature. We combined then the diluted DNA and the diluted Lipofectamine 2000, mixing gently, and we incubated for 20 minutes at room temperature, to allow DNA-Lipofectamine 2000 complexes formation. In the meantime we changed cell medium with 2 ml Opti-MEM. After 20 minutes of incubation we added the complexes to the plate and we left the cells in the incubator over-night. After about 16 hours we removed the complexes changing cell medium with their ordinary medium. 24 hours after removing the complexes we sub-cultured the cells diluting them 1:8, and supplementing culture medium with the selective

agent (G418, Gibco, final concentration 1 mg/ml). We maintained stable transfected cells in culture medium supplemented with the selective agent.

3.5 CELL STIMULATION AND TREATMENT WITH hERG1 INHIBITORS

HEK293 and HEK293 transfected cells were stimulated on fibronectin coated plates as described in Cherubini (2005).

For plates coating we used fibronectin 100 µg/ml in 1.5 ml of DMEM, for 1 hour in the incubator. After 1 hours fibronectin solution was poured off and non-specific binding sites were blocked incubating the plate with 1.5 ml of DMEM supplemented with heat-inactivated Bovine Serum Albumin (BSA) (Albumin Fraction V, Euroclone) (prepared as reported in Arcangeli 1993) (0.25 mg/ml final concentration) for 45 minutes in the incubator.

Before stimulation, cells were starved over-night, changing their medium with serum free medium. Cells were then detached using 5 mM EDTA in PBS, centrifuged at 1100 g for 10 minutes at room temperature and seeded on coated plates in 5 ml of DMEM added with 0.25 mg/ml BSA. Cells were stimulated for 45 minutes in the incubator.

When needed the cells were treated with hERG1 inhibitors such as 40 µM E-4031 or 1 µM ERG-toxin (kindly provided by Prof.ssa Restano Cassulini, Universitad National Autónoma de México (UNAM)). Before seeding cells on coated plates, they were incubated 30 minute with the inhibitors in suspension at 37°C. The cells were then seeded on the coated plates in presence of the same concentration of inhibitors, and left for 45 minutes in the incubator.

3.6 TOTAL PROTEIN EXTRACTION

10 cm petri dishes with confluent adherent cells were placed on ice, washed with ice-cold phosphate-buffered saline (PBS) and collected by scraping them with a rubber cell lifter. Cells were then and centrifuged at 2000 g 10 minutes and the pellet was resuspended in Lysis Buffer (150 mM NP-40, 150 mM NaCl, 50 mM Tris-HCl pH 8, 5 mM EDTA, 10 mM $Na_4P_2O_7$, 10 mM NaF, 0.4 mM Na_3VO_4 supplemented with protease inhibitors Complete Mini (Roche)) and incubated 20 minutes on ice. Lysed cells were then centrifuged at 16000 rpm,

10 minutes, 4°C, and the supernatant with total protein extract was collected and harvested at -80°C.

3.7 PROTEIN IMMUNOPRECIPITATION

For immunoprecipitation experiments we used 1.5 mg of total protein lysate, diluted in Wash Buffer (150 mM NP-40, 150 mM NaCl, 50 mM Tris-HCl pH 8, 5 mM EDTA, 10 mM $Na_4P_2O_7$) in a total volume of 300-400 µl. We performed a pre-cleaning step adding protein A or a protein A/G mix and incubating for 2 hours in a rolling tube at 4°C. We spin down the samples and transferred the supernatant in a new tube. We added the antibody for the protein of interest (5 µg of purified anti-hERG1 mAb, or 5 µg of TS2/16 mAb or 1 µl of anti-FAK per mg of total protein lysate) and we incubated the samples overnight in a rolling tube at 4°C. The antibody/antigen complex was pulled out of the sample adding protein A agarose or a protein A/G agarose mix and incubating for 2 hours in a rolling tube at 4°C. The agarose resin was then washed 3 times with 0.5 ml Wash Buffer and 3 times with 0.5 ml ice cold PBS. The samples were then boiled at 95°C for 5 minutes in 14 µl of Laemmli Buffer 2x, and analysed by SDS-PAGE and Western Blotting.

3.8 Sodium Dodecyl Sulphate PolyAcrylamide Gel Electrophoresis (SDS-PAGE)

To perform SDS-PAGE we prepared a polyacrilamide gel divided into an upper stacking gel at 4% acrylamide and the lower resolving gel at % acrylamide varying from 6% to 12.5%. In the stacking gel the samples are loaded and can be compacted as a thin migrating band, and in the resolving gel the samples are separated according to their molecular weight).

Resolving gel	6%	7.5%	10%
H_2O			
acrylamide (30%)-bis-acrylamide (0.8%)			
1.5 M Tris-HCl, pH 8.8	1,75 ml	1,75 ml	1,75 ml
10% SDS	70 µl	70 µl	70 µl
10% ammonium persulfate	70 µl	70 µl	70 µl
TEMED	7 µl	7 µl	7 µl

Stacking gel	4%
H_2O	2,4 ml
acrylamide (30%)-bis-acrylamide (0.8%)	534 µl
0.5 M Tris-HCl, pH 6.8	1 ml
10% SDS	40 µl
10% ammonium persulfate	40 µl
TEMED	8 µl

Samples were boiled at 95°C for 5 minutes, in 1x Laemmli Buffer (6,25 mM Tris-HCl pH 6,8, 1% glycerol, 2% SDS, 2% β-mercaptoethanol and 0,0012% bromophenol blue). The electrophoretic chamber was filled with Running Buffer 1x (prepared from a 5x mother: 0.5% Tris-base, 7.2% glycine, 0.5% SDS) and the run was performed at 150 V. As protein molecular weight marker we used 5 µl of Dual Colour Standard (Bio-Rad).

After SDS-PAGE, the separated proteins were transferred from gel to PVDF membrane by Western Blotting or were stained on the gel with Coomassie Brilliant Blue.

3.9 WESTERN BLOTTING

After SDS-PAGE, the separated proteins were transferred from gel to PVDF membrane (Amersham) by Western Blotting. The transfer was performed in Blotting Buffer (1.44%, 0.303% TrisHCl, 20% methanol) at 100 V for 1 hour.

After blotting, the membrane was incubated with T-PBS (0.1% Tween in PBS) containing 5% BSA (5%BSA-T-PBS) for 3-4 hours, on a rocking plate. After BSA has blocked the non-specific binding sites, the membrane was incubated with the primary antibody, overnight on a rocking plate at 4°C. Primary antibodies used in this work was: anti-hERG1 C54 1:1000 in 5%BSA-T-PBS; anti-β1A integrin RM12 1:1000 in 5%BSA-T-PBS; anti-β1D integrin RM26 1:1000 in 5%BSA-T-PBS; anti-FAK 1:500 in 5%BSA-T-PBS, anti-phospoTyr396-FAK 1:500 in 5%BSA-T-PBS. The day after, the membrane was washed with T-PBS three times for 15, 10, 10 minutes respectively, on a rocking plate. After the washing steps the membrane was incubated with the secondary antibody (anti-rabbit-HRP (Sigma) 1:10000 in 5%BSA-T-PBS or anti-mouse-HRP (Sigma)

1:5000) for 45 minutes at room temperature, on a rocking plate. After secondary antibody incubation the membrane was washed as previously described. Secondary antibody was revealed in the dark room using ECL (Amersham), according to manufacturers instruction.

4. ANTIBODY ENGINEERING

4.1 TOTAL RNA EXTRACTION

Frozen cell pellets of hybridomas producing anti-β1 integrin monoclonal antibodies (TS2/16 mAb or BV7 mAb) were kindly provided by prof. P. Defilippi, University of Turin. Total RNA was extracted from frozen cell pellets ($2x10^7$ cells) with TRIzol® Reagent (Ambion) according to manufacturer's instructions.
RNA concentration was determined by measuring OD260 and applying the Beer-Lambert Law. $A=\varepsilon cl$
Where extinction coefficient (ε) for single stranded RNA is 0,025 $(\mu g/ml)^{-1}$ cm^{-1} and the optical path (l) of the cuvette is 1 cm.
RNA purity was assessed measuring the ratio of absorption at 260 vs 280 nm, pure RNA $A_{260/280}$ is ≃2.

4.2 RNA REVERSE TRANSCRIPTION

TS2/16 or BV7 RNA was reverse transcribed into cDNA using oligo$(dT)_{12-18}$ primers (Invitrogen) and SuperScript® II Reverse Transcriptase (Invitrogen) according to manufacturer's instructions in a total volume of 40 µl.

Component	Stock concentration	Final concentration	Amount
RNA	---	100 ng/µl	4 µg
Oligo$(dT)_{12-18}$	500 µg/ml	25 µg/ml	2 µl
dNTPmix	10 mM each	0.5 mM	2 µl
PCR grade H_2O	---	---	18 µl

The mix was incubated in the thermocycler at 65°C for 5 minutes, and then quickly chilled on ice and added with the following components.

Component	Stock concentration	Final concentration	Amount
5x First Strand Buffer	5x	1x	8 µl
PCR grade H_2O	---	---	6 µl

The mix was then heated at 42°C for 2 minutes and then added with the enzyme.

Component	Stock concentration	Final concentration	Amount
SuperScript™ II RT	200 U/µl	5 U/µl	2 µl

The mix (40 µl) was then incubated at 42°C for 50 minutes and then the reaction was inactivated at 70°C for 15 minutes.

4.3 ISOLATION OF VARIABLE DOMAINS BY Polymerase Chain Reaction (PCR)

To isolate antibody variable domains (VL and VH) we performed a PCR with the primers reported in Wang et al. (2000) with modifications (Table 2).

Kappa light chain	Primer name	Sequence
Forward primer	degKappadir	GAYATTGTGMTSACMCARWCTMCA
Reverse primer	Kapparev	GGATACAGTTGGTGCAGCATC
IgG1 heavy chain	Primer name	Sequence
Forward primer	degH1dir	CAGGTTACTCTGAAAGWGTSTG
Forward primer	degH2dir	GAGGTCCARCTGCAACARTC
Forward primer	degH3dir	CAGGTCCAAACTUCAGCARCC
Forward primer	degH4dir	GAGGTGAASSTGGTGGAATC
Forward primer	degH5dir	GATGTGAACTTGGAAGTGTC
Reverse primer	IgG1rev	GGAAGATCTATAGACAGATGGGGGT GTCGTTTTGGC

Table 2. Primers used for the isolation of VL and VH variable domains, form Wang et al., (2000) with modifications.

There are two classes of light chain: kappa and lambda; but since the 95% of mouse antibodies have kappa light chain (Honjo and Alt, 1995) we chose primers specific for kappa light chain ignoring the lambda type. Forward primers

were degenerated, designed using protein sequence alignment of Framework1 (FRW1) of each chain variable region. Reverse primers were designed on the constant region (CH1) next to the end of the variable domain of each chain (Kappa light chain or IgG1 heavy chain). For kappa light chain we used only one primer pair, while for heavy chain we used 5 primer pairs composed by IgG1rev in combination with the 5 forward primers.
For VH isolation of both TS2/16 and BV7 we chose IgG1rev-degH4dir primer pair.
In order to prevent mutation due to DNA Polymerase, we used a high fidelity DNA polymerase with proof reading activity: KOD Hot Start DNA Polymerase (Novagen) using the following protocol.

Component	Stock concentration	Final concentration	Amount
10x Buffer	10x	1x	5 µl
$MgSO_4$	25 mM	1.5 mM	3 µl
dNTPs	2 mM each	0.2 mM each	5 µl
Forward primer	10 µM	0.3 µl	1.5 µl
Reverse primer	10 µM	0.3 µl	1.5 µl
DNA	---	---	10 ng
KOD Hot Start DNA Polymerase 1U/µl		0.02 U/µl	1 µl
PCR grade H_2O	---	---	to 50 µl

The mix was incubated in the thermocycler with following protocol

Step	Temperature	Time
1	95°C	2 min
2	95°C	20 sec
3	54°C (VH) or 46°C (VL)	10 sec
4	70°C	10 sec
5	70°C	5 min

Steps 2-4 were repeated 30 times

4.4 CLONING OF VARIABLE DOMAINS WITHOUT THE USE OF RESTRICTION ENZYMES

In order to sequence VH and VL variable domains we cloned them without the use of restriction enzymes in a vector suitable for DNA sequencing. We used

TA-Cloning Kit or Zero-Blunt Cloning kit (Invitrogen) following manufacturer's instructions.

4.5 DNA ELECTROPHORESIS AND PURIFICATION FROM AGAROSE GEL

DNA electrophoresis uses an electrical field to move the negatively charged DNA toward a positive electrode through an agarose gel matrix. PCR products and restriction enzyme digested DNA were run on agarose gel (1.5 % agarose in TAE (Tris, Acetic acid, EDTA) buffer) stained with ethidium bromide, alongside 2log DNA ladder (NEB) in order to separate different size fragments. Electrophoresis was run at 100 V. The band of interest was thus excised from gel with a clean scalpel and purified using QIAquick PCR Purification Kit (QIAGEN) following manufacturer's instructions. Purified DNA was eluted with 30 µl PCR grade H_2O.

4.6 Splicing by Overlap Extension PCR (SOE-PCR)

ScFv construct was assembled by Splicing by Overlap Extension PCR (SOE-PCR) in the order VL-linker-VH, using the primers described in (Wang et al 2000) with modifications (Table 3). The polypeptide linker joining the variable domains was designed as four GGGGS repeats.

Name	Sequence
VLFORSFI	CACGCGGCCCAGCCGGCCATGGCCGATATTGTGATGACACAGACTCCA
VLREVSOE	**GGAGCCGCCGCCGCC**AGAACCACCACCACCAGAACCACCACCACCGGATACAGTTGGTGCAGCATC
VHFORSOE	**GGCGGCGGCGGCTCC**GGTGGTGGTGGATCCGAGGTGAAGGTGGTGGAATC
VHREVNOT	ATAAGAATGCGGCCGCATAGACAGATGGGGGTGTCGTTTTGGC
VLFORXHO	CACGCCTCGAGTGATATTGTGATGACACAGACTCCA
VHREVAPALI	ACGCGTGCACTATAGACAGATGGGGGTGTCGTTTTGGC

Table 3. Primer designed to assemble the construct VL-linker-VH by SOE-PCR (VLREVSOE and VHFORSOE) and clone the sequence into pHenIX vector (VLFORSFI and VHREVNOT), or into scFv-hERG-pHenIX vector (VLFORXHO and VHREVAPALI). In red are the portions of the primers that anneal to the template, in green are the sequences added to clone the construct in frame with the expression cassette in pHenIX or in scFv-hERG1-pHenIX vector, underlined are the restriction sites, purple are the sequences added to facilitate enzyme digestion, and bold are the sequenced that overlap in SOE-PCR.

The protocol consists in two steps described in Figure 1. The first step allows to add: at the 3' end of VL, a sequence that encode the first three GGGGS repeats of the linker, and at the 5' end of VH. a sequence that encode the last two GGGGS repeats of the linker. During this step will be also attached at the 5' end of VL and at the 3' end of VH the restriction sites that will be used for the cloning of VL-linker-VH construct in the expression vector. The second step allows to join the two PCR products thanks to the overlapping sequences (15 bp) at the 3' end of VL and at the 5' end of VH.

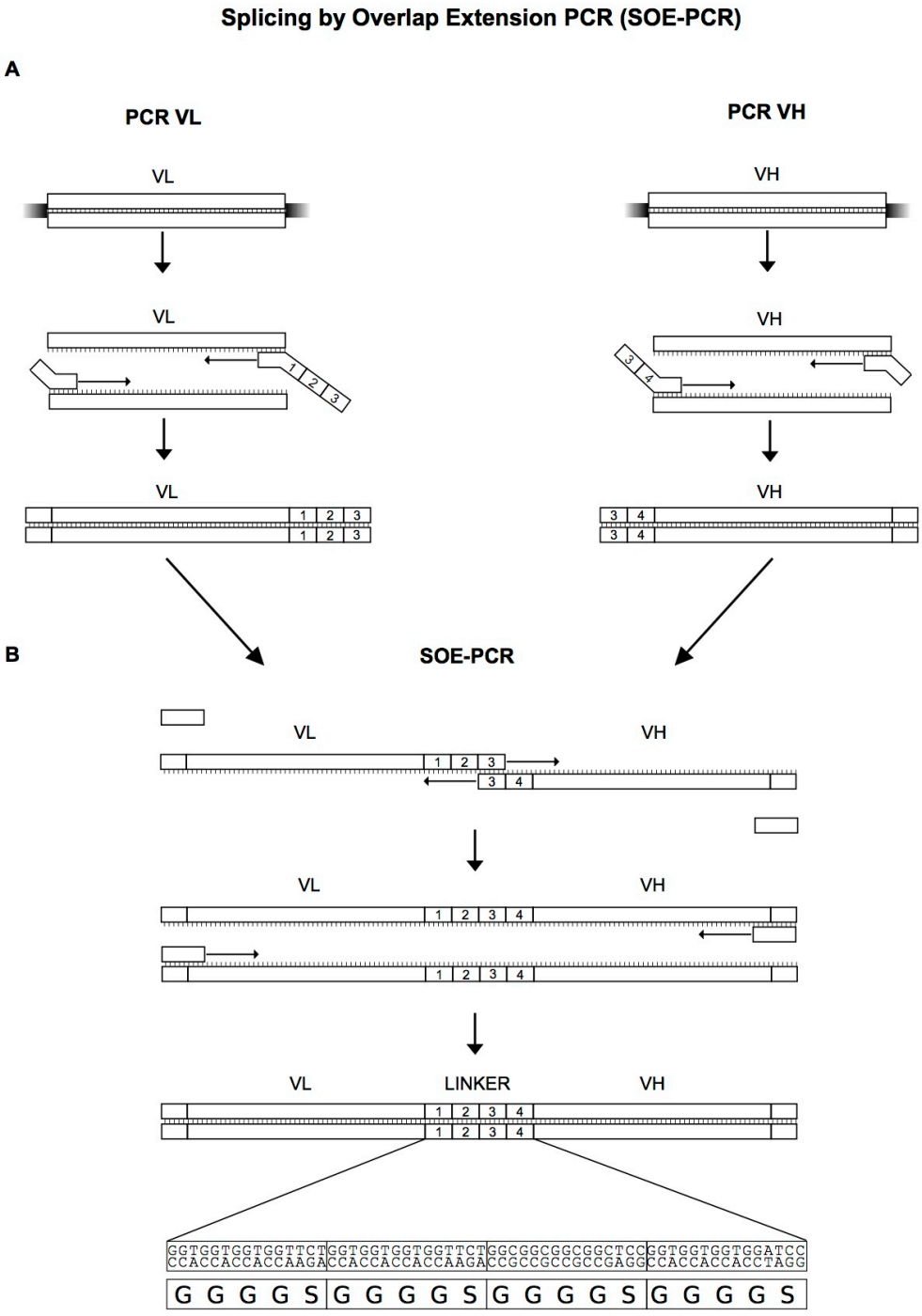

Figure 1. Scheme representing SOE-PCR method for scFv assembly in the order VL-linker-VH

In the first step we performed two parallel PCR: one with VLFORSFI-VLREVSOE primer pair and pCRII-VL template; and the other with VHFORSOE-VHREVNOT primer pair and pCRII-VH template. PCR protocol using KOD DNA Polymerase was performed as previously described.

In the second step, we settled up the SOE-PCR using as template 1 µl of each PCR reaction performed in the first step, and VLFORSFI-VHREVNOT primer pair, following the protocol below.

Component	Stock concentration	Final concentration	Amount
10x Buffer	10x	1x	5 µl
$MgSO_4$	25 mM	1.5 mM	3 µl
dNTPs	2 mM each	0.2 mM each	5 µl
VLFORSFI primer	10 µM	0.3 µl	1.5 µl
VHREVNOT primer	10 µM	0.3 µl	1.5 µl
PCR VL (STEP 1)	---	---	1 µl
PCR VH (STEP 1)	---	---	1 µl
KOD Hot Start DNA Polymerase 1U/µl		0.02 U/µl	1 µl
PCR grade H_2O	---	---	to 50 µl

The mix (50 µl) was incubated in the thermocycler according to the protocol below.

Step	Temperature	Time
1	95°C	2 min
2	95°C	20 sec
3	70°C	10 sec
4	70°C	10 sec
5	70°C	5 min

Steps 2-4 were repeated 30 times

4.7 PREPARATION OF ELECTROCOMPETENT E.Coli CELLS

To obtain electrocompetent E. Coli cells we inoculated a single colony of the desired E. Coli strain in 50 ml of Luria Broth (LB) medium (Invitrogen) overnight at 37°C on shaking. The following day we inoculated the bacterial suspension 1:10 in 1 l of LB medium and we grown the culture at 37°C on shaking till its optical density at 600 nm (OD_{600}) reached 0.8-1. The flasks were then incubated on ice for 30 minutes and then the bacterial suspension was centrifuged at 8000 g for 20 minutes at 4°C. Bacterial pellet was resuspended in 500 ml of ice cold sterile water and centrifuged as above. This step was repeated a first time resuspending the pellet with 250 ml and the second time

with 20 ml. Finally bacteria pellet was resuspended in 20 ml 10% sterile glycerol and transferred in 1.5 ml sterile tubes (50-100 µl/tube), frozen in N_2 liquid and harvested at -80°C.

4.8 TRANSFORMATION OF ELECTROCOMPETENT E. Coli CELLS

Electrocompetent E. Coli cells used in this work were transformed with plasmid DNA by electroporation. In this method we used 50 µl of electrocompetent E. Coli cells thawed on ice and transferred into a pre-chilled electroporation cuvette together with plasmid DNA (2-4 µl of ligation product or 10 ng of purified plasmid DNA). The cuvette was incubated 1 minute on ice and then placed into the Electroporator 2510 (Eppendorf) giving a 2500mV pulse. The cuvette was immediately placed on ice and the cells were recovered with 450 µl of SOC medium (SOB medium supplemented with 1 mM $MgSO_4$, 1 mM $MgCl_2$) and incubated for 1 hour at 37°C on shaking. Bacteria suspension was then plated on LB agar plates supplemented with the opportune antibiotic (ampicillin 50 µg/ml, kanamicin 25 µg/ml) and incubated lid-side down overnight at 37°C.

4.9 ANTI-hERG1 mAb LARGE SCALE PRODUCTION AND PURIFICATION

For large scale production of anti-hERG1 mAb, hybridoma clone A7 (patent # FI2006A000008) was cultivated in CELLine bioreactor CL1000 (INTEGRA Biosciences) as previously described. Hybridomas supernatant was harvested every 2 weeks, sub-culturing the cells 1:5. The harvested supernatant was dialysed against 20 mM sodium phosphate overnight at 4°C and then purified using HiTrap Protein A HP (GE Healthcare) following manufacturer's instructions. Purified antibody was then dialysed against PBS overnight at 4°C and harvested at -80°C. Antibody concentration was calculated as previously described.

RESULTS AND DISCUSSION

1. DEVELOPMENT AND CHARACTERISATION OF MONOCLONA ANTIBODIES AGAINST GLYCOLIPID ANTIGENS

Glycosphingolipids (GSL), play an important role in many pathways of cellular physiology, involved in cell adhesion and cell signalling, thanks to their ability to form, on the cell surface, clusters termed “glycosynapses” where they interact with functional molecules (Hakomori 2002). Many GSL was found over-expressed or altered in tumours compared to normal tissue (Durrant et al. 2012) The alteration of glycan structures on glycolipids suggests that they may be good targets for vaccines or mAbs based cancer immunotherapy.

Monosialoganglioside GM3 is the simplest ganglioside, it contains a trisaccharide head group composed of glucose, galactose and sialic acid bound to ceramide.

It is involved in adhesion and cell-signalling as ligand and as modulator of receptors activity. It has different roles depending on its co-expression with different receptors: it is able to inhibit the dimerisation of EGFR preventing cell proliferation but on the other hand it enhances uPAR signalling promoting proliferation. It is known that over-expression of GM3 in neuroectodermal tumour, including melanoma, is correlated with an invasive and metastatic phenotype. When GM3 overcome a threshold density level on plasma membrane it may assume a lactone or lactone-like conformation (Nores et al. 1987).

So lactone-like form of GM3 could be a target for suppressing tumour metastasis. A mimetic molecule of the lactone form of GM3 (mimGM3) (Figure 1) was produced in prof. Nativi’s laboratory (Department of Chemistry, University of Florence) and this molecule turned out to be more stable than GM3-lactone under physiological conditions (Arcangeli et al. 2010).

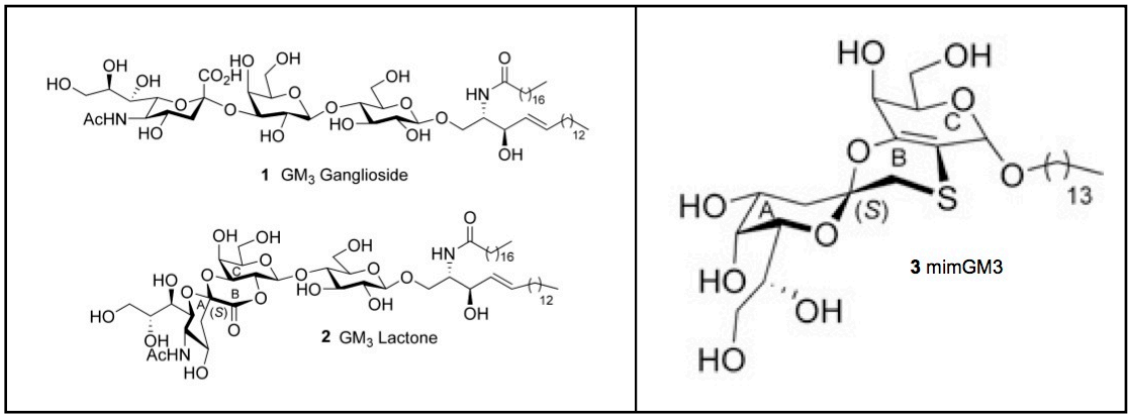

Figure 1: Chemical structure of GM3 (1), GM3-lactone (2) and the synthetic GM3-lactone mimetic molecule mimGM3 (3).

For these reasons we decided to produce a monoclonal antibody able to bind the lactone like form of GM3 using mimGM3 for mice immunisation, with the aim of inducing a strong immune response despite the lipid nature of the antigen.

1.1. GM3 AND GM3 LACTONE EXPRESSION IN CANCER CELL LINES

In order to find an appropriate cell line model within to test the biological effects of our antibodies, we evaluated the gangliosidic profile of different cancer cell lines. B16F1 murine melanoma cell line, MCF-7 and MDA-MB-231 breast cancer cell lines, and MIA PaCa-2 BxPC-3 and PANC-1 pancreatic ductal adenocarcinoma (PDAC) cell lines were amplified, scraped in cold PBS and pelleted. Lipid extract was performed and separated in neutral and acid glycolipid fractions as described in Materials and Methods. Gangliosides, contained in the acid glycolipid fraction was separated by Thin Layer Chromatography (TLC) and resolved with resorcinol reagent (Figure 2). Purified GM3 (lane 5), lactonised GM3 (lane 4 and 9) and Cronassial (a mix of GM1, GD1a, GD1b, GT1b) (lane 10) were used as standards.

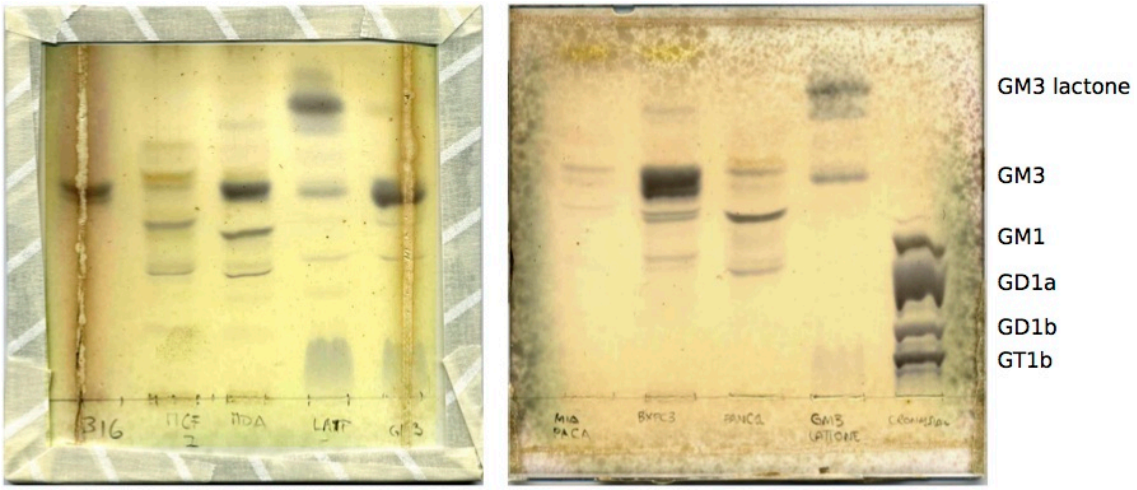

Figure 2. Picture of TLC plates of cell lines ganglioside extract resolved with resorcinol reagent. murine melanoma B16F1(lane 1), breast cancer MCF-7 (lane 2) and MDA-MB-231 (lane 3), PDAC MiaPaCa-2 (lane 6), BxPC-3 (lane 7) and PANC-1 (lane8). As standards were used: purified GM3 (lane 5), lactonised GM3 (lane 4 and 9) and Cronassial (a mix of GM1, GD1a, GD1b, GT1b) (lane 10).

As shown in Figure 2, B16F1 cell line has exclusively GM3, this result is consistent data reported in literature (Calorini et al. 1987), this cell line can thus be used as a cellular model expressing GM3.

As regard breast cancer cell lines, their gangliosides expression results quite similar for complex gangliosides, while it results different for GM3 expression. Densitometric analysis of GM3 relative bands in TLC plate, shows GM3 relative content in MCF-7 and MDA-MB-231; values were normalised versus cells number, and reported in the histogram as fold changes relative to MCF-7 cells (Figure 3).

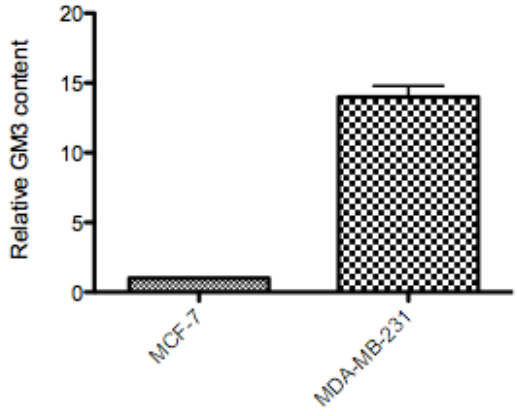

Figure 3. Histogram representing densitometric analysis of GM3 band in MCF-7 and MDA-MB-231 cell lines lipid extract (Figure 10). Values were calculated using ImageJ software and normalised versus cells number. Data are reported as fold change relative to GM3 expression in MCF-7.

These data show that in MDA-MB-231 cells, GM3 expression is approximately 14-fold more than in MCF-7, according to literature (Nohara et al. 1998).

From densitometric analysis of GM3 relative bands on TLC plate we found that GM3 expression is variable among PDAC cell lines. In the picture below, are shown GM3 expression values normalised versus cells number, and reported in the histogram as fold changes relative to MIA PaCa-2 cells.

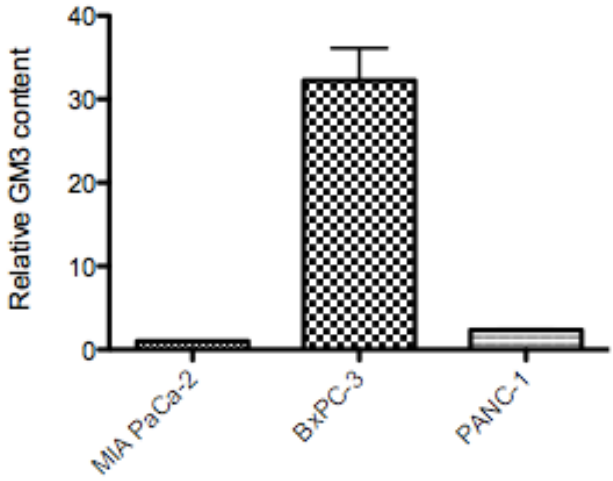

Figure 4. Histogram representing densitometric analysis of GM3 band in MIA PaCa-2, BxPC-2 and PANC-1 cell lines lipid extract (Figure 10). Values were calculated using ImageJ software and normalised versus cells number. Data are reported as fold change relative to GM3 expression in MIA PaCa-2.

From the results reported in Figure 4, we can extrapolate that in BxPC-3 GM3 expression is approximately 30-fold more than in MIA-PaCa-2 and 15-fold more than in PANC-1.

These data give an overview of GM3 expression in different cancer cell lines, using these results we can thus classify these cell lines for GM3 expression:

- high levels of GM3: B16F1, MDA-MB-231, BxPC-3
- low levels of GM3: MCF-7, MIA-PaCa-2, PANC-1

Our aim was to find a cellular model expressing GM3 lactone within to test our monoclonal antibody.

To evaluate GM3 lactone content in the analysed cell lines on TLC plate, we needed a GM3 lactone standard. We thus performed GM3 lactonisation, as

described in Materials and Methods. As expected from literature (Zhu et al. 1999), in the lactonised sample (lane 4 and 9, Figure 2) are present mainly two bands: a thin band relative to normal GM3, and bigger and faster moving band representing GM3 lactone. We can detect also another thin band located below the GM3 lactone band, maybe representing a different form of lactone (Yu et al. 1985).

As we can see in Figure 2, only in the lanes relative to the samples which express high level of GM3, is present a GM3 lactone comigrating band. This result is in agreement with the data found in literature. As reported in Nores et al. (1987), when GM3 is high expressed on the surface of plasma membrane of cancer cells, may assume a lactone or lactone like form. This conformational change occurs when GM3 expression, on plasma membrane, overcome a threshold density level and is favoured by the acid pH of tumour microenvironment.

From these data we can conclude that, the cell lines characterised by high GM3 expression level, express also GM3 lactone and can be used for in vitro assays with our monoclonal antibody.

1.2. MONOCLONAL ANTIBODIES DEVELOPMENT USING mimGM3

Hybridomas were produced according to Köhler and Milstein (1975) standard method as described in Materials and Methods. In brief, we performed two parallel immunisation protocols of Balb/c mice, using the stable mimetic of GM3 lactone, mimGM3, conjugated to two different carriers $Pam_3CysSer$ and Ovalbumin. For each immunised mouse, splenic cells were fused with NS0 myeloma cells. Each cell fusion product was resuspended and diluted (1:2, 1:4, 1:8 and 1:8) in complete culture medium added with the selective agent HAT. Dilutions were aliquoted each in a 24-well multiwell plate and left in the cell incubator for about two weeks. Two weeks after cell fusion, HAT selected hybridomas proliferated forming of visible colonies (Figure 5).

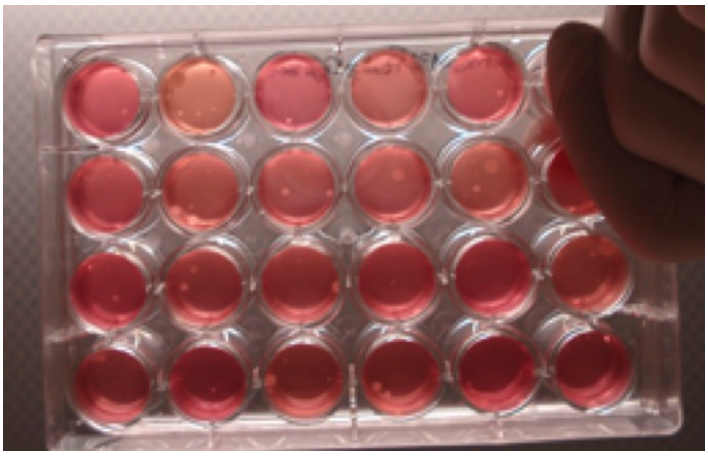

Figure 5: Picture of a 24-multiwell plate after 2 weeks from cell fusion, HAT selected hybridomas colonies are visible to the naked eye.

We tested hybridomas supernatants for the presence of antibodies able to bind GM3 by indirect enzyme-linked immunosorbent assay (ELISA) according to Arcangeli et al. (2010). Samples with an Optical Density at 450 nm (OD_{450}) greater than 0.1 were considered positive. In Figure 6 are shown ELISA results for each 24-multiwell plate analysed, in red are the positive wells.

mimGM3-Ovalbumin 1:2

	1	2	3	4	5	6
A	0.005	0	0.005	-0.044	-0.056	-0.01
B	-0.026	-0.027	-0.028	-0.024	-0.051	-0.042
C	-0.04	-0.015	-0.011	-0.054	-0.033	-0.038
D	-0.007	-0.027	-0.031	-0.014	-0.013	-0.032

mimGM3-Ovalbumin 1:4

	1	2	3	4	5	6
A	0.008	0.79	-0.029	-0.031	0	-0.035
B	-0.019	0	0.038	-0.014	0.773	0.42
C	-0.018	-0.034	-0.033	0.005	-0.015	0.024
D	-0.007	0.035	-0.029	0	0.015	0

mimGM3-Ovalbumin 1:8 A

	1	2	3	4	5	6
A	0.003	0.029	0.002	0	-0.036	0
B	-0.006	-0.015	-0.011	0.011	0	0.023
C	0	0.026	0	0	0.043	-0.013
D	0	0	-0.011	0	0.344	-0.022

mimGM3-Ovalbumin 1:8 B

	1	2	3	4	5	6
A	0	-0.012	0	0.03	-0.049	0
B	0	-0.03	0.029	0.008	0.024	0.016
C	0	0.003	0.028	0	0.027	-0.003
D	0	0.017	-0.006	0.025	0	0

mimGM3-Pam$_3$CysSer 1:2

	1	2	3	4	5	6
A	0.007	0.043	0.024	0.018	0.013	0.035
B	0.024	0.04	0.018	OUT	0.026	0.013
C	-0.03	0.011	0.057	0.067	0.078	0.049
D	0.077	0.181	0.074	0.054	0.032	0.086

mimGM3-Pam$_3$CysSer 1:4

	1	2	3	4	5	6
A	0.032	0.027	0.064	0.124	0.212	0.017
B	0.043	0.036	0.05	0.268	0.018	-0.006
C	-0.036	-0.007	0.052	0.097	0.132	0.065
D	0.092	0.469	0.158	0.028	-0.021	-0.013

mimGM3-Pam$_3$CysSer 1:8 A

	1	2	3	4	5	6
A	0.686	-0.044	-0.024	0.067	0.122	0.113
B	0.419	0.648	0.46	0.057	0.208	0.001
C	0.014	0.605	0.08	0.013	-0.003	-0.008
D	0	0.587	-0.014	-0.022	0.076	0

mimGM3-Pam$_3$CysSer 1:8 B

	1	2	3	4	5	6
A	0.05	0.038	0.014	-0.002	0.069	0.037
B	0.061	0.034	-0.008	-0.001	-0.002	0.021
C	0.023	0	0.048	-0.012	-0.004	0.005
D	0.045	-0.003	-0.025	-0.024	0.613	-0.005

Figure 6. Scheme representing indirect ELISA results obtained analysing 24-multiwell plate supernatants after 2 weeks from cell fusion, in red are the results considered positive (OD 450 nm > 0.1).

As shown in Figure 6, we obtained 4 positive supernatants from mimGM3-Ovalbumin immunisation and 18 from mimGM3-Pam$_3$CysSer immunisation.

From the positive wells, we isolated the colonies picking them up and transferring each one into a new well of a 24-multiwell plate. These hybridoma populations were then amplified and tested again by indirect ELISA against

GM3 in order to select the most suitable population for soft agar cloning (Figure 7).

	1	2	3	4	5	6
A	PCS B4 1:2	PCS B4 1:2	PCS B4 1:2	PCS B4 1:2	PCS B4 1:2	PCS B4 1:2
B	PCS B4 1:2	PCS B4 1:2	PCS B4 1:2	PCS B4 1:2	PCS B4 1:2	OVA B5 1:4
C	OVA B5 1:4	PCS D2 1:4	PCS D2 1:4	PCS D2 1:4	PCS D2 1:4	PCS D2 1:4
D	PCS D2 1:4	PCS D2 1:4	PCS B4 1:4	PCS B4 1:4	PCS B4 1:4	PCS B4 1:4

	1	2	3	4	5	6
A	0	0	0.1	0	0	0
B	0.016	0	0	0	0	OUT
C	0	0	0.025	0	1.672	0
D	0	0	0.371	0	2.408	0.035

Figure 7. Scheme representing indirect ELISA results obtained analysing supernatants from the 24-multiwell plate where we transferred the colonies picked up from positive wells shown in Figure 3, in red are the results considered positive (OD 450 nm > 1); data relative to other plates are not shown.

Since the samples were supernatants of confluent hybridoma cell cultures, we expected an antibody concentration higher then that of the cell fusion culture supernatants analysed the first time. For this reason, only samples with an OD_{450} greater than 1 were considered positive.

Thus we chose three populations for soft agar cloning: one for mimGM3-Ovalbumin (OVA B5 1:4 B6) and two from mimGM3-Pam_3CysSer immunisation (PCS D2 1:4 C5 and PCS B4 1:4 D5).

We tested the isotype of the three chosen hybridoma populations according to manufacturers instructions and we found that they were all IgM (Figure 8). This was an expected result, because the antigen used for mice immunisation was a non-proteic molecule. The synthetic molecule used to mimic the structure of GM3 lactone (mimGM3) is not a protein and, even if is more stable in blood stream than natural GM3-lactone (Arcangeli et al 2010), is not able to promote isotype switching from IgM to IgG. The carriers used to enhance immune system response were Ovalbumin (OVA), and Pam_3CysSer (a synthetic lipopeptide composed by three palmitic acids, one cystein and one serine amino acids). It is known that ovalbumin is not good as Keyhole Limpet Hemocyanin (KLH) in promoting immune response. While less data are

available regarding $Pam_3CysSer$ properties, lipopeptides are similar to the N terminus of bacteria lipoproteins, a characteristic that makes them strongly immunogenic (Hofmann et al. 1996). An evident difference of $Pam_3CysSer$ from other common carriers (such as OVA and KLH) is that one molecule of $Pam_3CysSer$ can be conjugated to only one antigen, a feature not so good for a carrier protein.

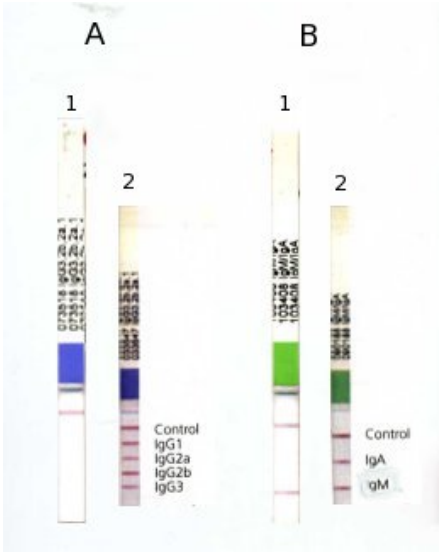

Figure 8. The strips used for isotype test show, with a red lane, the presence of (A.2) IgG1, IgG2a, IgG2b, IgG3 or (B.2) IgM and IgA. The three samples we analysed gave the same results: (A.1) no red lane, (B.1) a red lane corresponding to IgM isotype.

For monoclonal antibody production, clonal isolation of hybridomas was achieved after two subsequent cloning processes: manual colony picking, described above, and soft agar cloning.

Soft agar cloning was performed as described in Materials and Methods. After about 15 days from cell seeding, on the plates appeared visible colonies. Each clone was picked up, seeded in a 24-well multiwell plate, amplified and tested for its ability so secrete antibody which bind GM3 by indirect ELISA (Figure 9).

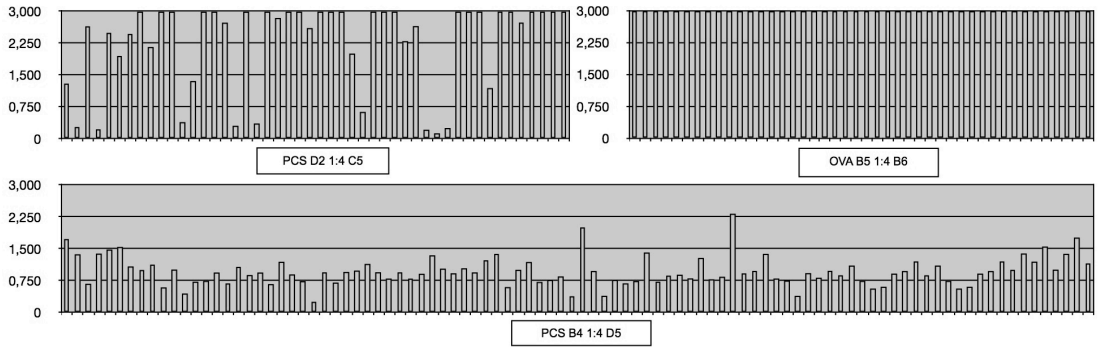

Figure 9: Histograms representing indirect ELISA results obtained analysing supernatants from the 24-multiwell plate where we transferred the clones obtained from soft agar cloning.

Indirect ELISA results, graphed in Figure 6, show that all OVA B5 1:4 C6 clones and many PCS D2 1:4 C5 clones have OD_{450} > 1.5, suggesting us that they are able to secrete antibody which bind GM3; while only a few PCS B4 1:4 B6 clones give positive results.

Positive clones were amplified and adapted to grow in an aminopterine free medium. Aminopterine remains inside the cells even if HAT is removed from culture medium, continuing to exploit its inhibitory effect on the novo synthesis of nucleotide bases. For this reason aminopterine was diluted from the culture by several passages of the cells in hypoxanthine-thymidine (HT) supplemented medium (approximately 2-3 weeks) before transferring into ordinary hybridoma growth medium DMEM High Glucose added with 4 mM L-Glutamine and 10% FBS FetalClone I (Hyclone).

We used indirect ELISA to find the best hybridoma clone able to bind GM3. We chose OVA C2 clone, which was thus amplified and cultivated in a bioreactor (CELLine, Integra Biosciences) for large scale mAb production. Bioreactor hybridomas supernatant was harvested every two weeks and purified using HiTrap IgM Purification HP (GE) as described in Materials and Methods (Figure 10).

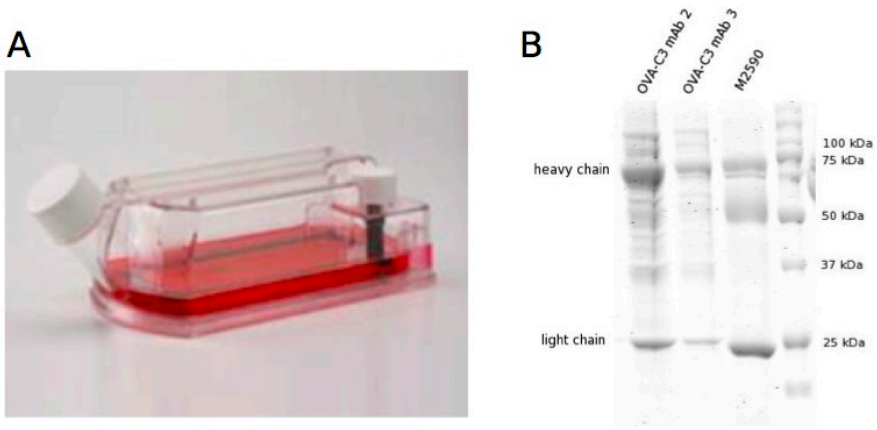

Figure 10. (A) Hybridoma bioreactor (CELLine) for large scale production of monoclonal antibodies; (B) Coomassie staining of protein gel electrophoresis, lane 1: purified OVA-C3 mAb second aliquot collected; lane 2: purified OVA-C2 mAb third aliquot collected; lane 3: anti-GM3 mAb M2590 (IgM).

1.3. EVALUATION OF ANTIBODY CROSS- REACTIVITY

In order to identify the clone capable of producing antibodies with the highest affinity for GM3, it was necessary to find the appropriate blocking solution for ELISA. Hybridomas supernatant was tested by ELISA, against three different blocking solution: PBS-BSA 10%, PBS-Skim Milk 5% and FBS FetalClone I (Figure 11).

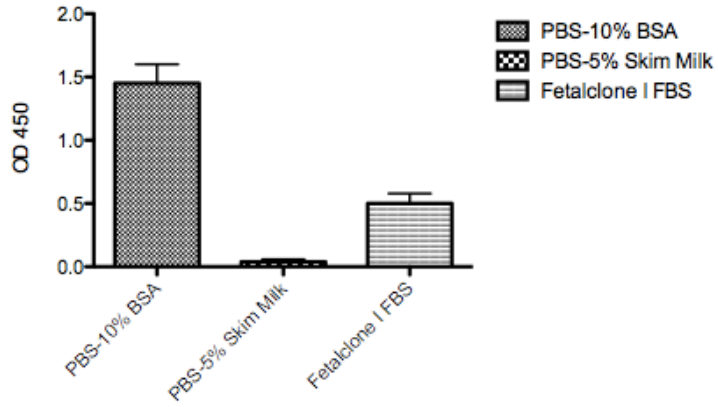

Figure 11: Histogram representing the results of an indirect ELISA obtained analysing hybridomas supernatant affinity for different kind of blocking solution (PBS-1'%BSA, PBS-5%Skim Milk, Fetalclone I FBS).

As shown in the picture above, hybridomas supernatant has a very high affinity for BSA and a lower one for FetalClone I, while it has not affinity for 5% Skim Milk-PBS, we obtained the same results both for OVA and PCS hybridomas. Hereafter, the affinity for GM3 of hybridomas supernatant was evaluated using Skim Milk as blocking solution, as described in Materials and Methods.

The strong affinity of our antibodies for BSA and FBS suggested us that they could cross-react with other molecules, such as different glycolipids. To verify this hypothesis we performed a Dot Blot assay using pre-casted strips with spotted glycolipids: sulfatides, GQ1b, GT1b, GT1a, GD3, GD1b, GD1a, GM3, GM2, GM1 (Zentech) as described in Materials and Methods.

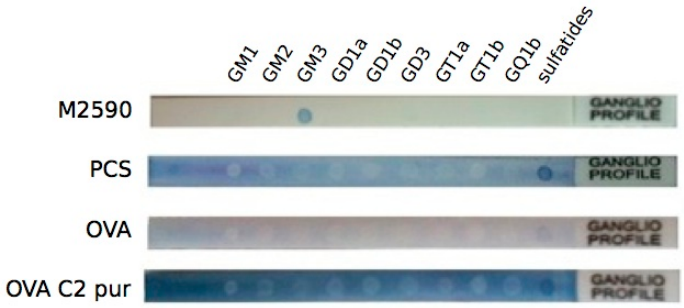

Figure 12. Pre casted Dot Blot assay strips using M2590, PCS antibody, OVA antibody and purified OVA-C2 mAb. Antibody binding is revealed as a blue spot.

The picture in Figure 12 show that the strip stained with M2590 has a dark blue spot corresponding to GM3, confirming that this commercial mAb selectively binds GM3. The others strips, stained with PCS, OVA and purified OVA C2 antibodies respectively, have not the blue spot corresponding to GM3, but they present a dark blue spot corresponding to sulfatides.

These results suggested that our antibodies cross-react with sulfatides.

The term sulfatides is usually used to address galactosyl-ceramide sulfate (SM4), but other times can refer to other sulfated glycolipids (such as lactosylceramide sulfate, SM3). The spot corresponding to sulfatides in the pre-casted strips used for dot-blot is composed by SM4 sulfatide extracted from bovine brain (Sigma).

To confirm these data we performed an indirect ELISA against equal amounts of GM3 and sulfatides (SM4) (Figure 13).

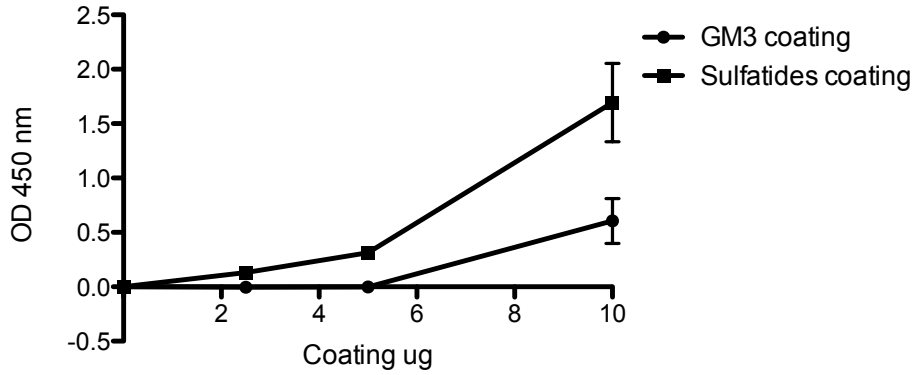

Figure 13. Results of indirect ELISA showing OVA C2 mAb affinity to GM3 or sulfatides.

The results shown in Figure 13 clearly indicate that, according to dot blot results, OVA C2 mAb binds better sulfatides than GM3.

Similar anti-ganglioside antibodies cross-reactions were found in literature. Townson et al., (2007) reported a study where both mouse and human antiganglioside antibodies resulted able to bind sulfatide, despite of their specificity for the glycan epitopes on the gangliosides against which they were raised and cloned. Another study (Boffey et al. 2004) show that some antiganglioside antibodies are polyreactive, cross-reacting with actin, thyroglobulin, tubulin or DNA.

The molecule used for mice immunisation in mAb production protocol (mimGM3) was developed, in prof. Nativi's lab, to mimic the lactone form of GM3. The results reported above demonstrate that our mAb has not a great affinity for GM3, but does not provide information about the affinity for GM3 lactone.

1.4. OVA C2 mAb AFFINITY FOR GM3 AND GM3 LACTONE

To evaluate OVA C2 affinity for GM3 lactone, we performed GM3 lactonisation (see Materials and Methods) using GM3 extracted from B16F1 cells (which are reported to express only GM3 ganglioside).

We run equal amounts of lactonised GM3 on three lanes of an aluminium TLC plate, we cut the plate separating the lanes and we stained one with resorcinol

reagent, one with OVA C2 mAb and one with M2590 mAb (Figure 14) (see Materials and Methods).

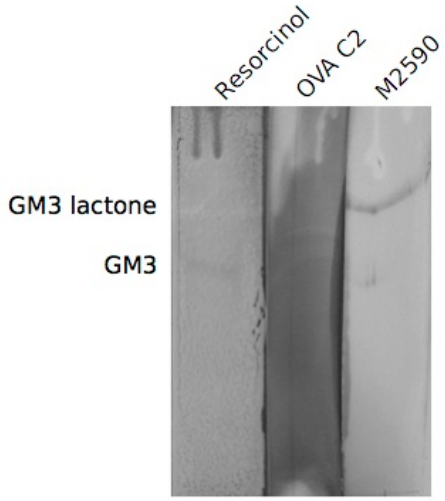

Figure 14. TLC plates of lactonised B16F1 ganglioside extract, stained respectively with resorcinol reagent, OVA C2 mAb and M2590 mAb. GM3 and GM3 lactone relative bands are indicated.

As shown in the picture above, lactonised B16F1 ganglioside extract separates in two bands on the TLC plate: a slower moving band corresponding to GM3 and a faster moving band corresponding to GM3 lactone (lane 1). As we can see in lane 2, OVA C2 mAb is not able to stain neither GM3 nor GM3 lactone; while in lane 3, M2590 mAb stains both GM3 and GM3 lactone. M2590 mAb is a commercial antibody produced immunising mice with B16 melanoma cells (Nores et al. 1987), and is reported to have stronger affinity for GM3 lactone than for GM3. Our data are thus in agreement with Nores report.

These results confirm that OVA C2 mAb has not affinity for GM3 and demonstrate that it is not able to bind GM3 lactone.

This result seems to be in contrast with ELISA results, which shown that at the highest concentration (10 μg) of GM3, OVA C2 give a positive signal (Figure 10), suggesting that it reacts with GM3. The signal we can see in ELISA assay is the OD_{450} due to the binding of the antibody to the compounds used to coat the wells, GM3 or sulfatides, and all the impurities contained in these samples. While the signal we can see in TLC staining assay is a band, due to the binding of the antibody to the compounds (GM3 or sulfatides) chromatographed on a TLC plate. TLC staining assay is thus more specific than ELISA, but it is less rapid and above all it is not suitable for the analysis of a great number of

samples at the same time. For these reason, even if it is high specific, TLC staining can not be used for antibody screening at the begin of hybridomas selection, but can only be used in a second phase to characterise a restrict number of antibodies.

1.5. GYCOLIPID SULFATE PROFILE IN CANCER CELL LINES

Since Dot Blot assay and ELISA results suggested that OVA C2 has high affinity for sulfatides, we decided to investigate the glycolipid sulfate profile of various cell lines and the ability of OVA C2 to bind sulfate containing glycolipids. In particular, we would like to investigate the presence of galactosil-ceramide sulphate (SM4 or sulfatide) in cancer cell lines.

In a first experiment, we prepared two twin TLC plates running equal amounts of B16F1 neutral glycolipid extract alongside with SM4 sulfatide standard (see Materials and Methods). We revealed one plate with Azure A reagent to visualise sulfate containing glycolipids, and we stained the other plate with OVA C2 mAb (Figure 15).

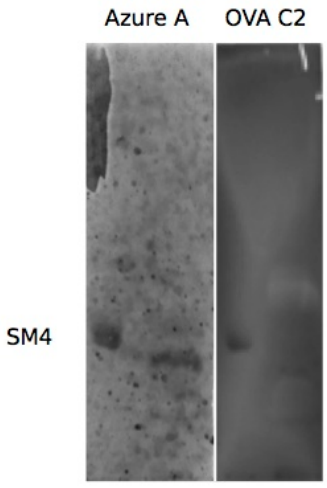

Figure 15. TLC plates of SM4 sulfatide standard (lanes 1, 3) and B16F1 neutral glycolipid extract (lanes 2, 4). Lanes 1-2 were stained with Azure A reagent, while lanes 3-4 with OVA C2 mAb. SM4 band is indicated.

Azure A staining of the TLC plate reveal in B16F1 lipid extract (lane 2) a band which run slower than SM4 standard band, maybe referring to the more complex SM3 sulfatide. OVA C2 mAb staining of TLC plate reveal a band relative to SM4 sulfatide in lane 3, while in lane 4 there are no detectable bands.

These results show that B16F1 cells do not express SM4 but a more complex sulfatide (probably SM3). Furthermore, the data demonstrate that OVA C2 mAb is able to bind SM4 sulfatide but not more complex sulfatides present in B16F1 lipid extract.

We performed an analogous experiment with PDAC cell lines. We prepared two twin TLC plates running equal amounts of MIA-PaCa-2, PANC-1 and BxPC-3 neutral glycolipid extracts alongside with SM4 sulfatide standard. We revealed one plate with Azure A reagent to visualise sulfate containing glycolipids, and we stained the other plate with OVA C2 mAb (Figure 16).

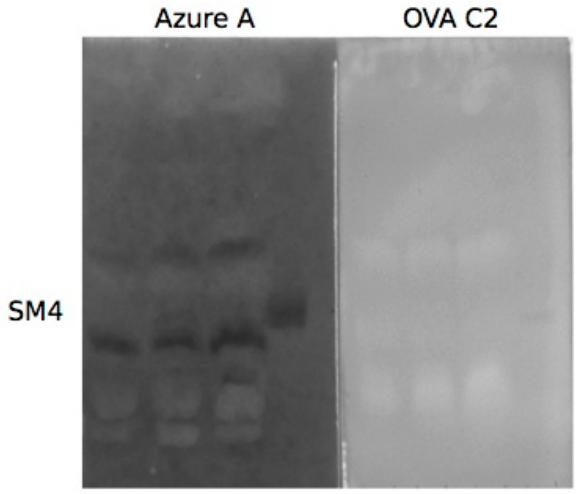

Figure 16. TLC plates of MIA-PaCa-2 (lanes 1, 5), PANC-1 (lanes 2, 6) and BxPC-3 (lanes 3, 7) neutral glycolipid extract alongside with SM4 sulfatide standard (lanes 4, 8) and. Lanes 1 to 4 were stained with Azure A reagent, while lanes 5 to 8 with OVA C2 mAb. SM4 band is indicated.

Azure A staining of the TLC plate reveal in PDAC cell lines lipid extract (lane 1 to 3) a band which run faster than SM4 standard band, maybe referring to the cholesterol sulfate, and a band which run slower than SM4, probably SM3 sulfatide. OVA C2 mAb staining of TLC plate reveal a band relative to SM4 sulfatide in lane 8, while in lane 5 to 7 there are no detectable bands.

These results show that MIA-PaCa-2, PANC-1 and BxPC-3 cells do not express SM4 but a more complex sulfatide (probably SM3) and other sulfate glycolipids (probably cholesterol sulfate). Furthermore, the data confirm that OVA C2 mAb is able to bind SM4 sulfatide but not other glycolipids sulfate present in PDAC cells lipid extracts.

SM4 (galactosil ceramide sulfate) separate in two visible bands on TLC plate and, as we can see in Figure 15 and 16, OVA C2 mAb stains mainly the slower moving band.

Niimura and Nagai (2008) used Negative ion Liquid Secondary Ion Mass Spectrometry (LSIMS) to analyse SM4s upper and lower band, extracted from canine MDCK cell lines. The analysis revealed that upper band was composed mainly from galactosil-ceramide sulfate containing non-hydroxy fatty acids (such as 24:0 or 24:1) while lower band was composed by SM4 containing hydroxy fatty acids (such as 24h:0) or the shorter chain length species (such as 16:0).

Our results, suggest that OVA C2 mAb has more affinity for hydrogenated fatty acids or short chain fatty acids (like 24h:0 and 16:0), than for non-hydroxy fatty acids.

1.6. OVA C2 mAb REACTIVITY IN IMMUNOHISTOCHEMISTRY

OVA C2 mAb was used in immunohystochemistry assay (IHC) on formalin fixed and paraffin embedded pancreatic tissue. As we can see in Figure 7, the antibody selectively bind a peculiar structure of pancreatic tissue: Langerhans Islets.

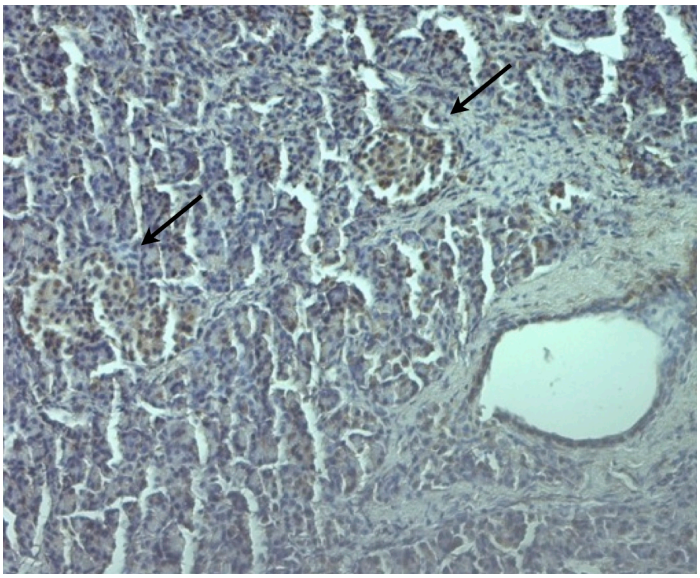

Figure 17. Immunohystochemistry on pancreatic tissue stained with OVA C2 mAb. The antibody stains specific structure (Langerhans Islets) indicated by arrows.

To confirm the result shown in the picture above, we performed IHC on pancreatic tissue contiguous slices using OVA C2 mAb (Figure 18, A) and anti-insulin antibody (Figure 18, B).

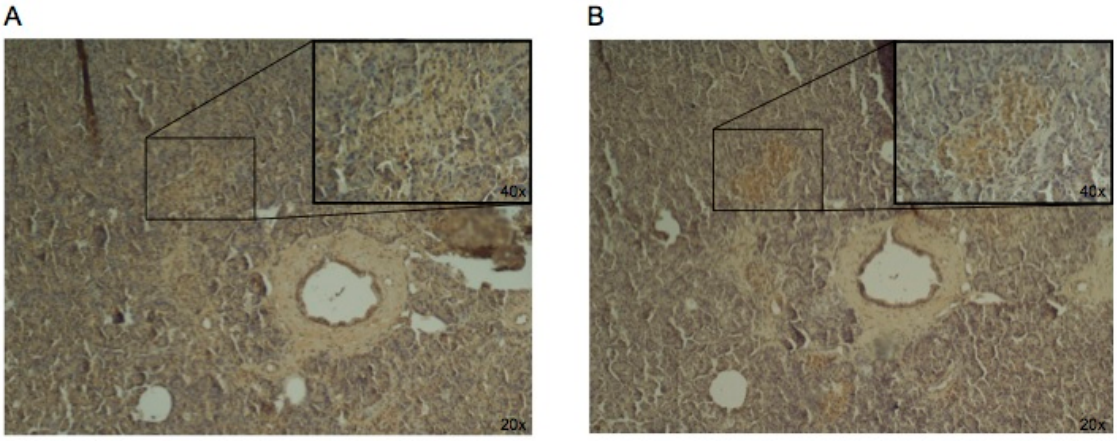

Figure 18. Immunohystochemistry on pancreatic tissue contiguous slices stained with OVA C2 mAb (A) and anti-insulin antibody (B). In both panels is shown the magnification (40x) of a Langerhans Islet.

In the picture above we can see that OVA C2 mAb (panel A) stains the same structures of anti-insulin antibody (panel B). This data demonstrate that OVA C2 mAb is able to bind Langerhans Islets.

OVA C2 mAb was used in IHC on various tissue which was reported to express sulfatides: jejunum, kidney, colon mucosa, colon adenocarcinoma, gastric mucosa and gastric adenocarcinoma (Takahashi and Suzuki 2012) but these tissue were not stained (data not shown).

SM4 sulfatides are the main glycolipid of Langerhans Islets β-cells, involved in insulin packaging and release. These molecules were found associated to insulin granules in β-cells (Blomqvist et al. 2002), and studies show that they preserve insulin crystals and facilitates insulin monomerisation during its secretion (Buschard et al. 2005). Sulfatides are one of the first example of non-protein chaperone (Takahashi and Suzuki 2012), promoting proinsulin folding and acting as a molecular chaperone for insulin (Osterbye et al. 2001). Furthermore, sulfatides are involved in insulin secretion activating ATP-sensitive potassium ion channels and stimulating calcium ion-dependent exocytosis (Buschard et al. 2002). Electrospray ionization tandem mass spectrometric

analysis on sulfatides extracted from brain and pancreatic islets show tissue specific differences for ceramide composition. Brain tissue has mainly SM4 with ceramide composed by long chain non-hydrogenated fatty acids (24:1, 24:0), while pancreatic islets has SM4 with ceramide composed by long chain fatty acid (24:0) but also short chain fatty acid (16:0), short chain fatty acid are a peculiar characteristic of β-cells SM4 (Hsu et al. 1998).

Our results show that OVA C2 mAb selectively stains SM4 lower band on TLC plates, SM4 lower band was found to be composed by hydrogenated fatty acid but also short chain fatty acids (such as 16:0). C16:0 isoform of sulfatide is predominantly found in secretory granules and on the surface β-cells plasma membrane. OVA C2 mAb stains Langerhans islets in IHC on pancreatic tissue, but not other sulfatide containing structure found in different tissues. These findings suggest that OVA C2 mAb selectively recognise C16:0 SM4 expressed in β-cells.

For these reasons we tested OVA C2 mAb binding on RIN 5F rat insulinoma β-cell line. In Figure 19 is shown immunofluorescence staining on RIN 5F cells cultured without glucose (A), or with 12 mM glucose (B).

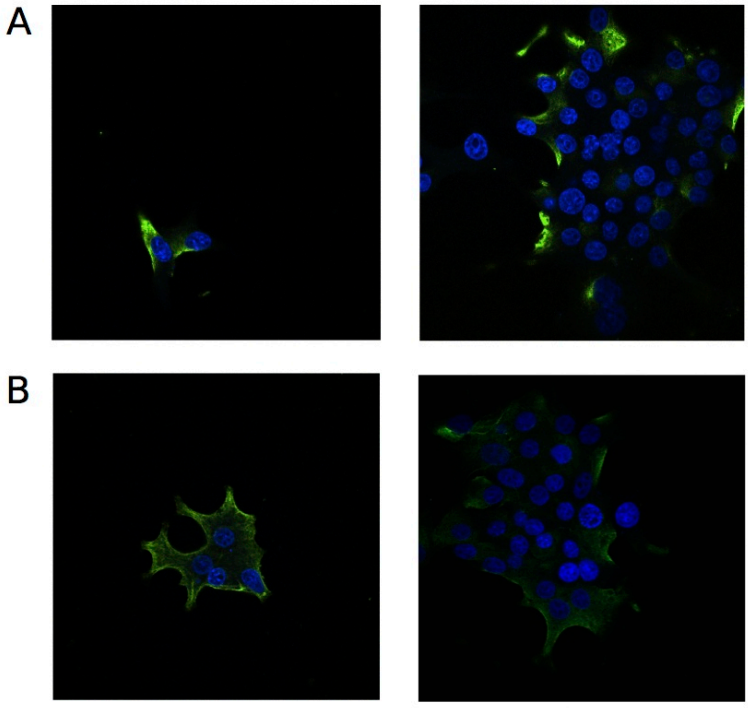

Figure 19. Immunofluorescence on RIN 5F stained with OVA C2 mAb (green) and DAPI (blue). RIN 5F were cultured without glucose (A) or with 12 mM glucose (B). Magnification 90x.

As shown in the picture above, OVA C2 mAb is able stain RIN 5F β-cells, and the staining pattern is different in the two culture conditions. In cells cultured without glucose (A) OVA C2 staining is not uniform, with intense spots localised in the cytoplasm, while in cells cultured in presence of 12 mM glucose (B), OVA C2 staining is uniform and localised at membrane level. These differences are probably correlated with the role of sulfatides in insulin packaging and release.

We will perform further experiment on RIN 5F cells, to test the effect of OVA C2 mAb treatment on insulin secretion. The ability to bind RIN 5F β-cells sulfatides suggest OVA C2 mAb as a possible tool for insulin oversecretion treatment in insulinoma cases.

2. STUDY OF THE MOLECULAR MECHANISMS INVOLVED IN hERG1-β1 INTEGRIN COMPLEX FORMATION

hERG1 channels are aberrantly expressed in several human cancers where they control different aspects of the neoplastic cell biology, such as cell proliferation, apoptosis, cell invasion, and angiogenesis. These effects seem to be often mediated by hERG1 recruitment into plasma membrane functional complexes, which generally include integrins and growth factor receptors .

Immunoprecipitations (IP) experiments evidenced that hERG1 forms macromolecular complexes mainly with the β1 subunit of integrin receptors ((Arcangeli et al. 1993), (Hofmann et al. 2001), (Cherubini et al. 2005), (Pillozzi et al. 2007), (Pillozzi et al. 2011), (Crociani et al. 2013)).

In acute myeloid leukaemia (AML), hERG1 is recruited on plasma membrane together with β1-integrin and vascular endothelial growth factor receptor-1 (FLT1), forming a macromolecular complex which mediates cell migration and invasion (Pillozzi et al. 2007). In acute lymphoblastic leukaemia (ALL) hERG1 forms macromolecular complexes with CXCR4 and β1integrin, triggering both extracellular signal-related kinase 1/2 (ERK1/2) and the phosphoinositide 3-kinase (PI3K)/Akt prosurvival signalling pathways (Pillozzi et al. 2011). Furthermore in colon adenocarcinoma cell lines, hERG1-β1 integrin complex recruits Focal Adhesion Kinase (FAK) which in turn activates PI3K and Akt signalling pathways, leading to Hypoxia Inducible Factor (HIF) activation and consequent VEGF-A and other tumour progression genes transcription (Crociani et al. 2013). hERG1 and β1 macromolecular complex can thus be considered an oncogenit unit.

FRET (Fluorescence Resonance Energy Transfer) experiments on HEK293 cells expressing CFP-hERG1 and integrin β1-YFP recombinant proteins demonstrate that hERG1 and β1 integrin directly interact to form a macromolecular complex. FRET experiments on cells cultured on fibronectin (FN) or BSA coated plates show that β1 complex formation is enhanced by FN-dependent integrin activation (manuscript in preparation).

The aim of the work presented in this thesis is to develop a bifunctional engineered antibody able to bind hERG1-β1 oncogenic unit, disrupting the complex and preventing downstream signalling. To address this goal the first step was to understand which portions of hERG1 channel and β1 integrin are involved in complex formation.

hERG1 channel is a tetrameric protein characterised by intra-subunits interactions (involving transmembrane domains) and inter-subunits interactions (involving both transmembrane and cytoplasmic domains) (Vandenberg et al. 2012). hERG1 interact with other proteins through its cytoplasmic domains: C terminal domain was found to interact with KCNQ1 channel (Ehrlich et al. 2004), ubiquitin ligase Nedd4-2 (Albesa et al. 2011), and PKA (Kagan and McDonald 2005); while even if it is not proven yet for hERG1, PAS domain is involved in protein-protein interaction both in prokaryote and eukaryotes (Becchetti and Arcangeli 2010). Furthermore, hERG1 cytoplasmic domains are substrate of various kinases, like PKA, PKB and PKC (Vandenberg et al. 2012), and specific phosphorylated residues are involved in protein interaction, e.g binding of 14-3-3ε to hERG requires intact PKA phosphorylation sites at S283 in the N terminus and at S1137 in the C terminus (Kagan and McDonald 2005).

β1 integrin is able to interact with other proteins with its extracellular region (fibronectin, vitronectin), transmembrane region (integrin α-subunit) and cytoplasmic region (kindlin, talin) (Campbell and Humphries 2011).

First of all, we investigated whether β1 cytoplasmic tail is able to bind intracellular domains of hERG1.

Each hERG1 α-subunit have two large cytoplasmic domains as shown in Figure 20. The N-terminal domain is composed by: the N-tail (residues 1-25), the Per-Arnt-Sim (PAS) domain (residues 26-135), and the proximal N-tail (residues 136-376). The C-terminal region is composed by: the C-linker (residues 666-748), the cyclic nucleotide binding domain (cNBD) (residues 749-872) and the distal C-tail (residues 873-1159).

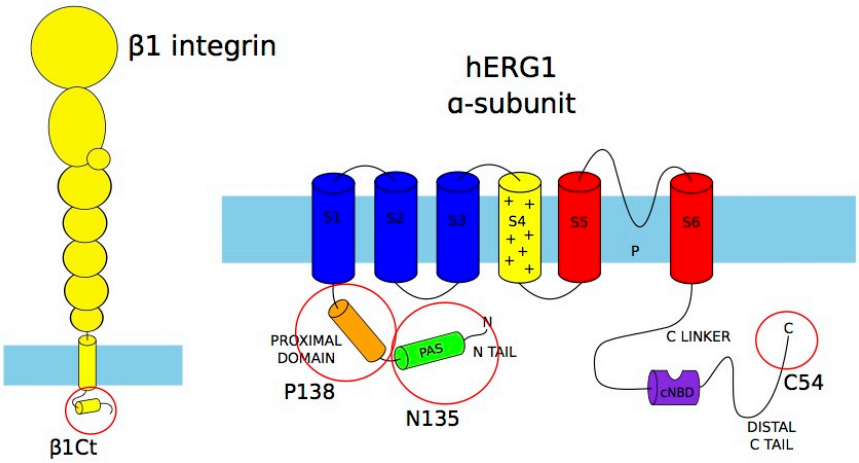

Figure 20. Cartoon representing β1 and hERG1 cytoplasmic domains used for GST-pull down assay: β1Ct, N135 (N-tail and PAS domain, in red); P138 (proximal N-terminus); C54 (last 54 amino acids of C-taill), in the red circles.

To investigate the interaction between β1 cytoplasmic tail and hERG1 cytoplasmic domains, we decided to perform GST pull down assay. We expressed GST-fusion protein in E. Coli, using β1 cytoplasmic tail and single hERG1 intracellular domains sequences cloned into pGEX2T vector.

hERG1 N-terminal domain was divided in two portions: GST-P138 (proximal N-terminus) and GST-N135 (PAS, N-tail). As regard hERG1 C-terminal domain, we used two constructs: GST-C54 (containing the last 54 amino acids of hERG1) and GST-H1Ct (containing the whole C-terminal domain). Unfortunately, despite many attempts, we cannot succeed in GST-H1Ct expression (data not shown).

We thus expressed and purified GST-P138, GST-N135 and GST-C54. We expressed also GST-β1Ct (containing the whole cytoplasmic domain of β1), and we cut GST by thrombin digestion. Purified β1Ct was thus used in combination to GST-P138, GST-N135 and GST-C54 in pull down assay. GST-fusion proteins were pulled down using Glutatione Sepharose 4B resin and analysed by SDS-page and Coomassie staining as described in Materials and Methods (Figure 21)

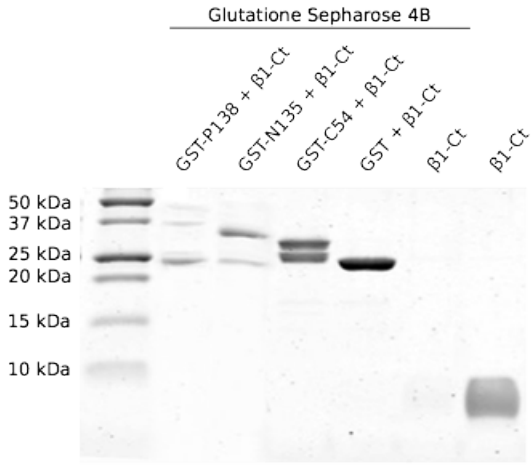

Figure 21. GST pull down assay. Picture of protein gel stained with Coomassie reagent. GST fusion proteins incubated with purified β1Ct and pulled down with Glutatione Sepharose 4B: GST-P138 (lane 2), GST-N135 (lane 3), GST-C54 (lane 4). As negative controls we used GST+ β1Ct (lane 5) and β1Ct (lane 6) incubated with Glutatione Sepharose 4B; as positive control in SDS-page we used purified β1Ct (lane 7). Protein molecular weight marker (lane 1).

As shown in the picture above, we cannot detect β1Ct band (7 kDa) in none of the lanes with pulled down GST-fusion protein hERG1 domains, but only in the control lane, loaded with β1Ct (lane7). The experiment was repeated varying ionic strength and pH conditions, but we obtained the same results (data not shown). This data suggest that, in these experimental conditions, β1Ct is not able to bind hERG1 N-terminal domains and distal C-tail. These findings does not provide information about the interaction between β1 cytoplasmic domain and the full-length hERG1 C terminal domain or the whole hERG1 tetramerised cytoplasmic domains.

We proceeded then to evaluate whether complex formation involves β1 cytoplasmic tail and the whole hERG1 cytoplasmic domains or involves other regions of the two proteins.

To address this goal we performed a “Fishing” experiment in HEK293 cells over-expressing hERG1 (HEK293-hERG1 clone 5) and HEK293 wild type, using GST-β1Ct fusion protein as a molecular bait and pulling down the bait with Glutatione Sepharose 4B resin (Figure 22).

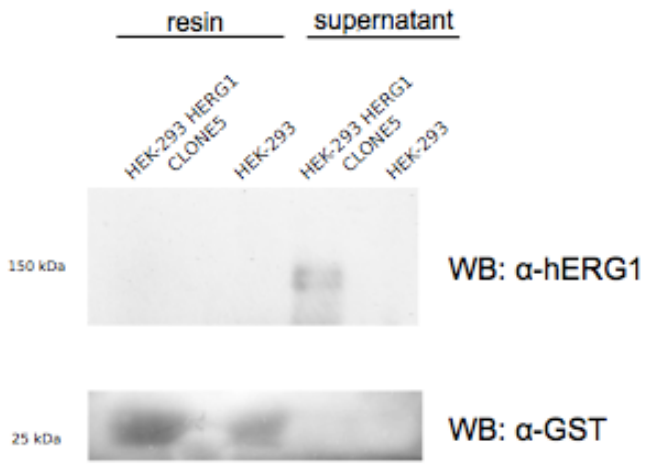

Figure 22. “Fishing” assay. Immunoblot with anti-hERG1 antibody (C54) (≃155 kDa) and anti-GST antibody (26 kDa). Resin: GST pulled down proteins: HEK293 hERG1 clone 5 (lane 1), HEK293 wild type (lane 2). Supernatant, containing non-pulled down protein: HEK293 hERG1 clone 5 (lane 3), HEK293 wild type (lane 4).

In Figure 22, we can see that hERG1 (155 kDa) was not pulled down by GST-β1Ct bait (lane 1), but remains in the supernatant (lane 3). Non transfected HEK293 were used as negative control.
“Fishing” experiment results show that GST-β1Ct is not able to bind hERG1 channel in total protein lysate, suggesting that β1 cytoplasmic domain does not interact neither with the whole intracellular domains of tetramerised hERG1.

To confirm these data we performed an experiment using two hERG1 mutants, hERG1-Δ-2-370 and hERG1-ΔC+RD (Figure 23). hERG1-Δ-2-370 is composed by hERG1 lacking the N-terminal domain (residues 2-370) (Viloria et al. 2000); while hERG1-ΔC+RD is formed by hERG1 lacking the whole C-terminal domain except for 104 amino acids (residues 1018–1122) crucial for membrane trafficking (Kupershmidt et al. 1998).

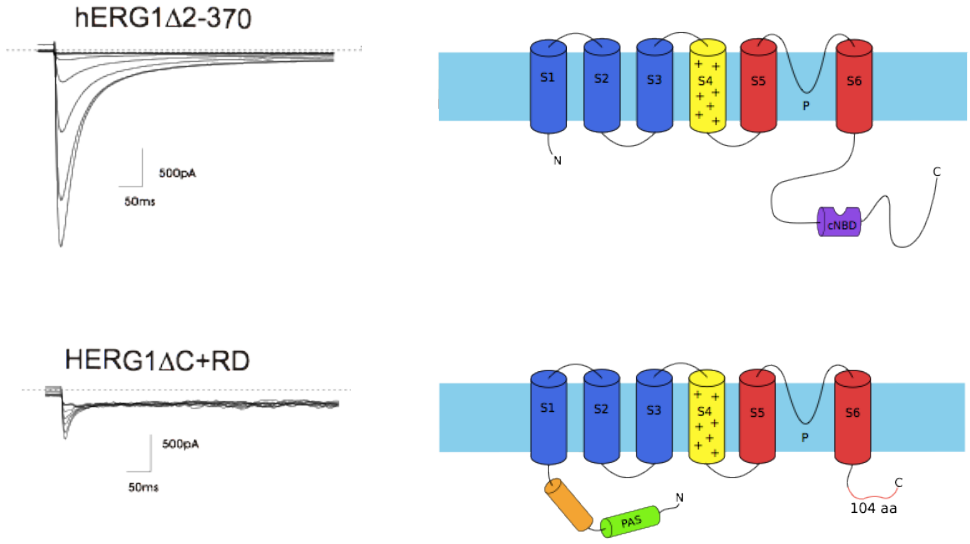

Figure 23. hERG1-Δ-2-370 and hERG1-ΔC+RD mutants: on the right are shown hERG current recorded by patch clamp technique in transfected HEK293 cells; on the left are shown cartoons representing mutants structure.

We performed immunoprecipitation (IP) experiments, with anti-hERG1 mAb, on reconstituted models of HEK293 cells expressing hERG1 mutants (Figure 24). Membrane expression of both functional hERG1-Δ-2-370 and hERG1-ΔC+RD was evaluated measuring hERG current by patch clamp technique (Figure 23, left panels).

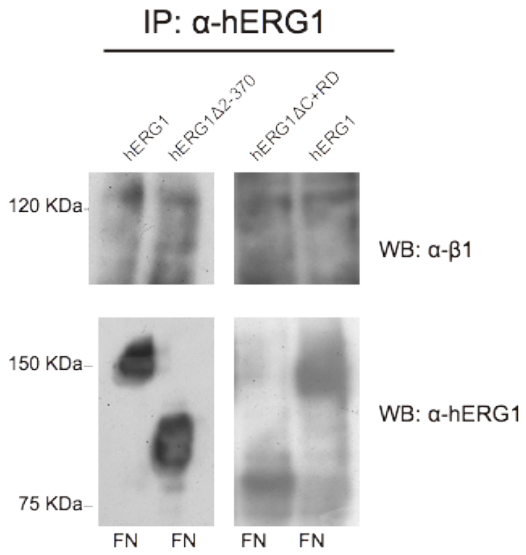

Figure 24. Immunoprecipitation experiment (IP). Transfected HEK293 cells were stimulated on fibronectin (FN) coated plates and total protein extract was immunoprecipitated using anti-hERG1 mAb. Immunoblot with anti-β1 integrin antibody (RM12) (≈130 kDa) and reprobing with anti hERG1 antibody (C54): hERG1 (≈155 kDa) (lanes 1 and 4), HEK293-hERG1-Δ-2-370 (≈100 kDa) (lane 2), HEK293-hERG1-ΔC+104 (≈90 kDa) (lane 3).

HEK293 expressing hERG1 wild type and hERG1 mutants were seeded on fibronectin (FN) to engage β1-integrin and cell extracts were immunoprecipitated with anti-hERG1 mAb. Immunoblot with anti-β1 integrin antibody (RM12) and the reprobing with anti-hERG1 antibody (C54), show that β1 integrin (≃130 kDa) co-immunoprecipitate with hERG1 wild type (≃155 kDa) (Figure 24, lanes 1 and 4), in agreement with previous data (Cherubini 2005). Furthermore β1 integrin immunoprecipitate with both hERG1-Δ-2-370 (≃100 kDa) and hERG1-ΔC+RD (≃90 kDa) (Figure 24, lanes 2 and 3, respectively).
These results demonstrate that hERG1 cytoplasmic domains are not necessary for complex formation, indicating that hERG1-β1 interaction may involve transmembrane or extracellular portions of these proteins.

To investigate the mechanisms involved in complex formation, we evaluated hERG1-β1 co-immunoprecipitation in HEK293-hERG1 cells treated with hERG1 blockers such as E4031 and ERG-toxin (Figure 25).

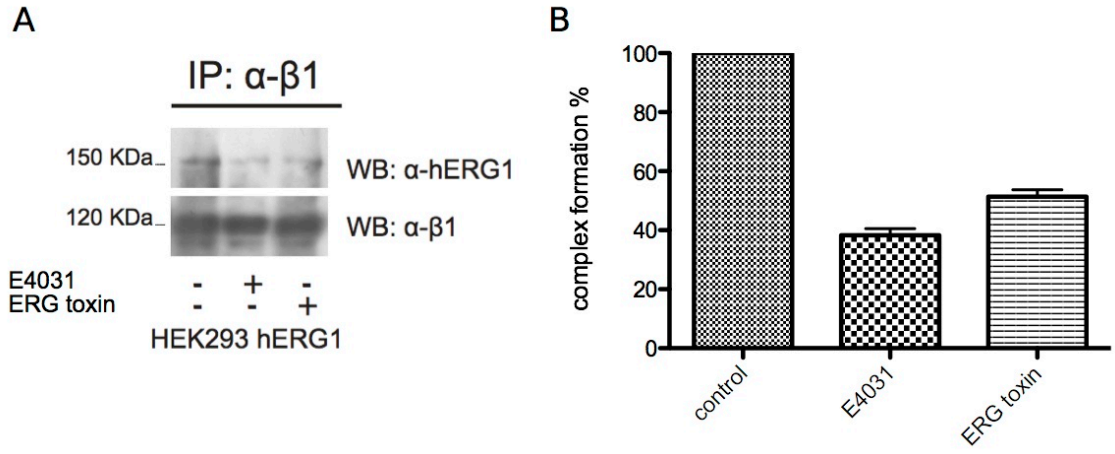

Figure 25. Immunoprecipitation experiment (IP). HEK293 cells stably expressing hERG1 treated with hERG1 blokers E4031 or ERG-toxin. Total protein extract was immunoprecipitated using anti-β1 integrin mAb (TS2/16). (A) Immunoblot with anti-hERG1 mAb (C54) (≃155 kDa) and reprobing with anti-β1 antibody (RM12) (≃130 kDa). Treatments: control (lane 1), E4031 (lane 2), ERG-toxin (lane 3). (B) Histogram representing complex formation %, densitometric analysis was performed using ImageJ software. For each condition, the amount of co-immunoprecipitated hERG1 was normalised versus immunoprecipitated β1-integrin.

As shown in Figure 25, E4031 (lane 2) inhibit complex formation, according to previous findings (Cherubini et al. 2005). Complex formation is also prevented by ERG-toxin (lane 3), confirming that hERG1 blockers influence hERG1-β1 interaction.

hERG1 blockers reduce ERG current binding the channel in different ways. The common feature of these molecules is indeed the reduction of ERG-current. To investigate if ion flux is important for complex formation we compared hERG1-β1 co-immunoprecipitation in transfected HEK293, expressing the non-conductive mutant hERG1-G628S, and in HEK293-hERG1 (Figure 26).

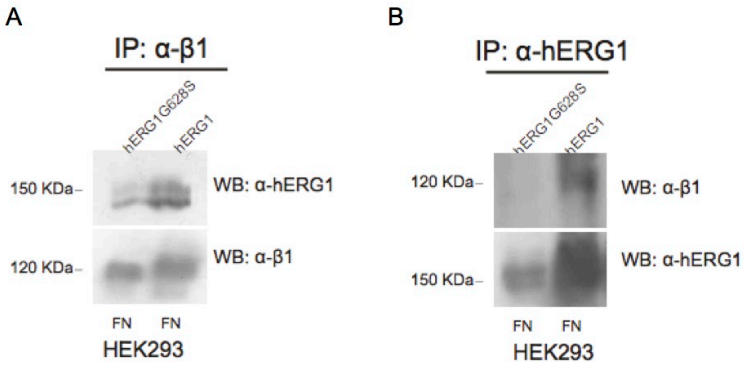

Figure 26. Immunoprecipitation experiment (IP). HEK293-hERG1-G628S (non conductive mutant) and HEK293-hERG1 (wild type). Total protein extract was immunoprecipitated using anti-β1 integrin mAb (TS2/16) (A) or anti-hERG1 mAb (B). Immunoblot with anti-hERG1 mAb (C54) (≃155 kDa) and reprobing with anti-β1 antibody (RM12) (≃130 kDa).

The results in Figure 26 show that hERG1-G628S co-immunoprecipitate with β1 integrin (lane 1), even if less than hERG1 wild type (lane 2), suggesting that the effect of G628S mutation is similar to that of hERG1 blockers and that ion flux has a role in complex formation.

hERG1 channel is a voltage gated channel, with a voltage sensor formed by the S4 transmembrane segments, rich in basic amino acids. S4 segments move in the membrane bilayer following depolarisation, inducing conformational changes that regulate channel opening. S4 transmembrane domains are thus involved both in ion flux and in protein conformational changes.

To study the effect of ion flux and channel conformational changes on hERG1-β1 complex formation, we performed hERG1-β1 co-IP experiments on transfected HEK293 expressing the mutants: hERG1-K525C and hERG1-K531C. Both mutants have a point mutation in the S4 transmembrane domain. K525 is one of the three outer positive charges of S4 segment, while R531 is one of the three inner positive charges of S4 (Figure 27, A). A study reports that K525C mutation causes a prominent hyperpolarising shift in hERG1 activation curve and induces channel opening at negative holding voltage, stabilising the

open state; whereas R531C mutation causes a depolarising shift in hERG1 activation curve, stabilising the closed states (Zhang et al. 2004). These findings were confirmed by patch clamp technique on HEK293 expressing hERG1 wild type, hERG1-K525C or hERG1-K531C used in our experiments (Figure 27 B, C).

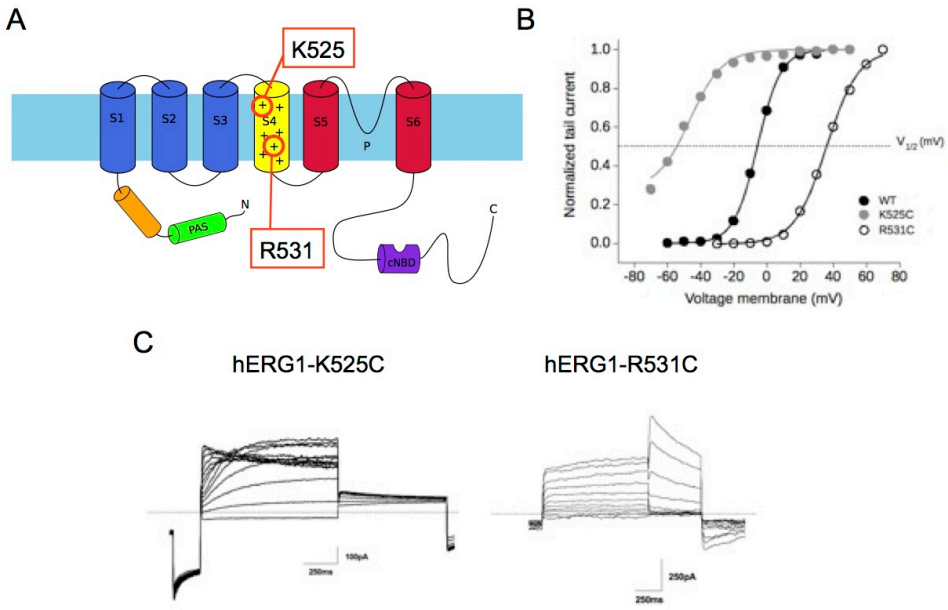

Figure 27. hERG1 S4 mutants K525C and R531C. (A) Cartoon of hERG1 α-subunit and its transmembrane domains, the position of S4 positive amino acids K525 and R531 is shown. (B) Activation curve of hERG1 wild type, hERG1-K525C and hERG1-R531C. (C) hERG current in HEK293 expressing hERG1-K525C and hERG1-R531C.

We evaluated hERG1-β1 co-immunoprecipiation on HEK293 expressing hERG1 wild type, hERG1-K525C or hERG1-K531C. Cells were seeded on fibronectin (FN) to engage β1-integrin and cell extracts were immunoprecipitated with anti-β1 integrin mAb (TS2/16) (Figure 28).

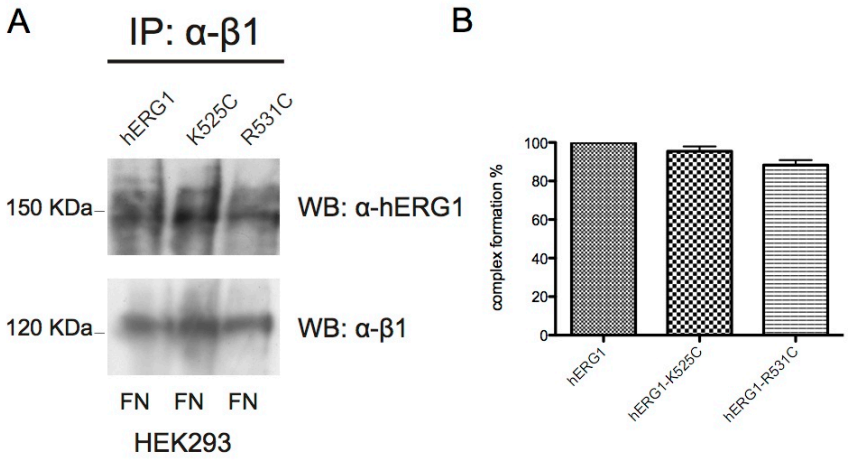

Figure 28. (A) Immunoprecipitation experiment (IP) on HEK293-hERG1 (wild type), and S4 mutants HEK293-hERG1-K525C and HEK293-hERG1-R531C. Total protein extract was immunoprecipitated using anti-β1 integrin mAb (TS2/16). Immunoblot with anti-hERG1 mAb (C54) (≃155 kDa) and reprobing with anti-β1 antibody (RM12) (≃130 kDa). (B) Histogram representing densitometric analysis of hERG1 co-immunoprecipitated with β1-integrin. Values were calculated using ImageJ software and normalised versus immunoprecipitated β1-integrin.

In Figure 28 (A), immunoblot with anti-hERG1 mAb (C54) and reprobing with anti-β1 antibody (RM12) show that β1 integrin (≃130 kDa) co-immunoprecipitate with hERG1 S4 mutants as well as with hERG1 wild type (≃155 kDa). Densitometric analysis shows that complex formation is similar in the three samples, suggesting that the point mutations in S4 segment does not prevent complex formation.

Since our previous works demonstrate that hERG1 blockers prevent complex-related downstream signalling ((Cherubini et al. 2005), (Pillozzi et al. 2007), (Pillozzi et al. 2011), (Crociani et al. 2013)), we investigated FAK phosphorylation on tyrosine 397 in the hERG1 mutants described above (Figure 29).

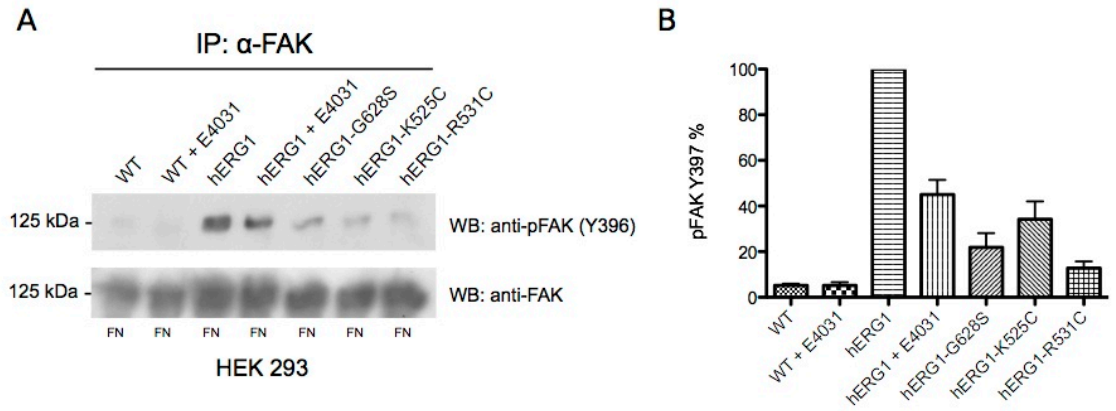

Figure 29. (A) Immunoprecipitation experiment (IP) on HEK293 wild type (WT), HEK293-hERG1, HEK293-hERG1-G628S, HEK293-hERG1-K525C and HEK293-hERG1-R531C. All the cells were stimulated on fibronectin. Total protein extract was immunoprecipitated using anti-FAK antibody. Immunoblot with anti-pFAK-Y397 antibody (≃125 kDa) and reprobing with anti-anti-FAK antibody (≃125 kDa). (B) Histogram representing densitometric analysis of phosphorylated (Y397) FAK amount. Values were calculated using ImageJ software and normalised versus immunoprecipitated FAK amount.

To study the effect of E4031 treatment on FAK phosphorylation, we evaluated FAK phosphorylation on HEK293 wild type and HEK293-hERG1 treated or not with 40 μM E4031. In all the samples β1-integrin was engaged, seeding the cells on FN. Cell extracts were immunoprecipitated with anti-FAK antibody and revealed with anti-pFAK-Y397 antibody (Figure 29, A). Densitometric analysis was performed on three independent experiments, using Image J software, and the values reported in the histogram (Figure 29, B) were normalised against immunoprecipitated total FAK amount. Our results confirm that FAK phosphorylation is strongly enhanced by hERG1 channel expression and inhibited by E4031 treatment (Cherubini et al. 2005). Furthermore, the histogram show that FAK phosphorylation is strongly inhibited when β1-integrin is expressed together with G628S, K525C or R531C mutants.

Many works show the cross-talk between K^+ channels and integrin function. Brown. et al. described that homophilic ligation or antibody cross-linking of PECAM-1 (CD31) expressed by macrophages inhibited Kv11.1 current promoting macrophage β1 integrin binding of apoptotic cells or Latex beads that had been opsonised with fibronectin (Vernon-Wilson et al. 2007). Levite et al. (2000) reported that depolarisation of T-lymphocytes through the inhibition of K^+ efflux via Kv1.3 was sufficient to activate β1 integrin function (Levite et al. 2000). Depolarisation affect the activation, or open probability, of Kv channels,

which should be sufficient to promote K^+ efflux and integrin-dependent adhesion. Integrin engagement is responsible for cellular hyperpolarisation, which may be due to intracellular signalling events affecting surface expression or activity of ion channels (Brown and Dransfield 2008).

hERG1 channels are voltage gated channel, their opening and ion flow are dependent on membrane voltage. S4 transmembrane segments are the so-called voltage sensors, due to their content in basic amino acids. When the plasma membrane is hyperpolarised, S4 transmembrane domains are attracted by the negative charges inside the cell and hERG1 channel is closed. During membrane depolarisation, negative charges move from the inside to the outside of the cell and S4 segments move in the membrane bilayer following depolarisation. This movement leads to conformational changes that lead to channel opening and potassium ion flow outside of the cell, the flow goes on until the membrane is repolarised. S4 transmembrane domains are thus involved both in ion flux and in hERG1 conformational changes. Brown et al. (2008) speculate that the conformation of β1 integrins is sensitive to small changes in membrane potential. This may be due to integrin coassociation with voltage-gated ion channels in which a conformational change within the voltage-sensor is relayed or transmitted to the integrin (Brown 1990, Olivotto et al. 1996). It was known that integrin-dependent binding of either CHO or SH-SY5Y neuroblastoma cells to fibronectin can promote FAK association with either Kv2.1 or Kv11.1 potassium channels, and that adhesion-dependent stimulation of K^+ efflux is essential for phosphorylation of FAK at residue Y397 and may regulate Y576/577 phosphorylation in a Src dependent manner (Wei et al. 2008). Our results show that FAK phosphorylation is strongly inhibited when β1-integrin is expressed together with G628S, K525C or R531C mutants. These findings suggest that ion flux and hERG1 voltage related conformation are crucial for FAK phosphorylation and in turn for complex-related signalling. Our results are thus consistent with the works described above and with Brown hypothesis, suggesting that the voltage sensor could transmit a conformational change to β1-integrin leading to integrin related downstream signalling. LaFlamme group, reported that expression of the integrin β1 cytoplasmic domain in the context of a chimeric transmembrane receptor with the

transmembrane and extracellular subunit of the interleukin-2 receptor, inhibit FAK phosphorylation at Y397 in primary fibroblasts (Berrier et al. 2008). These results suggest that the transmembrane and extracellular domain of β1 are required for FAK activation. We can thus speculate that hERG1 interact with beta1 integrin at transmembrane level, transmitting conformational changes during channel opening, that lead to integrin signalling activation. Engaged beta1 integrin in turn stabilise the open state of the channel.

For these reasons a bispecific antibody able to target hERG1-β1 complex could be a valid tool to block complex related signalling.

3. DEVELOPMENT OF ENGINEERED ANTIBODIES ABLE TO TARGET hERG1-β1 ONCOGENIC UNIT

The aim of the second part of the work presented in this thesis is to develop a bifunctional engineered antibody able to bind hERG1-β1 oncogenic unit, disrupting the complex and preventing downstream signalling.

Bispecific antibodies (bsAbs) are molecules capable of a strong and specific binding with two different antigens. The new generation of recombinant bsAb fragments are nowadays emerging as tool with many practical applications in cancer therapy: such as to retarget effector cells toward tumour cells (Chames and Baty 2009) but also to inhibit downstream signalling pathway of oncogenic units (McDonagh et al. 2012). Bispecific single chain diabody (scDb) are composed by the variable domains (VH and VL) of two antibodies connected by three peptide linkers. The compact and medium size (60 kDa) of these molecules confers good tumour penetration, expression and solubility (Chames et al. 2009). The strategy we would like to use is to develop a bispecific scDb able to bind the oncogenic unit hERG1 channel/β1 integrin. Our engineered protein should be able to bind hERG1 and to simultaneously block β1 signalling and disrupt the complex.

For this aim we will use the variable domains (VH and VL) of anti-hERG1 mAb (which binds the extracellular domain S5-P (peptide EQPHMDSRIGWLHN) of hERG1) and of β1 integrin mAb BV7 or TS2/16 (which binds the extracellular domain of β1 integrin).

Our recent work, demonstrate that anti-hERG1 mAb is able to reduce hERG current and inhibit cell motility of PDAC cell lines (manuscript in preparation).

We have already isolated anti-hERG1 mAb variable domains: mRNA was purified from total RNA extracted from hybridomas secreting anti-hERG1 mAb (Clone A12, patented by the University of Florence, n° FI2006A000008), mRNA was reverse transcribed into cDNA and VH and VL were isolated by PCR using specific primers (Wang et al. 2000); the variable domains were then cloned into

the pCR-Blunt vector with Zero Blunt PCR Cloning Kit (Invitrogen) and sequenced.

Using anti-hERG1 mAb VH and VL variable domains we developed a single chain variable fragment (scFv), anti-hERG1-scFv. This recombinant antibody is able to bind the peptide EQPHMDSRIGWLHN in ELISA assay.

Prior to develop the bispecific scDb we decided to produce and characterise anti-β1 integrin scFv, engineering both BV7 and TS2/16. Those monoclonal antibodies bind the extracellular portion of β1 integrin, BV7 was found to block β1 integrin (Morello et al. 2011), while TS2/16 activate β1 integrin (Garcia et al. 1998).

3.1. BV7 mAb ENGINEERING

To isolate heavy chain (VH) and light chain (VL) variable domains of anti-β1-integrin mAb BV7, the first step was the extraction of total RNA from frozen BV7-hybridoma cell pellet (kindly provided by prof. Defilippi, University of Turin). Total RNA was reverse transcribed into cDNA and VH and VL were isolated by PCR using specific primers as described in Materials and Methods.

In order to choose the best degenerated forward primer for the isolation of VH we performed five parallel PCR reactions using the primer pairs listed below:

DegH1dir-IgG1rev

DegH2dir-IgG1rev

DegH3dir-IgG1rev

DegH4dir-IgG1rev

DegH5dir-IgG1rev

The expected size of VH is around 350-400 bp. In Figure 30 is shown the electrophoretic run of PCR products alongside with 2log DNA ladder (NEB).

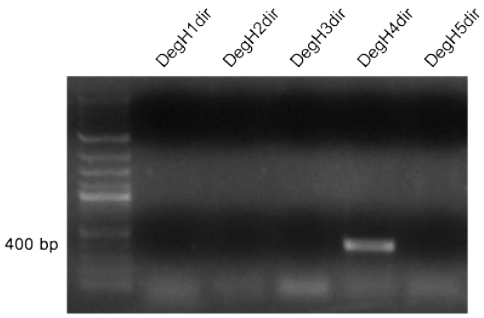

Figure 30. Electrophoretic run: (lane 1) 2log DNA ladder; (lane 2-6) PCR products performed with the primer pairs composed by IgG1rev in combination with five degenerated forward primers.

As shown in Figure 30 the primer pair DegH4dir-IgG1rev is the only one that give a PCR product of the correct size, it was thus chosen to isolate VH.

To isolate variable domains we used an high fidelity DNA polymerase (KOD Hot Start DNA Polymerase (Novagen)) as described in Materials and Methods.

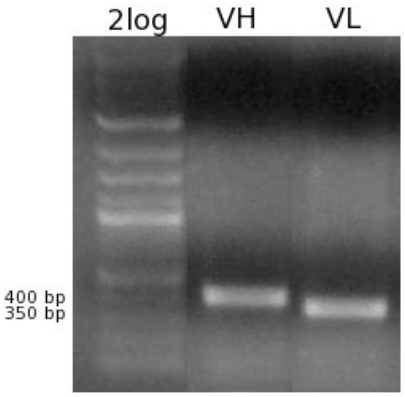

Figure 31. Electrophoretic run: (lane 1) 2log DNA ladder; (lane 2) isolated VH (≃400 bp), (lane 2) isolated VL (≃350 bp).

PCR products of the correct size (350-400 bp, Figure 31) were purified from agarose gel using QIAquick PCR Purification Kit (QIAGEN) and cloned without using restriction enzymes into pCR-Blunt vector (Invitrogen) following Zero Blunt PCR Cloning kit (Invitrogen) instructions. Ligation products were used to transform electrocompetent DH5α. Transformed DH5α colonies were picked up and grown in LB medium to extract plasmid DNA for sequencing. At first, we chose 3 colonies for VL and 3 colonies for VH. For each sample, the variable domain was sequenced using both M13rev and M13for universal primers. DNA sequencing was performed by Primm srl.

Electropherograms were analysed using FinchTV (Geospiza, Inc) software. Nucleotide sequences were translated using ExPASy Translate Tool and predicted amino acid sequences were analysed using Kabat scheme (www.bioinf.org.uk) in order to identify CDRs.

In Figure 32 (A) is shown the nucleotide sequence obtained comparing six electropherograms: forward and reverse sequences of pCR-Blunt-VL, extracted form three different colonies; in red are the primers used for VL isolation. In Figure 32 (B) is shown VL amino acid sequence, predicted translating nucleotide sequence. Following Kabat numbering scheme, we identified the conserved key amino acids delimiting CDRs regions: conserved amino acids on Framework regions are highlighted in yellow, and CDRs are highlighted in blue.

A

```
GATATTGTGATCACCCAGTCTCCATCCTCCCTGTCTGCCTCTCTGGGAGACAGAGTC
ACCATCAGTTGCAGGGCAAGTCAGGACATTAGGAATTATTTAAACTGGTATCAGCAG
AAACCAGATGGAACTGTTAAACTCCTCATCTACTACACATCAAGATTACACTCAGGA
GTCCCATCAAGGTTCAGTGGCAGTGGGTCTGGAACAGATTATTCTCTCACCATTACC
AACCTGGAGCAAGAAGATATTGCCACTTACTTTTGCCAACAGGGTAATACTCTTCCA
TGGACGTTCGGTGGAGGCACCAAGCTGGGAATCAAGCGGGCTGATGCTGCACCAACT
GTATCC
```

B

```
                              CDR L1                        CDR L2
DIVITQSPSSLSASLGDRVTISCRASQDIRNYLNWYQQKPDGTVKLLIYYTSRLHSG

                                      CDR L3
VPSRFSGSGSGTDYSLTITNLEQEDIATYFCQQGNTLPWTFGGGTKLGIKRADAAPT


VS
```

Figure 32. (A) DNA sequence of TS2/16 light chain variable domain (VL), isolated using the primers highlighted in red; (B) predicted amino acid sequence of VL and CDRs analysis according to Kabat scheme: highlighted in yellow are the conserved amino acids used to identify the CDRs (highlighted in blue).

The analysis shown in Figure 32, with CDRs and Frameworks identification, suggests that VL domain is correctly isolated.

As regard VH domain, some clues suggested that the isolated sequence was not correct. The electropherograms of the 3 samples analysed, show a VH sequence long 389 bp. Since to isolate variable domains by PCR, we used primers designed from amino acid sequence alignment, VH and VL sequence

length should be a multiple of 3 bases. Therefore the isolated VH sequence has not a correct length.
We translated the nucleotide sequence and proceeded to Kabat CDRs analysis (Figure 33).

In Figure 33 (A) is shown the nucleotide sequence obtained comparing six electropherograms: forward and reverse sequences of pCR-Blunt-VH, extracted form three different colonies, in red are the primers used for VH isolation. In Figure 33 (B) is shown VH amino acid sequence, predicted translating the nucleotide sequence. Following Kabat numbering scheme, we identify the conserved key amino acids delimiting CDRs regions: conserved amino acids on Framework regions are highlighted in yellow, and CDRs are highlighted in blue.

A

```
GAGGTGAAGCTGGTGGAATCTGGGGGAGGCTTAGTGCAGCCTGGAGAGTCCCTGAAA
CTCTCCTGTGAATCCAATGAATACGAATTCCCTTCCCATGATTTGTCTTGGGTCCGC
AAGACTCCGGAGAAGAGGCTGGAGTTGGTCGCAGCCATTAATAGTGATGGTGGTAGC
ACCTACTATCCAGACACCATGGAGAGACGATTCATCATCTCCAGAGACAATACCAAG
AAGACCCTGTACCTGCAAATGAGCAGTCTGAGGTCTGAGGACACAGCCTTGTATTAC
TGTGCAAGCGTCTATTCTAGGTACGACGGTTCTACTTTGACTTCTGGGGCCAAGGCA
CCACTCTCACAGTCTCCTCAGCCAAAACGACACCCCCATCTGTCTAT
```

B

```
                                    CDR H1                CDR H2
EVKLVESGGGLVQPGESLKLSCESNEYEFPSHDLSWVRKTPEKRLELVAAINSDGGS

                                                ????????????????
TYYPDTMERRFISRDNTKKTLYLQMSSLRSEDTALYYCASVYSRYDGSTLTSGAKA

??????????????
PLSQSPQPKRHPHLS
```

Figure 33. (A) DNA sequence of TS2/16 heavy chain variable domain (VH), isolated using the primers highlighted in red; (B) predicted amino acid sequence of VH and CDRs analysis according to Kabat scheme: highlighted in yellow are the conserved amino acids used to identify the CDRs (highlighted in blue).

As shown in Figure 33, we identified CDR-H1 and CDR-H2, but not CDR-H3. We could only identify the beginning of CDR-H3 (33 residues after the end of

CDR-H2 and 3 residues after a C), but not its end (WGXG, where X can be any amino acid).

Since VH sequence is not a multiple of 3 bases, we hypothesised a deletion or a insertion mutation inside the CDR-H3, and we tried to translate the nucleotide sequence from the other two reading frames, looking for WGXG motif.

Translating from the third reading frame we finally found the sequence which delimit the end of CDR-H3 (Figure 34).

```
GEAGGIWGRLSAAWRVPETLL-IQ-IRIPFP-FVLGPQDSGEEAGVGRSH---WW-
HLLSRHHGETIHHLQRQYQEDPVPANEQSEV-GHSLVLLCKRLF-
VRRFYFDFWGQGTTLTVSSAKTTPPSVY
```

Figure 34. Amino acid sequence obtained translating VH nucleotide sequence from the third reading frame. The symbol - indicates the presence of a STOP codon. Blue is the sequence from the last STOP codon to the end of the sequence, which contains the amino acids that delimit the end of CDR-H3 (highlighted in yellow).

This result suggested that a deletion of 1 base (or 1+n bases, where n is a multiple of 3) or an insertion of 2 bases (or 2+n, where n is a multiple of 3) occurred within the CDR-H3 sequence.

We predicted a possible original VH amino acid sequence considering correct:

- the sequence at least until the C at the end of Framework 3 and in particular until the CASVYS sequence included (because insertion or deletion in ASVYS region will result in stop codons formation);
- the sequence after WGQG motif included, translated from the third frame (Figure 35).

Question marks indicate the unknown amino acids (Figure 35, A). Basing on this predicted sequence we predicted the nucleotide sequence within the mutation could be occurred, highlighted in green (Figure 35, B).

A

```
                                  CDR H1                 CDR H2
EVKLVESGGGLVQPGESLKLSCESNEYEFPSHDLSWVRKTPEKRLELVAAINSDGGS

                                                CDR H3
TYYPDTMERRFISRDNTKKTLYLQMSSLRSEDTALYYCASVYS?????????WGQG


TTLTVSSAKTTPPSVY
```

B

```
GAGGTGAAGCTGGTGGAATCTGGGGGAGGCTTAGTGCAGCCTGGAGAGTCCCTGAAA
CTCTCCTGTGAATCCAATGAATACGAATTCCCTTCCCATGATTTGTCTTGGGTCCGC
AAGACTCCGGAGAAGAGGCTGGAGTTGGTCGCAGCCATTAATAGTGATGGTGGTAGC
ACCTACTATCCAGACACCATGGAGAGACGATTCATCATCTCCAGAGACAATACCAAG
AAGACCCTGTACCTGCAAATGAGCAGTCTGAGGTCTGAGGACACAGCCTTGTATTAC
TGTGCAAGCGTCTATTCTAGGTACGACGGTTCTACTTTGACTTCTGGGGCCAAGGCA
CCACTCTCACAGTCTCCTCAGCCAAAACGACACCCCCATCTGTCTAT
```

Figure 35. (A) Predicted original VH amino acid sequence reconstructed using the reliable sequence translated from the first frame and from the third frame. Question marks indicate the unknown amino acids. (B) VH nucleotide sequence, with highlighted the predicted sequence within the mutation could be occurred.

To reject the hypothesis of a bias during VH isolation, we repeated the process by reverse transcribing BV7 RNA into cDNA using three methods: random primers, Oligo-dT, and by first strand synthesis using IgG1rev specific primer. We isolated VH by PCR as previously described and we sequenced the PCR product, in order to see if there were heterozygous mutations, but we obtained the same result. In addition we repeated the whole process starting from new frozen hybridomas cell pellet, but we still obtained the same result.

We performed a bioinformatic analysis to check if the frameshift mutation causes STOP codon formation in the adjacent CH1 domain.

From IMGT database we downloaded three CH1 cDNA sequences of IgG1 produced in Balb/c mice. BV7 mAb was indeed produced in Balb/c mice (Martin-Padura et al. 1994).

We joined, in silico, the conserved CH1 nucleotide sequence and our VH nucleotide sequence, we translated the whole sequence and we found a lot of STOP codon in CH1 region (Figure 36). We performed this analysis for each of the three CH1 cDNA sequences and we obtained the same result.

This analysis suggests that, unless another opportune insertion or deletion occurred at the begin of CH1 sequence, the frameshift mutation in CDR-H3 region causes STOP codons formation in CH1 domain, leading to the formation of a truncated protein which certainly is not an IgG1.
To verify this hypothesis, we decided to isolate and sequence VH-CH1 region. Using CH1 sequences alignment, we designed a reverse primer that anneal at the end of CH1 domain.

VHCH1rev: CTTGTCCACCTTGGTGCTGC

We isolated VH-CH1 region by PCR using DegH4dir and VHCH1rev, and we sequenced the PCR product.

Nucleotide sequence of VH-CH1 domain
GAGGTGAAGCTGGTGGAATCTGGGGGAGGCTTAGTGCAGCCTGGAGAGTCCCTGAAA CTCTCCTGTGAATCCAATGAATACGAATTCCCTTCCCATGATTTGTCTTGGGTCCGC AAGACTCCGGAGAAGAGGCTGGAGTTGGTCGCAGCCATTAATAGTGATGGTGGTAGC ACCTACTATCCAGACACCATGGAGAGACGATTCATCATCTCCAGAGACAATACCAAG AAGACCCTGTACCTGCAAATGAGCAGTCTGAGGTCTGAGGACACAGCCTTGTATTAC TGTGCAAGCGTCTATTCTAGGTACGACGGTTCTACTTTGACTTCTGGGGCCAAGGCA CCACTCTCACAGTCTCCTCAGCCAAAACGACACCCCCATCTGTCTATccactggccc ctggatctgctgcccaaactaactccatggtgaccctgggatgcctggtcaagggct atttccctgagccagtgacagtgacctggaactctggatccctgtccagcggtgtgc acaccttcccagctgtcctggagtctgacctctacactctgagcagctcagtgactg tcccctccagccctcggcccagcgagaccgtcacctgcaacgttgcccacccggcca gcagcaccaaggtggacaag
Translated amino acid sequence
EVKLVESGGGLVQPGESLKLSCESNEYEFPSHDLSWVRKTPEKRLELVAAINSDGGS TYYPDTMERRFIISRDNTKKTLYLQMSSLRSEDTALYYCASVYSRYDGSTLTSGAKA PLSQSPQPKRHPHLSihwpldllpkltpw-pwdawsraislsq-q- pgtldpcpavctpsqlswsltstl-aaq- lsppalgparpspatlptrpaaprw

Figure 36. VH-CH1 nucleotide sequence and its translated amino acid sequence. The symbol - indicates the presence of a STOP codon. In red are primer sequences, in capital letters is VH region and in lowercase letters is CH1 region.

As shown in Figure 36, the frameshift causes STOP codon formation in CH1 region. The result shown is based on VH-CH1 PCR product forward and

reverse sequencing. In DNA electropherogram we could not detect heterozygous mutations. This result demonstrate that hybridomas used for BV7 engineering are no longer able to secrete functional complete IgG.
Among the CDRs, CDR-H3 is the most important for antigen binding, and the most variable. Mutation in CDR-H3 occurs more frequently than in other portion of heavy chain variable domain. Since hybridomas are no longer controlled by the rigid regulation mechanism of the immune system, they can accumulate mutations upon prolonged culture, which are not evident from functional analysis of cell supernatant as long as a sufficient number of cells still produce the correct antibody chains (Strebe et al. 2010). Variable domains sequence heterogeneity is one of the main problems in functional cloning of variable regions from hybridoma cell lines. As reported for the Myc1-9E10 (anti-c-myc) hybridoma cell line, isolated VH and VL PCR product may not necessarily code for functional variable regions (Fuchs et al. 1997). These problems may be minimised by extracting RNA from freshly produced hybridoma subclone (Strebe et al. 2010).
For these reasons BV7 could not be used for anti-β1-scFv development.

We thus decided to produce anti-β1 scFv and hERG1-β1-bispecific antibody engineering another anti-β1-integrin monoclonal antibody named TS2/16.

3.2. TS2/16 mAb ENGINEERING

3.2.1 ISOLATION OF VARIABLE DOMAINS (VH E VL)

The first step to isolate heavy chain (VH) and light chain (VL) variable domains of anti-β1-integrin mAb TS2/16, was the extraction of total RNA from frozen TS2/16-hybridoma cell pellet (kindly provided by prof. Defilippi, University of Turin). Total RNA was reverse transcribed into cDNA and VH and VL were isolated by PCR using specific primers as described in Materials and Methods.
In order to choose the best degenerated forward primer for the isolation of VH we performed five parallel PCR reactions using the primer pairs listed below:
DegH1dir-IgG1rev
DegH2dir-IgG1rev
DegH3dir-IgG1rev

DegH4dir-IgG1rev

DegH5dir-IgG1rev

The expected size of VH is around 350-400 bp. In Figure 37 is shown the electrophoretic run of PCR products alongside with 2log DNA ladder (NEB).

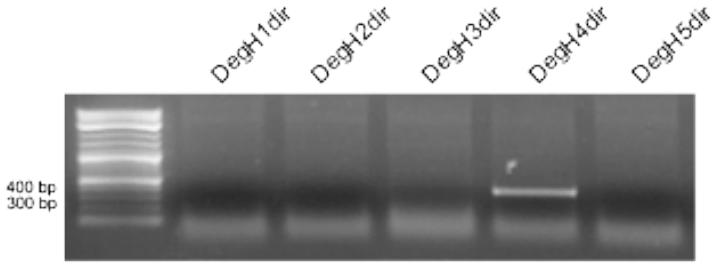

Figure 37. Electrophoretic run: (lane 1) 2log DNA ladder; (lane 2-6) PCR products performed with the primer pairs composed by IgG1rev in combination with five degenerated forward primers.

As shown in the picture above, the primer pair DegH4dir-IgG1rev is the only one that give a PCR product of the correct size, and therefore it was chosen to isolate VH.

To isolate variable domains we used an high fidelity DNA polymerase (KOD Hot Start DNA Polymerase (Novagen)) as described in Materials and Methods.

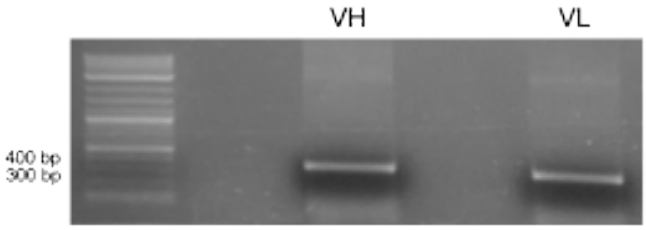

Figure 38. Electrophoretic run: (lane 1) 2log DNA ladder; (lane 2) isolated VH (≃400 bp), (lane 2) isolated VL (≃350 bp).

PCR products of the correct size (about 350-400 bp, Figure 38) were purified from agarose gel using QIAquick PCR Purification Kit (QIAGEN) and cloned without using restriction enzymes into pCR-Blunt vector (Invitrogen) following Zero Blunt PCR Cloning kit (Invitrogen) instructions. Ligation products were used to transform electrocompetent DH5α. Transformed DH5α colonies were picked up and grown in LB medium to extract plasmid DNA for sequencing. We chose 3 colonies for VL and 4 colonies for VH. For each sample, the variable

domain was sequenced using both M13rev and M13for universal primers. DNA sequencing was performed by Primm srl.

Electropherograms were analysed using FinchTV (Geospiza, Inc) software. Nucleotide sequences were translated using ExPASy Translate Tool and predicted amino acid sequences were analysed using Kabat scheme (www.bioinf.org.uk) in order to identify CDRs.

In Figure 39 (A) is shown the nucleotide sequence obtained comparing six electropherograms: forward and reverse sequences of pCR-Blunt-VL, extracted form three different colonies; in red are the primers used for VL isolation. In Figure 39 (B) is shown VL amino acid sequence, predicted translating the nucleotide sequence. Following Kabat numbering scheme, we identify the conserved amino acids delimiting CDRs regions: conserved amino acids on Framework regions are highlighted in yellow, and CDRs are highlighted in blue.

A

```
GATATTGTGATGACACAGACTCCAACCACCATGGCTGCATCTCCCGGGGACAAGATC
ACTATCACCTGCAGTGTCAGTTCAATTATAAGTTCCAATTACCTGCATTGGTATAGT
CAGAAGCCAGGATTCTCCCCTAAACTCTTGATTTATAGGACATCCAATCTGGCTTCT
GGAGTCCCACCTCGCTTCAGTGGCAGTGGGTCTGGGACCTCTTACTCTCTCACAATT
GGCACCATGGAGGCTGAAGATGTTGCCACTTACTACTGCCAGCAGGGTTCTGATATT
CCACTCACGTTCGGTGATGGGACCAAGCTGGACCTGAAACGGGCTGATGCTGCACCA
ACTGTATCC
```

B

```
                              CDR L1                          CDR L2
DIVMTQTPTTMAASPGDKITITCSVSSIISSNYLHWYSQKPGFSPKLLIYRTSNLAS

                                     CDR L3
GVPPRFSGSGSGTSYSLTIGTMEAEDVATYYCQQGSDIPLTFGDGTKLDLKRADAAP


TVS
```

Figure 39. (A) DNA sequence of TS2/16 light chain variable domain (VL), isolated using the primers highlighted in red; (B) predicted amino acid sequence of VL and CDRs analysis according to Kabat scheme: highlighted in yellow are the conserved amino acids used to identify the CDRs (highlighted in blue).

In Figure 40 (A) is shown the nucleotide sequence obtained comparing eight electropherograms: forward and reverse sequences of pCR-Blunt-VH, extracted form four different colonies; in red are the primers used for VH isolation. In

Figure 40 (B) is shown VH amino acid sequence, predicted translating the nucleotide sequence. Following Kabat numbering scheme, we identify the conserved amino acids delimiting CDRs regions: conserved amino acids on Framework regions are highlighted in yellow, and CDRs are highlighted in blue.

A

```
GAGGTGAAGGTGGTGGAATCTGGGGGAGGCTTAGTGAAGCCTGGAGGGTCCCTGAAA
CTCTCCTGTGCAGCCTCTGGATTCACTTTCAGTAGCTATACCATGTCTTGGGTTCGC
CAGACTCCGGAGAAGAGGCTGGAGTGGGTCGCAACCATAAGTAGTGGTGGTTCTTAC
ACCTACTATCCAGACAGTGTGAAGGGCCGATTCACCATTTCCAGAGACAAAGCCAAG
AACACCCTGTATTTGCAAATGGGCAGTCTGAAGTCTGAGGACACAGCCATGTATTAC
TGTACAAGAATAGGTTACGACGAAGATTATGCTATGGACCACTGGGGTCAAGGAACC
TCAGTCACCGTCTCCTCAGCCAAAACGACACCCCCATCTGTCTAT
```

B

```
                                CDR H1                          CDR H2
EVKVVESGGGLVKPGGSLKLSCAASGFTFSSYTMSWVRQTPEKRLEWVATISSGGSY

                                                        CDR H3
TYYPDSVKGRFTISRDKAKNTLYLQMGSLKSEDTAMYYCTRIGYDEDYAMDHWGQGT


SVTVSSAKTTPPSVY
```

Figure 40. (A) DNA sequence of TS2/16 heavy chain variable domain (VH), isolated using the primers highlighted in red; (B) predicted amino acid sequence of VH and CDRs analysis according to Kabat scheme: highlighted in yellow are the conserved amino acids used to identify the CDRs (highlighted in blue).

The analysis shown in the picture above, with CDRs and Frameworks identification, suggested us that the variable domains are correctly isolated and they are suitable to be used for the developing of recombinant antibodies.

3.2.2. DEVELOPMENT OF TS2/16-scFv

A single chain variable fragment (scFv) is an engineered antibody composed by VH and VL domains joined by a polypeptide linker. These recombinant proteins can be assembled in two ways: VL-linker-VH and VH-linker-VL. As reported in Pluckthun et al (1996), in the whole length antibody, the distance between the C-terminus of VL and the N-terminus of VH is around 39-43 Å, while the distance between the C-terminus of VH and the N-terminus of VL is around 32-34 Å. For this reason, to recreate a similar structure in an scFv, the linker

joining the variable domains should be longer for VL-VH orientation (20-25 residues) than for VH-VL one (15-20 residues). Linker length and primary sequence are crucial for the correct assembly of the scFv: too short linkers may cause dimerisation or multimerisation of the molecule.
The final goal of our project was to develop a bispecific single chain diabody (scDb) against hERG1 channel and β1-integrin. Prior to develop the scDb, we needed to produce and characterise an anti-hERG1-scFv and an anti-β1-scFv. These two scFv should be in the same conformation that they will assume in the scDb. Anti-hERG1-scFv construct was previously assembled in our lab, in the order VH-linker-VL. For these reasons, we decided to assemble TS2/16-scFv construct in the order VL-linker-VH, with a 20 amino acids linker composed by four GGGGS tandem repeats.
Anti-hERG1-scFv was assembled in pHenIX vector (a plasmid used for scFv assembly end expression in E. Coli). PhenIX vector carries indeed two multicloning sites separated by a sequence which codes for a 15 amino acid linker $(GGGGS)_3$. At the 5' end of the double multicloning site, there is a sequence coding for pelB, a leader peptide for periplasm exportation, and at the 3' a sequence coding for the Myc Tag. This expression vector, has a twofold function, can be used for scFv assembly and expression as a soluble protein, or can be used for phage display technology. PHenIX have indeed, in frame with the expression cassette, the gene for M13 filamentous phage protein III (pIII). The expression cassette and pIII gene are separated by the stop codon TAG, named Amber, which can be suppressed by some host strains carrying the tRNA genes that recognise UAG codon (such as glnV and tyrT).
In this work we decided to not use phage display technology, thus we worked with non-amber-suppressor bacteria strains (BL21 and HB2151).

As explained above, to assemble the scFv in the order VL-VH we need a peptide linker of 20 residues $(GGGGS)_4$, so we could not assemble the scFv construct using the two multicloning site of pHenIX vector.
For this reason, we decided to assemble the construct by SOE-PCR, using the primers described in (Schaefer et al. 2010) with modifications (Table 1). In red are the portions of the primers that anneal to the template, in green are the

sequences added to clone the construct in frame with the expression cassette in pHenIX vector, underlined are the restriction sites, purple are the sequences added to facilitate enzyme digestion, and bold are the sequenced that overlap in SOE-PCR. VLFORSFI and VHREVNOT anneal at the 5' end of VL and at the 3' end of VH respectively and add restriction sites to clone the construct into pHenIX vector. While VLREVSOE and VHREVSOE anneal at the 3' end of VL and at the 5' end of VH and introduce at the 3' end of VL, a sequence that encode the first three GGGGS repeats of the linker, and at the 5' end of VH, a sequence that encode the last two GGGGS repeats of the linker, respectively.

Name	Sequence
VLFORSFI	CACGCGGCCCAGCCGGCCATGGCCGATATTGTGATGACACAGACTCCA
VLREVSOE	**GGAGCCGCCGCCGCC**AGAACCACCACCACCAGAACCACCACCACCGGATACAGTTGGTGCAGCATC
VHFORSOE	**GGCGGCGGCGGCTCC**GGTGGTGGTGGATCCGAGGTGAAGGTGGTGGAATC
VHREVNOT	ATAAGAATGCGGCCGCATAGACAGATGGGGGTGTCGTTTTGGC

Table 1. Primer designed to assemble the construct VL-linker-VH by SOE-PCR and clone the sequence into pHenIX vector. In red are the portions of the primers that anneal to the template, in green are the sequences added to clone the construct in frame with the expression cassette in pHenIX vector, underlined are the restriction sites, purple are the sequences added to facilitate enzyme digestion, and bold are the sequenced that overlap in SOE-PCR.

Variable domains, each cloned in pCR-Blunt vector, were amplified respectively with VLFORSFI-VLREVSOE e VHFORSOE-VHREVNOT primer pairs (Figure 41, A and B). To assemble the construct VL-linker-VH we joined the two PCR products by SOE-PCR, thanks to the overlapping sequences (15 bp) at the 3' end of VL and at the 5' end of VH and VLFORSFI-VHREVNOT primer pair (Figure 41, C).

A First step PCR (VL)

CACGCGGCCCAGCCGGCCATGGCCGATATTGTGATGACACAGACTCCAACCACCATG
GCTGCATCTCCCGGGGACAAGATCACTATCACCTGCAGTGTCAGTTCAATTATAAGT
TCCAATTACCTGCATTGGTATAGTCAGAAGCCAGGATTCTCCCCTAAACTCTTGATT
TATAGGACATCCAATCTGGCTTCTGGAGTCCCACCTCGCTTCAGTGGCAGTGGGTCT
GGGACCTCTTACTCTCTCACAATTGGCACCATGGAGGCTGAAGATGTTGCCACTTAC
TACTGCCAGCAGGGTTCTGATATTCCACTCACGTTCGGTGATGGGACCAAGCTGGAC
CTGAAACGGGCTGATGCTGCACCAACTGTATCCGGTGGTGGTGGTTCTGGTGGTGGT
GGTTCT**GGCGGCGGCGGCTCC**

B First step PCR (VH)

GGCGGCGGCGGCTCCGGTGGTGGTGGATCCGAGGTGAAGGTGGTGGAATCTGGGGGA
GGCTTAGTGAAGCCTGGAGGGTCCCTGAAACTCTCCTGTGCAGCCTCTGGATTCACT
TTCAGTAGCTATACCATGTCTTGGGTTCGCCAGACTCCGGAGAAGAGGCTGGAGTGG
GTCGCAACCATAAGTAGTGGTGGTTCTTACACCTACTATCCAGACAGTGTGAAGGGC
CGATTCACCATTTCCAGAGACAAAGCCAAGAACACCCTGTATTTGCAAATGGGCAGT
CTGAAGTCTGAGGACACAGCCATGTATTACTGTACAAGAATAGGTTACGACGAAGAT
TATGCTATGGACCACTGGGGTCAAGGAACCTCAGTCACCGTCTCCTCAGCCAAAACG
ACACCCCCATCTGTCTATGCGGCCGCATTCTTAT

C Second step SOE-PCR (VL-linker-VH)

CACGCGGCCCAGCCGGCCATGGCCGATATTGTGATGACACAGACTCCAACCACCATG
GCTGCATCTCCCGGGGACAAGATCACTATCACCTGCAGTGTCAGTTCAATTATAAGT
TCCAATTACCTGCATTGGTATAGTCAGAAGCCAGGATTCTCCCCTAAACTCTTGATT
TATAGGACATCCAATCTGGCTTCTGGAGTCCCACCTCGCTTCAGTGGCAGTGGGTCT
GGGACCTCTTACTCTCTCACAATTGGCACCATGGAGGCTGAAGATGTTGCCACTTAC
TACTGCCAGCAGGGTTCTGATATTCCACTCACGTTCGGTGATGGGACCAAGCTGGAC
CTGAAACGGGCTGATGCTGCACCAACTGTATCCGGTGGTGGTGGTTCTGGTGGTGGT
GGTTCT**GGCGGCGGCGGCTCC**GGTGGTGGTGGATCCGAGGTGAAGGTGGTGGAATCT
GGGGGAGGCTTAGTGAAGCCTGGAGGGTCCCTGAAACTCTCCTGTGCAGCCTCTGGA
TTCACTTTCAGTAGCTATACCATGTCTTGGGTTCGCCAGACTCCGGAGAAGAGGCTG
GAGTGGGTCGCAACCATAAGTAGTGGTGGTTCTTACACCTACTATCCAGACAGTGTG
AAGGGCCGATTCACCATTTCCAGAGACAAAGCCAAGAACACCCTGTATTTGCAAATG
GGCAGTCTGAAGTCTGAGGACACAGCCATGTATTACTGTACAAGAATAGGTTACGAC
GAAGATTATGCTATGGACCACTGGGGTCAAGGAACCTCAGTCACCGTCTCCTCAGCC
AAAACGACACCCCCATCTGTCTATGCGGCCGCATTCTTAT

Figura 41. Nucleotidic sequence of PCR product for VL (A) and for VH (B) and SOE-PCR product (C) to assemble the construct SfiI-VL-linker-VH-NotI ready to be cloned SfiI-NotI into pHenIX vector.

SOE-PCR product was then purified from agarose gel, double digested with SfiI and NotI restriction enzymes, and cloned in pHenIX vector, as described in Materials and Methods.

In Figure 42 is shown a cartoon representing TS2/16 mAb and the engineered TS2/16-scFv, together with its pHenIX-VL-VH construct.

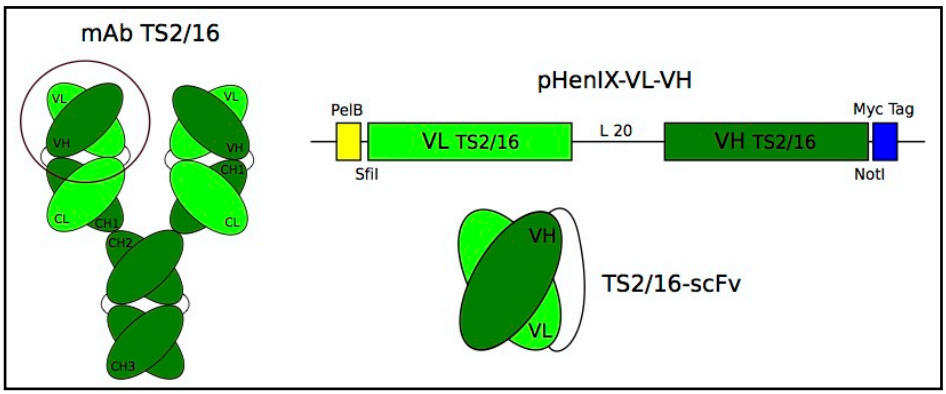

Figure 42. TS2/16 mAb engineering, through VL-linker-VH assembly in pHenIX vector, to produce TS2/16-scFv.

Cloning success was evaluated by SfiI/NotI enzymatic digestion of plasmid DNA extracted from single transformed colonies as described in Materials and Methods. As shown in Figure 43, SfiI/NotI enzymatic digestion generates two bands: a 4500 bp band (pHenIX) and a 850 bp band (VL-linker-VH).

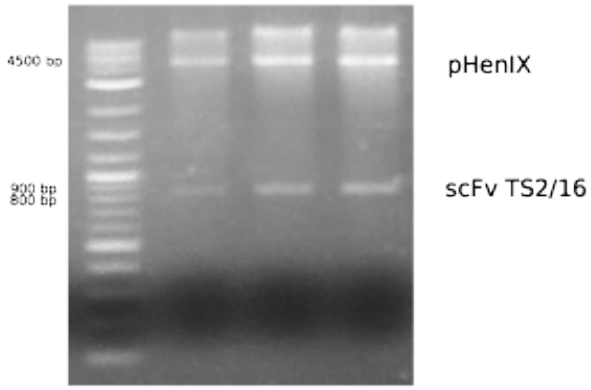

Figure 43. DNA electrophoresis of SfiI/NotI-digested plasmidic DNA. DNA was extracted from 3 BL21(DE3)Gold colonies, transformed with the ligation product of SfiI/NotI digested pHenIX and SfiI-VL-linker-VH-NotI).

Plasmid DNA pHenIX-VL-linker-VH was sequenced by Primm srl to verify if the construct is cloned in frame in the expression cassette. In Figure 44 is reported the nucleotide sequence of TS2/16-scFv in pHenIX vector and its translated sequence.

Nucleic acid sequence of TS2/16-scFv

ATGAAATACCTATTGCCTACGGCAGCCGCTGGATTGTTATTACTCGCGGCCCAGCCG
GCCATGGCCGATATTGTGATGACACAGACTCCAACCACCATGGCTGCATCTCCCGGG
GACAAGATCACTATCACCTGCAGTGTCAGTTCAATTATAAGTTCCAATTACCTGCAT
TGGTATAGTCAGAAGCCAGGATTCTCCCCTAAACTCTTGATTTATAGGACATCCAAT
CTGGCTTCTGGAGTCCCACCTCGCTTCAGTGGCAGTGGGTCTGGGACCTCTTACTCT
CTCACAATTGGCACCATGGAGGCTGAAGATGTTGCCACTTACTACTGCCAGCAGGGT
TCTGATATTCCACTCACGTTCGGTGATGGGACCAAGCTGGACCTGAAACGGGCTGAT
GCTGCACCAACTGTATCC**GGTGGTGGTGGTTCTGGTGGTGGTGGTTCTGGCGGCGGC**
GGCTCCGGTGGTGGTGGATCCGAGGTGAAGGTGGTGGAATCTGGGGGAGGCTTAGTG
AAGCCTGGAGGGTCCCTGAAACTCTCCTGTGCAGCCTCTGGATTCACTTTCAGTAGC
TATACCATGTCTTGGGTTCGCCAGACTCCGGAGAAGAGGCTGGAGTGGGTCGCAACC
ATAAGTAGTGGTGGTTCTTACACCTACTATCCAGACAGTGTGAAGGGCCGATTCACC
ATTTCCAGAGACAAAGCCAAGAACACCCTGTATTTGCAAATGGGCAGTCTGAAGTCT
GAGGACACAGCCATGTATTACTGTACAAGAATAGGTTACGACGAAGATTATGCTATG
GACCACTGGGGTCAAGGAACCTCAGTCACCGTCTCCTCAGCCAAAACGACACCCCCA
TCTGTCTATGCGGCCGCAGAACAAAAACTCATCTCAGAAGAGGATCTGAATGGGGCC
GCATAG

Amino acid sequence of TS2/16-scFv expressed in E. Coli

MKYLLPTAAAGLLLLAAQPAMADIVMTQTPTTMAASPGDKITITCSVSSIISSNYLH
WYSQKPGFSPKLLIYRTSNLASGVPPRFSGSGSGTSYSLTIGTMEAEDVATYYCQQG
SDIPLTFGDGTKLDLKRADAAPTVS**GGGGSGGGGSGGGGSGGGGS**EVKVVESGGGLV
KPGGSLKLSCAASGFTFSSYTMSWVRQTPEKRLEWVATISSGGSYTYYPDSVKGRFT
ISRDKAKNTLYLQMGSLKSEDTAMYYCTRIGYDEDYAMDHWGQGTSVTVSSAKTTPP
SVYAAAEQKLISEEDLNGAA

Figure 44. Nucleic acid sequence of TS2/16-scFv construct cloned in pHenIX vector and its translation into protein sequence; highlighted in yellow is pelB, in light green is VL, in dark green is VH, in blue is Myc Tag sequence, bold is linker sequence.

We will express TS2/16-scFv in E. Coli HB2151 non suppressor strain, in order to check protein correct assembly. Afterwards, for high scale production, will clone TS2/16-scFv construct in pPIC9K vector, for the expression of 6xHis tagged proteins in Pichia Pastoris. TS2/16-scFv-6xHis will be concentrated from yeast culture supernatant and purified using Ni-NTA Agarose resin (Qiagen). To evaluate the ability to bind β1 integrin, purified TS2/16-scFv-6xHis will be tested by cell-ELISA, using GD25 cell line (β1 integrin deficient), and GD25-β1A (stably transfected β1 integrin cDNA).

3.3. DEVELOPMENT of hERG1-β1 BISPECIFIC Single Chain Diabody (scDb)

The final goal of the project is to develop a bispecific antibody able to target both hERG1 channel and β1 integrin. The bispecific antibody format that we chose is the single chain diabody (scDb): a recombinant protein composed by the variable domains (VH and VL) of two antibodies connected by three peptide linkers (A, M and B) (Figure 45). Linkers length is crucial for protein proper assembly, Volkel et al (2001) reported that for scDb assembly A and B linkers should be 2-6 residues each, and linker M ≥ 13 residues. Shortening linker sequences results in protein chain opening, preventing intra-chain domain pairing (VHA-VLA and VHB-VLB) and promoting dimerisation (Völkel et al. 2001).

To develop a hERG1-β1-scDb we assembled together anti-hERG1 mAb and anti β1 integrin mAb (TS2/16) variable domains, as shown in Figure 45.

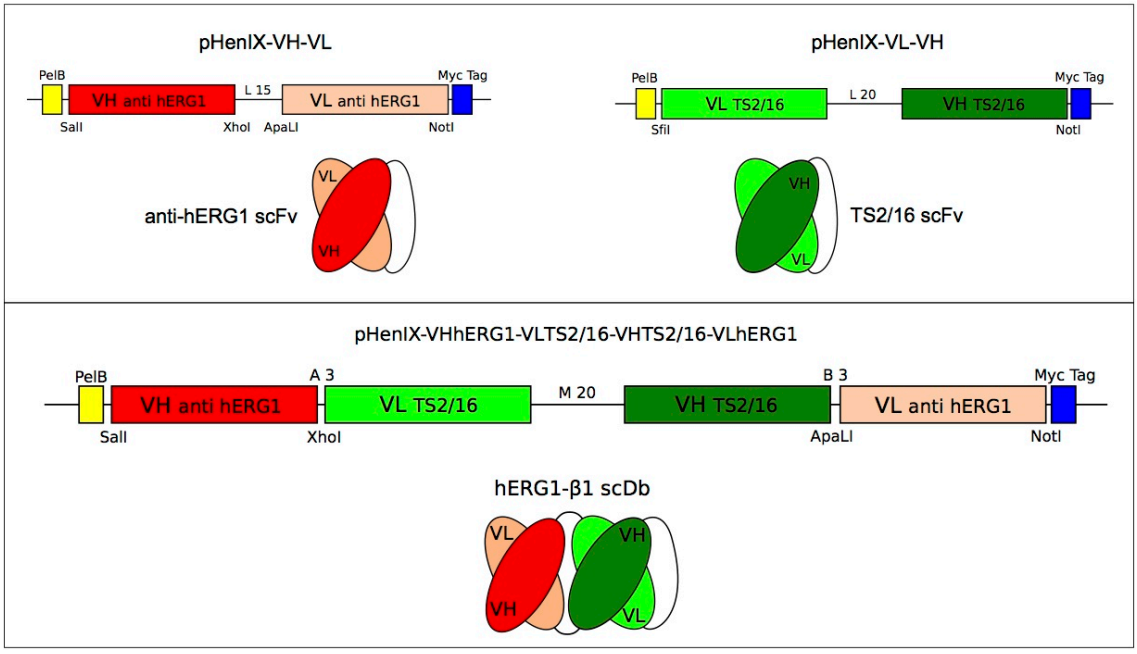

Figure 45. Cartoon representing hERG1-β1 single chain diabody assembly.

To assemble the scDb we ideated a rapid methodic, which consist in replacing anti-hERG1-scFv linker with VL-linker-VH (TS2/16 scFv) construct (Figure 46).

ATGAAATACCTATTGCCTACGGCAGCCGCTGGATTGTTATTACTCGCGGCCCAGCCG
GCCATGGCCCAGGTGCAGCTGCAGGTCGACGAGGTCCAACTGCAACAGTCTGGACCT
GAACTGGTGAAGCCTGGGGCTTCTGTGAAGATATCCTGCAAGACTTCAGGATACACA
TTCACTGAATACACCGTTCACTGGGTGAAACAGAGCCATGGAAAGAGCCTTGAATGG
ATTGGAGGCATTAATCCTAATGGTGGTACTACCTATAATCAGAAGTTCAAGGGCAAG
GCCACATTGACTATTGACAAGTCCTCCAGCTCAGCCTTCATGGAGCTCCGCAGCCTG
ACATCTGAGGATTCTGCAGTCTATTACTTTGCAACAGGTTGGGGACCTGACTACTGG
GGCCAAGGCACCACTCTCACAGTCTCCTCAGCCAAAACAACACCCCCATCAGTCTAT
CCACTGGCCCCTGGCTCGAGTGGTGGAGGCGGTTCAGGCGGAGGTGGCTCTGGCGGT
AGTGCACTTGATATTGTGCTGACACAATCTCCACTCACTTTGTCGGTTAACATTGGT
CAACCAGCCTCTATCTCTTGCAAGTCAAGTCAGAGCCTCTTATATACTAATGGAAAA
ACCTATTTTAATTGGTTATTACAGAGGCCAGGCCAGTCTCCAAAGCGCCTAATCTAT
CTGGTGTCTAAACTGGACTCTGGAGTCCCTGACAGGTTCACTGGCAGTGGATCAGGA
ACAGATTTTACACTGAAAATCAGCAGAGTGGAGGCTGAAGATTTGGGAGTTTATTAC
TGCGCGCAAGGTACACATTTTCCGTGGACGTTCGGTGGAGGGACCAAGCTGGAAATC
AAACGGGCTGATGCTGCACCAACTGTATCCGCGGCCGCAGAACAAAAACTCATCTCA
GAAGAGGATCTGAATGGGGCCGCA**TAG**

Figure 46. Nucleic acid sequence of anti-hERG1 scFv cloned in pHenIX vector. Dark red is VH and light red is VL.

VL-linker-VH (TS2/16-scFv) was assembled by SOE-PCR as previously described, except that we used the primers shown in Table 2.

Name	Sequence
VLFORXHO	CACGCCTCGAGTGATATTGTGATGACACAGACTCCA
VLREVSOE	**GGAGCCGCCGCCGCC**AGAACCACCACCACCAGAA CCACCACCACCGGATACAGTTGGTGCAGCATC
VHFORSOE	**GGCGGCGGCGGCTCC**GGTGGTGGTGGATCCGAG GTGAAGGTGGTGGAATC
VHREVAPALI	ACGCGTGCACTATAGACAGATGGGGGTGTCGTTTT GGC

Table 2. Primer designed to assemble the construct VL-linker-VH by SOE-PCR and clone the sequence in place of anti-hERG1-scFv linker, to form hERG1-β1-scDb. In red are the portions of the primers that anneal to the template, in green are the bases added to generate A and B scDb linkers, underlined are the restriction sites added to clone the construct in place of anti-hERG1-scFv linker, purple are the sequences added to facilitate enzyme digestion, and bold are the sequenced that overlap in SOE-PCR.

VLFORXHO and VHREVAPALI primers were designed to add, at the 5' and 3' ends of the construct, the appropriate restriction sites (XhoI and ApaLI) for the cloning in place of the anti-hERG1-scFv linker. The sequences added with these primers allow at the same time to clone the construct and generate A and B linkers. For scDb proper assembly, A and B linker sequences were designed

to code for a 3 residues peptide (GSS and SAL respectively), and linker M for a 20 amino acid polypeptide (the same of TS2/16-scFv) (Plückthun et al. 1996).

CACGCCTCGAGTGATATTGTGATGACACAGACTCCAACCACCATGGCTGCATCTCCC
GGGGACAAGATCACTATCACCTGCAGTGTCAGTTCAATTATAAGTTCCAATTACCTG
CATTGGTATAGTCAGAAGCCAGGATTCTCCCCTAAACTCTTGATTTATAGGACATCC
AATCTGGCTTCTGGAGTCCCACCTCGCTTCAGTGGCAGTGGGTCTGGGACCTCTTAC
TCTCTCACAATTGGCACCATGGAGGCTGAAGATGTTGCCACTTACTACTGCCAGCAG
GGTTCTGATATTCCACTCACGTTCGGTGATGGGACCAAGCTGGACCTGAAACGGGCT
GATGCTGCACCAACTGTATCCGGTGGTGGTGGTTCTGGTGGTGGTGGTTCTGGCGGC
GGCGGCTCCGGTGGTGGTGGATCCGAGGTGAAGGTGGTGGAATCTGGGGGAGGCTTA
GTGAAGCCTGGAGGGTCCCTGAAACTCTCCTGTGCAGCCTCTGGATTCACTTTCAGT
AGCTATACCATGTCTTGGGTTCGCCAGACTCCGGAGAAGAGGCTGGAGTGGGTCGCA
ACCATAAGTAGTGGTGGTTCTTACACCTACTATCCAGACAGTGTGAAGGGCCGATTC
ACCATTTCCAGAGACAAAGCCAAGAACACCCTGTATTTGCAAATGGGCAGTCTGAAG
TCTGAGGACACAGCCATGTATTACTGTACAAGAATAGGTTACGACGAAGATTATGCT
ATGGACCACTGGGGTCAAGGAACCTCAGTCACCGTCTCCTCAGCCAAAACGACACCC
CCATCTGTCTATAGTGCACGCGT

Figure 47. Nucleic acid sequence of the construct XhoI-VL-linker-VH-ApaLI obtained engineering TS2/16 mAb by SOE-PCR. Light green is VL, dark green is VH, yellow is the linker that code for a 20 residues polypeptide $(GGGGS)_4$.

XhoI-VL-linker-VH-ApaLI SOE-PCR product (Figure 47) was XhoI/ApaLI digested and cloned in place of anti-hERG1 scFv linker sequence. Cloning success was evaluated by SfiI/NotI enzymatic digestion of plasmid DNA extracted from single transformed colonies as described in Materials and Methods. If the insert is correctly cloned, SfiI/NotI enzymatic digestion generates two bands: a the 4500 bp band (pHenIX) and a 1700 bp band (scDb, VH_{hERG1}-A-$VL_{\beta1}$-M-$VH_{\beta1}$-B-VL_{hERG1}) (Figure 48).

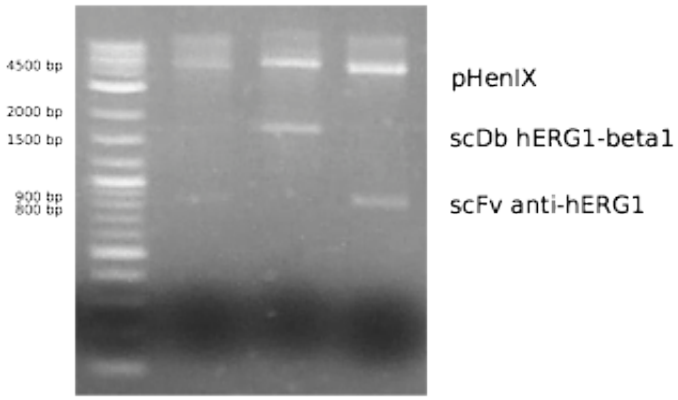

Figure 48. DNA electrophoresis of SfiI/NotI-digested plasmidic DNA. DNA was extracted from 3 BL21(DE3)Gold colonies, transformed with the ligation product of XhoI/ApaLI digested pHenIX-hERG1scFv and TS2/16 XhoI-VL-linker-VH-ApaLI).

As shown in the picture above, only one of the three sample analysed was positive (1700 bp scDb band, lane 3). While in the other two samples (lane 2 and 4), SfiI/NotI digestion generates the 4500 pb pHenIX band and an 850 bp band corresponding to anti-hERG1-scFv, suggesting that the vector re-ligated to itself.
The positive sample was sequenced by Primm srl to check if scDb sequence is in frame with pHenIX expression cassette.

In Figure 49 are shown the nucleic acid sequence and the translated amino acid sequence of hERG1-β1-scDb construct cloned in pHenIX vector. Highlighted in yellow is pelB, in light green is VL, in dark green is VH, in blue is Myc Tag sequence, bold are A, M, B linker sequence, underlined are XhoI and ApaLI restriction sites used for scDb assembly.

Nucleic acid sequence of hERG1-β1-scDb

ATGAAATACCTATTGCCTACGGCAGCCGCTGGATTGTTATTACTCGCGGCCCAGCCG
GCCATGGCCCAGGTGCAGCTGCAGGTCGACGAGGTCCAACTGCAACAGTCTGGACCT
GAACTGGTGAAGCCTGGGGCTTCTGTGAAGATATCCTGCAAGACTTCAGGATACACA
TTCACTGAATACACCGTTCACTGGGTGAAACAGAGCCATGGAAAGAGCCTTGAATGG
ATTGGAGGCATTAATCCTAATGGTGGTACTACCTATAATCAGAAGTTCAAGGGCAAG
GCCACATTGACTATTGACAAGTCCTCCAGCTCAGCCTTCATGGAGCTCCGCAGCCTG
ACATCTGAGGATTCTGCAGTCTATTACTTTGCAACAGGTTGGGGACCTGACTACTGG
GGCCAAGGCACCACTCTCACAGTCTCCTCAGCCAAAACAACACCCCCATCAGTCTAT
CCACTGGCCCCT**GGCTCGAG**TGATATTGTGATGACACAGACTCCAACCACCATGGCT
GCATCTCCCGGGGACAAGATCACTATCACCTGCAGTGTCAGTTCAATTATAAGTTCC
AATTACCTGCATTGGTATAGTCAGAAGCCAGGATTCTCCCCTAAACTCTTGATTTAT
AGGACATCCAATCTGGCTTCTGGAGTCCCACCTCGCTTCAGTGGCAGTGGGTCTGGG
ACCTCTTACTCTCTCACAATTGGCACCATGGAGGCTGAAGATGTTGCCACTTACTAC
TGCCAGCAGGGTTCTGATATTCCACTCACGTTCGGTGATGGGACCAAGCTGGACCTG
AAACGGGCTGATGCTGCACCAACTGTATCC**GGTGGTGGTGGTTCTGGCGGCGGCGGC**
TCCGGTGGTGGTGGATCCGAGGTGAAGGTGGTGGAATCTGGGGGAGGCTTAGTGAAG
CCTGGAGGGTCCCTGAAACTCTCCTGTGCAGCCTCTGGATTCACTTTCAGTAGCTAT
ACCATGTCTTGGGTTCGCCAGACTCCGGAGAAGAGGCTGGAGTGGGTCGCAACCATA
AGTAGTGGTGGTTCTTACACCTACTATCCAGACAGTGTGAAGGGCCGATTCACCATT
TCCAGAGACAAAGCCAAGAACACCCTGTATTTGCAAATGGGCAGTCTGAAGTCTGAG
GACACAGCCATGTATTACTGTACAAGAATAGGTTACGACGAAGATTATGCTATGGAC
CACTGGGGTCAAGGAACCTCAGTCACCGTCTCCTCAGCCAAAACGACACCCCCATCT
GTCTAT**AGTGCACTG**GATATTGTGCTGACACAATCTCCACTCACTTTGTCGGTTAAC
ATTGGTCAACCAGCCTCTATCTCTTGCAAGTCAAGTCAGAGCCTCTTATATACTAAT
GGAAAAACCTATTTTAATTGGTTATTACAGAGGCCAGGCCAGTCTCCAAAGCGCCTA
ATCTATCTGGTGTCTAAACTGGACTCTGGAGTCCCTGACAGGTTCACTGGCAGTGGA
TCAGGAACAGATTTTACACTGAAAATCAGCAGAGTGGAGGCTGAAGATTTGGGAGTT
TATTACTGCGCGCAAGGTACACATTTTCCGTGGACGTTCGGTGGAGGGACCAAGCTG
GAAATCAAACGGGCTGATGCTGCACCAACTGTATCCGCGGCCGCAGAACAAAAACTC
ATCTCAGAAGAGGATCTGAATGGGGCCGCATAG

Amino acid sequence of hERG1-β1-scDb

MKYLLPTAAAGLLLLAAQPAMAQVQLQVDEVQLQQSGPELVKPGASVKISCKTSGYT
FTEYTVHWVKQSHGKSLEWIGGINPNGGTTYNQKFKGKATLTIDKSSSSAFMELRSL
TSEDSAVYYFATGWGPDYWGQGTTLTVSSAKTTPPSVYPLAP**GSS**DIVMTQTPTTMA
ASPGDKITITCSVSSIISSNYLHWYSQKPGFSPKLLIYRTSNLASGVPPRFSGSGSG
TSYSLTIGTMEAEDVATYYCQQGSDIPLTFGDGTKLDLKRADAAPTVS**GGGGSGGGG**
SGGGGSGGGGSEVKVVESGGGLVKPGGSLKLSCAASGFTFSSYTMSWVRQTPEKRLE
WVATISSGGSYTYYPDSVKGRFTISRDKAKNTLYLQMGSLKSEDTAMYYCTRIGYDE
DYAMDHWGQGTSVTVSSAKTTPPSVY**SAL**DIVLTQSPLTLSVNIGQPASISCKSSQS
LLYTNGKTYFNWLLQRPGQSPKRLIYLVSKLDSGVPDRFTGSGSGTDFTLKISRVEA
EDLGVYYCAQGTHFPWTFGGGTKLEIKRADAAPTVSAAAEQKLISEEDLNGAA

Figure 49. Nucleic acid sequence of hERG1-β1-scDb construct cloned in pHenIX vector and its translation into protein sequence; highlighted in yellow is pelB, in light green is VL, in dark green is VH, in blue is Myc Tag sequence, bold are A, M, B linker sequence, underlined are XhoI and ApaLI restriction sites used for scDb assembly.

We will express hERG1-β1-scDb in E. Coli HB2151 non suppressor strain, in order to check protein correct assembly. Afterwards, for high scale production, will clone hERG1-β1-scDb in pPIC9K vector, for expression of 6xHis tagged proteins in Pichia Pastoris. hERG1-β1-scDb-6xHis will be concentrated from yeast culture supernatant and purified using Ni-NTA Agarose resin (Qiagen).

To evaluate the ability to bind both hERG1 and β1 integrin, purified bispecific-scDb will be tested by cell-ELISA, using GD25 cell line (which lacks the expression of both β1 integrin and hERG1 channel), and GD25 transfected either with hERG1 and β1 integrin cDNA.

To study the biological effect of the bispecific-scDb, we will evaluate hERG1-β1 co-immunoprecipitation and FAK phosphorylation on tyrosine 397, in HEK293-hERG1 cells treated with hERG1-β1-scDb.

CONCLUSION

1. DEVELOPMENT AND CHARACTERISATION OF MONOCLONAL ANTIBODIES AGAINST GLYCOLIPID ANTIGENS

1.1 GM3 AND GM3 LACTONE EXPRESSION IN CANCER CELL LINES

In order to find an appropriate cell line model within to test the biological effect of anti-GM3 lactone antibodies, we investigated the gangliosidic profile of different cancer cell lines: B16F1 murine melanoma cell line, MCF-7 and MDA-MB-231 breast cancer cell lines, and MIA-PaCa-2, BxPC-3 and PANC-1 pancreatic ductal adenocarcinoma (PDAC) cell lines.

Our results confirmed that B16F1 cell line has exclusively GM3, as already reported in literature. This cell line can thus be used as a cellular model over-expressing GM3. In breast cancer cell lines (MDA-MB-231 and MCF-7), gangliosides profile results quite similar for complex gangliosides, while it is different for GM3 expression. In MDA-MB-231, GM3 expression is approximately 14-fold more than in MCF-7, according to literature (Nohara et al. 1987). There are no data in literature regarding gangliosides expression in PDAC cell lines. Our findings show that in BxPC-3 cell line, GM3 expression is approximately 30-fold more than in MIA-PaCa-2 and 15-fold more than in PANC-1.

We can thus classify the analysed cell lines for GM3 expression:

- high levels of GM3: B16F1, MDA-MB-231, BxPC-3
- low levels of GM3: MCF-7, MIA-PaCa-2, PANC-1

Among these cell lines, we found that only the cell lines characterised by high GM3 expression level, express also GM3 lactone. This result is in agreement with the data found in literature. As reported in Nores et al (1987), when GM3 is high expressed on the surface of plasma membrane of cancer cells, may

assume a lactone or lactone like form. This conformational change occurs when GM3 expression, on plasma membrane, overcome a threshold density level and is favoured by the acid pH of tumour microenvironment.

We can thus conclude that B16F1, MDA-MB-231 and BxPC-3 cell lines, over-expressing GM3, can be used as models within to test anti-GM3 lactone antibodies.

1.2. MONOCLONAL ANTIBODIES DEVELOPMENT USING mimGM3

We developed two hybridomas populations (OVA and PCS) using, for mice immunisation, a stable GM3 lactone mimetic molecule, mimGM3, conjugated to two different carriers $Pam_3CysSer$ (PCS) and Ovalbumin (OVA).
The antibodies produced by both PCS and OVA hybridomas were all IgM, suggesting that the synthetic molecule used to mimic the structure of GM3 lactone (mimGM3) even if is more stable in blood stream than natural GM3-lactone (Arcangeli et al 2010), is not able to promote isotype switching from IgM to IgG.
The hybridomas producing the highest level of antibodies were cloned, in order to obtain hybridomas producing monoclonal antibodies.
The antibodies produced by both PCS and OVA hybridomas shown cross-reactivity with other molecules in ELISA, such as BSA, fetal bovine serum, and another class of glycolipids: sulfatides.
A comparative ELISA against GM3 and sulfatides shown that OVA C2 mAb binds better sulfatides than GM3.
Further analysis, confirmed that OVA C2 mAb binds to sulfatides (Dot blot assay and TLC staining), but shown that it is not able to bind neither GM3 (Dot blot assay and TLC staining) nor GM3 lactone (TLC staining).

1.3. OVA C2 mAb CHARACTERISATION

Since Dot Blot assay and ELISA results suggested that OVA C2 mAb has high affinity for sulfatides, we decided to investigate the glycolipid sulfate profile of various cell lines and the ability of OVA C2 mAb to bind sulfate containing glycolipids. We investigated the gangliosidic profile of different cancer cell lines:

B16F1, MIA-PaCa-2, BxPC-3 and PANC-1, which turned out to not express SM4 but a more complex sulfatide (probably SM3).

TLC staining on SM4 sulfatide and on B16F1, MIA-PaCa-2, BxPC-3 and PANC-1 lipid extract suggests that OVA C2 mAb react with SM4 but not with SM3 sulfatide.

Our results show that OVA C2 mAb selectively stains SM4 lower band on TLC plates, SM4 lower band was found to be composed by hydrogenated fatty acid and short chain fatty acids (such as 16:0). C16:0 isoform of sulfatide is predominantly found in secretory granules and on the surface β-cells plasma membrane. OVA C2 mAb stains Langerhans islets in IHC on pancreatic tissue, but not other sulfatide containing structure found in different tissues. These findings suggest that OVA C2 mAb selectively recognise C16:0 SM4 expressed in β-cells.

Immunofluorescence staining of RIN 5F β-cells insulinoma confirmed that OVA C2 mAb is able to bind sulfatides expressed on β-cells. Moreover, our preliminary results show that the staining pattern depends on culture conditions: in cells cultured without glucose OVA C2 mAb give an intense, not uniform, cytoplasmic staining, while in presence of 12 mM glucose (B), it give a well defined membrane staining. These differences are probably correlated with the role of sulfatides in insulin packaging and release.

The ability to bind RIN 5F β-cells sulfatides suggest OVA C2 mAb as a possible tool for insulin oversecretion treatment in insulinoma cases. Therefore, we will perform further experiment on RIN 5F cells to test the effect of OVA C2 mAb treatment on insulin secretion.

2. STUDY OF THE MOLECULAR MECHANISMS INVOLVED IN HERG1-B1 INTEGRIN COMPLEX FORMATION

The aim of second part of the work presented in this thesis is to develop a bifunctional engineered antibody able to bind hERG1-β1 oncogenic unit, disrupting the complex and preventing downstream signalling.

To address this goal the first step was to understand which portions of hERG1 channel and β1 integrin are involved in complex formation.

- GST pull down assay using β1 cytoplasmic tail and single hERG1 intracellular domains expressed in E. Coli as GST-fusion proteins suggested that, in these experimental conditions, β1Ct is not able to bind hERG1 N-terminal domains and hERG1 distal C-tail.
- "Fishing" experiment in HEK293 cells over-expressing hERG1 total protein lysate, using GST-β1Ct fusion protein as a molecular bait, show that GST-β1Ct is not able to bind hERG1 channel in total protein lysate, suggesting that β1 cytoplasmic domain does not interact with the whole intracellular domains of tetramerised hERG1.
- hERG1-β1 co-immunoprecipitation experiments in transfected HEK293 expressing hERG1-Δ-2-370 and hERG1-ΔC+RD hERG1 mutants, demonstrate that hERG1 cytoplasmic domains are not necessary for complex formation.

These results indicate that hERG1-β1 interaction may involve transmembrane or extracellular portions of the two proteins.

To investigate the mechanisms involved in complex formation and complex related signalling, we evaluated hERG1-β1 co-immunoprecipitation and FAK signalling in transfected HEK293, treated or not with hERG1 blockers, and we found that:

- 40 μM E4031 inhibit complex formation and FAK signalling, according to previous findings (Cherubini 2005). Complex formation is also prevented by ERG-toxin, confirming that hERG1 blockers influence hERG1-β1 interaction.
- The non-conductive mutant hERG1-G628S is able to complex with β1 integrin but less than hERG1 wild type, suggesting that ion flux has a role in complex formation.
- FAK phosphorylation on Y397 is strongly inhibited when β1-integrin is expressed together with the non conductive hERG1 mutant hERG1-G628S or the S4 mutants hERG1-K525C or hERG1-R531C.

These findings suggest that ion flux and hERG1 voltage related conformation are crucial for FAK phosphorylation and in turn for complex-related signalling.
Therefore a bispecific antibody able to target hERG1-β1 complex and block integrin related signalling could be a valid tool for cancer immunotherapy.

3. DEVELOPMENT OF ENGINEERED BISPECIFIC ANTIBODIES ABLE TO TARGET hERG1-β1 ONCOGENIC UNIT

We engineered two anti-β1 integrin monoclonal antibodies BV7 and TS2/16 directed against the extracellular portion of β1 integrin, isolating their variable domains (VH and VL).
We engineered TS2/16 mAb to produce a single chain variable fragment (TS2/16-scFv) assembling the variable domains in the order VL-linker-VH.
We designed the construct for a bispecific single chain diabody (scDb), able to bind hERG1 and β1 integrin using isolated variable domains of anti-hERG1 mAb (already isolated in our lab) and of TS2/16 mAb. We assembled hERG1-β1-scDb construct in the order: VH_{hERG1}-linkerA-$VL_{\beta1}$-linkerM-$VH_{\beta1}$-linkerB-VL_{hERG1}.
We will clone both TS2/16-scFv and hERG1-β1-scDb in pPIC9K vector, for expression of 6xHis tagged proteins in Pichia Pastoris. TS2/16-scFv-6xHis and hERG1-β1-scDb-6xHis will be concentrated from yeast culture supernatant and purified using Ni-NTA Agarose resin (Qiagen).
Purified TS2/16-scFv-6xHis will be tested by cell-ELISA to evaluate its ability to bind β1 integrin. Cell-ELISA will be performed using GD25 cell line (which lacks the expression of both β1 integrin and hERG1 channel), and GD25-β1A (stably transfected β1 integrin cDNA).
As regards hERG1-β1-scDb we will evaluate its ability to bind both hERG1 and β1 integrin, by cell-ELISA, using GD25 cell line, and GD25 transfected either with hERG1 and β1 integrin cDNA.
To study the biological effect of the bispecific-scDb, we will evaluate hERG1-β1 co-immunoprecipitation and FAK phosphorylation on tyrosine 397, in HEK293-hERG1 cells treated with hERG1-β1-scDb.

REFERENCES

Afrasiabi E, Hietamaki M, Viitanen T, Sukumaran P, Bergelin N, Tornquist K. Expression and significance of HERG (KCNH2) potassium channels in the regulation of MDA-MB-435S melanoma cell proliferation and migration. Cellular signalling. 2010;22(1):57-64.

Alberts B, Johnson A, Lewis J, al e. Molecular Biology of the Cell. 4th edition: New York: Garland Science; 2002.

Albesa M, Grilo LS, Gavillet B, Abriel H. Nedd4-2-dependent ubiquitylation and regulation of the cardiac potassium channel hERG1. Journal of molecular and cellular cardiology. 2011;51(1):90-8.

Arcangeli A, Becchetti A. Complex functional interaction between integrin receptors and ion channels. Trends in cell biology. 2006;16(12):631-9.

Arcangeli A, Becchetti A, Mannini A, Mugnai G, De Filippi P, Tarone G, Del Bene MR, Barletta E, Wanke E, Olivotto M. Integrin-mediated neurite outgrowth in neuroblastoma cells depends on the activation of potassium channels. The Journal of cell biology. 1993;122(5):1131-43.

Arcangeli A, Crociani O, Lastraioli E, Masi A, Pillozzi S, Becchetti A. Targeting ion channels in cancer: a novel frontier in antineoplastic therapy. Current medicinal chemistry. 2009;16(1):66-93.

Arcangeli A, Romoli MR, Boni L, Gerlini G, Tofani L, Urso C, Borgognoni L. High hERG1 expression in advanced melanoma. Melanoma research. 2013;23(3): 185-90.

Arcangeli A, Toma L, Contiero L, Crociani O, Legnani L, Lunghi C, Nesti E, Moneti G, Richichi B, Nativi C. Stable GM3 lactone mimetic raises antibodies specific for the antigens expressed on melanoma cells. Bioconjug Chem. 2010;21(8):1432-8.

Becchetti A, Arcangeli A. Integrins and ion channels: molecular complexes and signaling. Advances in experimental medicine and biology. 2010;674:v-vii.

Berrier AL, Jones CW, LaFlamme SE. Tac-beta1 inhibits FAK activation and Src signaling. Biochemical and biophysical research communications. 2008;368(1):62-7.

Bianchi L, Wible B, Arcangeli A, Taglialatela M, Morra F, Castaldo P, Crociani O, Rosati B, Faravelli L, Olivotto M, Wanke E. herg encodes a K+ current highly conserved in tumors of different histogenesis: a selective advantage for cancer cells? Cancer research. 1998;58(4):815-22.

Blomqvist M, Osterbye T, Mansson JE, Horn T, Buschard K, Fredman P. Sulfatide is associated with insulin granules and located to microdomains of a cultured beta cell line. Glycoconj J. 2002;19(6):403-13.

Boffey J, Nicholl D, Wagner ER, Townson K, Goodyear C, Furukawa K, Furukawa K, Conner J, Willison HJ. Innate murine B cells produce anti-disialosyl antibodies reactive with Campylobacter jejuni LPS and gangliosides that are polyreactive and encoded by a restricted set of unmutated V genes. Journal of neuroimmunology. 2004;152(1-2):98-111.

Brown GC. Electrostatic coupling between membrane proteins. FEBS letters. 1990;260(1):1-5.

Brown SB, Dransfield I. Electric fields and inflammation: may the force be with you. TheScientificWorldJournal. 2008;8:1280-94.

Burnet M. Cancer: a biological approach. III. Viruses associated with neoplastic conditions. IV. Practical applications. British medical journal. 1957;1(5023): 841-7.

Buschard K, Blomqvist M, Osterbye T, Fredman P. Involvement of sulfatide in beta cells and type 1 and type 2 diabetes. Diabetologia. 2005;48(10): 1957-62.

Buschard K, Hoy M, Bokvist K, Olsen HL, Madsbad S, Fredman P, Gromada J. Sulfatide controls insulin secretion by modulation of ATP-sensitive K(+)-channel activity and Ca(2+)-dependent exocytosis in rat pancreatic beta-cells. Diabetes. 2002;51(8):2514-21.

Calorini L, Fallani A, Tombaccini D, Mugnai G, Ruggieri S. Lipid composition of cultured B16 melanoma cell variants with different lung-colonizing potential. Lipids. 1987;22(9):651-6.

Campbell ID, Humphries MJ. Integrin structure, activation, and interactions. Cold Spring Harbor perspectives in biology. 2011;3(3).

Chames P, Baty D. Bispecific antibodies for cancer therapy: the light at the end of the tunnel? MAbs. 2009;1(6):539-47.

Chames P, Van Regenmortel M, Weiss E, Baty D. Therapeutic antibodies: successes, limitations and hopes for the future. Br J Pharmacol. 2009;157(2): 220-33.

Charpin C, Bhan AK, Zurawski VR, Jr., Scully RE. Carcinoembryonic antigen (CEA) and carbohydrate determinant 19-9 (CA 19-9) localization in 121 primary and metastatic ovarian tumors: an immunohistochemical study with the use of monoclonal antibodies. International journal of gynecological pathology : official journal of the International Society of Gynecological Pathologists. 1982;1(3):231-45.

Cherubini A, Hofmann G, Pillozzi S, Guasti L, Crociani O, Cilia E, Di Stefano P, Degani S, Balzi M, Olivotto M, Wanke E, Becchetti A, Defilippi P, Wymore R, Arcangeli A. Human ether-a-go-go-related gene 1 channels are physically linked to beta1 integrins and modulate adhesion-dependent signaling. Molecular biology of the cell. 2005;16(6):2972-83.

Cherubini A, Taddei GL, Crociani O, Paglierani M, Buccoliero AM, Fontana L, Noci I, Borri P, Borrani E, Giachi M, Becchetti A, Rosati B, Wanke E, Olivotto M, Arcangeli A. HERG potassium channels are more frequently expressed in

human endometrial cancer as compared to non-cancerous endometrium. British journal of cancer. 2000;83(12):1722-9.

Coste H, Martel MB, Got R. Topology of glucosylceramide synthesis in Golgi membranes from porcine submaxillary glands. Biochim Biophys Acta. 1986;858(1):6-12.

Crociani O, Lastraioli E, Boni L, Pillozzi S, Romoli MR, D'Amico M, Stefanini M, Crescioli S, Taddei A, Bencini L, Bernini M, Farsi M, Beghelli S, Scarpa A, Messerini L, Tomezzoli A, Vindigni C, Morgagni P, Saragoni L, Giommoni E, Gasperoni S, Dicostanzo F, Roviello F, Demanzoni G, Bechi P, Arcangeli A. hERG1 channels regulate VEGF-A secretion in human gastric cancer: clinicopathologial correlations and therapeutical implications. Clinical cancer research : an official journal of the American Association for Cancer Research. 2014.

Crociani O, Zanieri F, Pillozzi S, Lastraioli E, Stefanini M, Fiore A, Fortunato A, D'Amico M, Masselli M, De Lorenzo E, Gasparoli L, Chiu M, Bussolati O, Becchetti A, Arcangeli A. hERG1 channels modulate integrin signaling to trigger angiogenesis and tumor progression in colorectal cancer. Scientific reports. 2013;3:3308.

Ding XW, Yang WB, Gao S, Wang W, Li Z, Hu WM, Li JJ, Luo HS. Prognostic significance of hERG1 expression in gastric cancer. Digestive diseases and sciences. 2010;55(4):1004-10.

Dunn GP, Bruce AT, Ikeda H, Old LJ, Schreiber RD. Cancer immunoediting: from immunosurveillance to tumor escape. Nat Immunol. 2002;3(11):991-8.

Dunn GP, Bruce AT, Sheehan KC, Shankaran V, Uppaluri R, Bui JD, Diamond MS, Koebel CM, Arthur C, White JM, Schreiber RD. A critical function for type I interferons in cancer immunoediting. Nat Immunol. 2005;6(7):722-9.

Durrant LG, Noble P, Spendlove I. Immunology in the clinic review series; focus on cancer: glycolipids as targets for tumour immunotherapy. Clinical and experimental immunology. 2012;167(2):206-15.

Ehrlich JR, Pourrier M, Weerapura M, Ethier N, Marmabachi AM, Hebert TE, Nattel S. KvLQT1 modulates the distribution and biophysical properties of HERG. A novel alpha-subunit interaction between delayed rectifier currents. J Biol Chem. 2004;279(2):1233-41.

Ehrlich P. Ueber den jetzigen stand der karzinomforschung Ned Tijdschr Geneeskd1909. p. 73–290.

Folch J, Lees M, Sloane Stanley GH. A simple method for the isolation and purification of total lipides from animal tissues. J Biol Chem. 1957;226(1): 497-509.

Fontana L, D'Amico M, Crociani O, Biagiotti T, Solazzo M, Rosati B, Arcangeli A, Wanke E, Olivotto M. Long-term modulation of HERG channel gating in hypoxia. Biochemical and biophysical research communications. 2001;286(5):857-62.

Fuchs P, Breitling F, Little M, Dubel S. Primary structure and functional scFv antibody expression of an antibody against the human protooncogen c-myc. Hybridoma. 1997;16(3):227-33.

Galfre G, Milstein C. Preparation of monoclonal antibodies: strategies and procedures. Methods Enzymol. 1981;73(Pt B):3-46.

Galfrè G, Milstein C. Preparation of monoclonal antibodies: strategies and procedures. Methods Enzymol. 1981;73(Pt B):3-46.

Garcia AJ, Takagi J, Boettiger D. Two-stage activation for alpha5beta1 integrin binding to surface-adsorbed fibronectin. J Biol Chem. 1998;273(52):34710-5.

Gong Q, Anderson CL, January CT, Zhou Z. Role of glycosylation in cell surface expression and stability of HERG potassium channels. American journal of physiology Heart and circulatory physiology. 2002;283(1):H77-84.

Grillo-Lopez AJ, Hedrick E, Rashford M, Benyunes M. Rituximab: ongoing and future clinical development. Seminars in oncology. 2002;29(1 Suppl 2): 105-12.

Hakomori S, Zhang Y. Glycosphingolipid antigens and cancer therapy. Chemistry & biology. 1997;4(2):97-104.

Hakomori S-i. The glycosynapse. Proceedings of the National Academy of Sciences. 2002;99(1):225-32.

Hamilton WB, Helling F, Lloyd KO, Livingston PO. Ganglioside expression on human malignant melanoma assessed by quantitative immune thin-layer chromatography. International journal of cancer Journal international du cancer. 1993;53(4):566-73.

Hofmann A, Erhard M, Schmidt P, Bessler W, Wiesmuller H, Zinsmeister P, Stangassinger M, Losch U. [Lipopeptides as adjuvants for the immunisation of laying hens]. Altex. 1996;13(5):26-9.

Hofmann G, Bernabei PA, Crociani O, Cherubini A, Guasti L, Pillozzi S, Lastraioli E, Polvani S, Bartolozzi B, Solazzo V, Gragnani L, Defilippi P, Rosati B, Wanke E, Olivotto M, Arcangeli A. HERG K+ channels activation during beta(1) integrin-mediated adhesion to fibronectin induces an up-regulation of alpha(v)beta(3) integrin in the preosteoclastic leukemia cell line FLG 29.1. J Biol Chem. 2001;276(7):4923-31.

Holliger P, Prospero T, Winter G. "Diabodies": small bivalent and bispecific antibody fragments. Proceedings of the National Academy of Sciences of the United States of America. 1993;90(14):6444-8.

Hsu FF, Bohrer A, Turk J. Electrospray ionization tandem mass spectrometric analysis of sulfatide. Determination of fragmentation patterns and characterization of molecular species expressed in brain and in pancreatic islets. Biochim Biophys Acta. 1998;1392(2-3):202-16.

Hynes RO. Integrins: bidirectional, allosteric signaling machines. Cell. 2002;110(6):673-87.

Irie A, Koyama S, Kozutsumi Y, Kawasaki T, Suzuki A. The molecular basis for the absence of N-glycolylneuraminic acid in humans. J Biol Chem. 1998;273(25):15866-71.

Jehle J, Schweizer PA, Katus HA, Thomas D. Novel roles for hERG K(+) channels in cell proliferation and apoptosis. Cell death & disease. 2011;2:e193.

Jeschke U, Mylonas I, Shabani N, Kunert-Keil C, Schindlbeck C, Gerber B, Friese K. Expression of sialyl lewis X, sialyl Lewis A, E-cadherin and cathepsin-D in human breast cancer: immunohistochemical analysis in mammary carcinoma in situ, invasive carcinomas and their lymph node metastasis. Anticancer research. 2005;25(3a):1615-22.

Kagan A, McDonald TV. Dynamic control of hERG/I(Kr) by PKA-mediated interactions with 14-3-3. Novartis Foundation symposium. 2005;266:75-89; discussion -99.

Kannagi R. Molecular mechanism for cancer-associated induction of sialyl Lewis X and sialyl Lewis A expression—The Warburg effect revisited. Glycoconj J. 2003;20(5):353-64.

Kim R, Emi M, Tanabe K. Cancer immunoediting from immune surveillance to immune escape. Immunology. 2007;121(1):1-14.

Kohler G, Milstein C. Continuous cultures of fused cells secreting antibody of predefined specificity. Nature. 1975;256(5517):495-7.

Köhler G, Milstein C. Continuous cultures of fused cells secreting antibody of predefined specificity. Nature. 1975;256(5517):495-7.

Koike T, Kimura N, Miyazaki K, Yabuta T, Kumamoto K, Takenoshita S, Chen J, Kobayashi M, Hosokawa M, Taniguchi A, Kojima T, Ishida N, Kawakita M, Yamamoto H, Takematsu H, Suzuki A, Kozutsumi Y, Kannagi R. Hypoxia induces adhesion molecules on cancer cells: A missing link between Warburg effect and induction of selectin-ligand carbohydrates. Proceedings of the National Academy of Sciences of the United States of America. 2004;101(21):8132-7.

Kontermann RE. Recombinant bispecific antibodies for cancer therapy. Acta pharmacologica Sinica. 2005;26(1):1-9.

Kupershmidt S, Snyders DJ, Raes A, Roden DM. A K+ channel splice variant common in human heart lacks a C-terminal domain required for expression of rapidly activating delayed rectifier current. J Biol Chem. 1998;273(42): 27231-5.

Lastraioli E, Bencini L, Bianchini E, Romoli MR, Crociani O, Giommoni E, Messerini L, Gasperoni S, Moretti R, Di Costanzo F, Boni L, Arcangeli A. hERG1 Channels and Glut-1 as Independent Prognostic Indicators of Worse Outcome in Stage I and II Colorectal Cancer: A Pilot Study. Translational oncology. 2012;5(2):105-12.

Lastraioli E, Guasti L, Crociani O, Polvani S, Hofmann G, Witchel H, Bencini L, Calistri M, Messerini L, Scatizzi M, Moretti R, Wanke E, Olivotto M, Mugnai G, Arcangeli A. herg1 gene and HERG1 protein are overexpressed in colorectal cancers and regulate cell invasion of tumor cells. Cancer research. 2004;64(2):606-11.

Lastraioli E, Romoli MR, Arcangeli A. Immunohistochemical biomarkers in gastric cancer research and management. International journal of surgical oncology. 2012;2012:868645.

Lastraioli E, Taddei A, Messerini L, Comin CE, Festini M, Giannelli M, Tomezzoli A, Paglierani M, Mugnai G, De Manzoni G, Bechi P, Arcangeli A. hERG1 channels in human esophagus: evidence for their aberrant expression in the malignant progression of Barrett's esophagus. Journal of cellular physiology. 2006;209(2):398-404.

Legate KR, Wickstrom SA, Fassler R. Genetic and cell biological analysis of integrin outside-in signaling. Genes & development. 2009;23(4):397-418.

Levite M, Cahalon L, Peretz A, Hershkoviz R, Sobko A, Ariel A, Desai R, Attali B, Lider O. Extracellular K(+) and opening of voltage-gated potassium channels activate T cell integrin function: physical and functional association between Kv1.3 channels and beta1 integrins. The Journal of experimental medicine. 2000;191(7):1167-76.

Lin H, Xiao J, Luo X, Wang H, Gao H, Yang B, Wang Z. Overexpression HERG K(+) channel gene mediates cell-growth signals on activation of oncoproteins SP1 and NF-kappaB and inactivation of tumor suppressor Nkx3.1. Journal of cellular physiology. 2007;212(1):137-47.

Makhlouf AM, Fathalla MM, Zakhary MA, Makarem MH. Sulfatides in ovarian tumors: clinicopathological correlates. International Journal of Gynecological Cancer. 2004;14(1):89--93.

Martin-Padura I, Bazzoni G, Zanetti A, Bernasconi S, Elices MJ, Mantovani A, Dejana E. A novel mechanism of colon carcinoma cell adhesion to the endothelium triggered by beta 1 integrin chain. J Biol Chem. 1994;269(8): 6124-32.

Masi A, Becchetti A, Restano-Cassulini R, Polvani S, Hofmann G, Buccoliero AM, Paglierani M, Pollo B, Taddei GL, Gallina P, Di Lorenzo N, Franceschetti S, Wanke E, Arcangeli A. hERG1 channels are overexpressed in glioblastoma multiforme and modulate VEGF secretion in glioblastoma cell lines. British journal of cancer. 2005;93(7):781-92.

McDonagh CF, Huhalov A, Harms BD, Adams S, Paragas V, Oyama S, Zhang B, Luus L, Overland R, Nguyen S, Gu J, Kohli N, Wallace M, Feldhaus MJ, Kudla AJ, Schoeberl B, Nielsen UB. Antitumor activity of a novel bispecific antibody that targets the ErbB2/ErbB3 oncogenic unit and inhibits heregulin-induced activation of ErbB3. Mol Cancer Ther. 2012;11(3):582-93.

McKhann GM, Ho W. The in vivo and in vitro synthesis of sulphatides during development. Journal of neurochemistry. 1967;14(7):717-24.

Millard M, Odde S, Neamati N. Integrin targeted therapeutics. Theranostics. 2011;1:154-88.

Miyoshi E, Moriwaki K, Nakagawa T. Biological function of fucosylation in cancer biology. Journal of biochemistry. 2008;143(6):725-9.

Morello V, Cabodi S, Sigismund S, Camacho-Leal MP, Repetto D, Volante M, Papotti M, Turco E, Defilippi P. beta1 integrin controls EGFR signaling and tumorigenic properties of lung cancer cells. Oncogene. 2011;30(39):4087-96.

Morichika H, Hamanaka Y, Tai T, Ishizuka I. Sulfatides as a predictive factor of lymph node metastasis in patients with colorectal adenocarcinoma. Cancer. 1996;78(1):43--7.

Moriwaki K, Miyoshi E. Fucosylation and gastrointestinal cancer. World journal of hepatology. 2010;2(4):151-61.

Muller-Loennies S, Gronow S, Brade L, MacKenzie R, Kosma P, Brade H. A monoclonal antibody against a carbohydrate epitope in lipopolysaccharide differentiates Chlamydophila psittaci from Chlamydophila pecorum, Chlamydophila pneumoniae, and Chlamydia trachomatis. Glycobiology. 2006;16(3):184-96.

Natarajan A, Xiong CY, Albrecht H, DeNardo GL, DeNardo SJ. Characterization of site-specific ScFv PEGylation for tumor-targeting pharmaceuticals. Bioconjug Chem. 2005;16(1):113-21.

Niimura Y, Nagai K. Metabolic responses of sulfatide and related glycolipids in Madin-Darby canine kidney (MDCK) cells under osmotic stresses. Comparative biochemistry and physiology Part B, Biochemistry & molecular biology. 2008;149(1):161-7.

Nohara K, Wang F, Spiegel S. Glycosphingolipid composition of MDA-MB-231 and MCF-7 human breast cancer cell lines. Breast Cancer Res Treat. 1998;48(2):149-57.

Nores GA, Dohi T, Taniguchi M, Hakomori S. Density-dependent recognition of cell surface GM3 by a certain anti-melanoma antibody, and GM3 lactone as a possible immunogen: requirements for tumor-associated antigen and immunogen. Journal of immunology (Baltimore, Md : 1950). 1987;139(9): 3171-6.

Oliva J, Valdés Z, Casacó A, Pimentel G, González J, Álvarez I, Osorio M, Velazco M, Figueroa M, Ortiz R, Escobar X, Orozco M, Cruz J, Franco S, Díaz M, Roque L, Carr A, Vázquez A, Mateos C, Rubio M, Pérez R, Fernández LE. Clinical evidences of GM3 (NeuGc) ganglioside expression in human breast cancer using the 14F7 monoclonal antibody labelled with 99mTc. Breast Cancer Res Treat. 2006;96(2):115-21.

Olivotto M, Arcangeli A, Carla M, Wanke E. Electric fields at the plasma membrane level: a neglected element in the mechanisms of cell signalling. BioEssays : news and reviews in molecular, cellular and developmental biology. 1996;18(6):495-504.

Osterbye T, Jorgensen KH, Fredman P, Tranum-Jensen J, Kaas A, Brange J, Whittingham JL, Buschard K. Sulfatide promotes the folding of proinsulin, preserves insulin crystals, and mediates its monomerization. Glycobiology. 2001;11(6):473-9.

Patsenker E, Stickel F. Role of integrins in fibrosing liver diseases. American Journal of Physiology - Gastrointestinal and Liver Physiology. 2011;301(3):G425-G34.

Petrecca K, Atanasiu R, Akhavan A, Shrier A. N-linked glycosylation sites determine HERG channel surface membrane expression. The Journal of Physiology. 1999;515(1):41-8.

Pillozzi S, Arcangeli A. Physical and functional interaction between integrins and hERG1 channels in cancer cells. Advances in experimental medicine and biology. 2010;674:55-67.

Pillozzi S, Brizzi MF, Bernabei PA, Bartolozzi B, Caporale R, Basile V, Boddi V, Pegoraro L, Becchetti A, Arcangeli A. VEGFR-1 (FLT-1), beta1 integrin, and hERG K+ channel for a macromolecular signaling complex in acute myeloid leukemia: role in cell migration and clinical outcome. Blood. 2007;110(4): 1238-50.

Pillozzi S, Masselli M, De Lorenzo E, Accordi B, Cilia E, Crociani O, Amedei A, Veltroni M, D'Amico M, Basso G, Becchetti A, Campana D, Arcangeli A. Chemotherapy resistance in acute lymphoblastic leukemia requires hERG1 channels and is overcome by hERG1 blockers. Blood. 2011;117(3):902-14.

Plückthun A, Krebber A, Krebber C, Horn U, Knüpfer U, Wenderoth R, Nieba L, Proba K, Riesenberg D. Producing antibodies in Escherichia coli: Fom PCR to fermentation. In: McCafferty J HH, editor. Antibody engineering: a practical approach Oxford: IRL press 1996. p. 203–52

Regina Todeschini A, Hakomori SI. Functional role of glycosphingolipids and gangliosides in control of cell adhesion, motility, and growth, through glycosynaptic microdomains. Biochim Biophys Acta. 2008;1780(3):421-33.

Sanz L, Cuesta Ángel M, Compte M, ÁLvarez-Vallina L. Antibody engineering: facing new challenges in cancer therapy1. Acta Pharmacologica Sinica. 2005;26(6):641--8.

Schaefer J, Honegger A, Plückthun A. Construction of scFv Fragments from Hybridoma or Spleen Cells by PCR Assembly. In: Kontermann R, Dübel S, editors. Antibody Engineering: Springer Berlin Heidelberg; 2010. p. 21-44.

Scott AM, Wolchok JD, Old LJ. Antibody therapy of cancer. Nature reviews Cancer. 2012;12(4):278-87.

Shao XD, Wu KC, Hao ZM, Hong L, Zhang J, Fan DM. The potent inhibitory effects of cisapride, a specific blocker for human ether-a-go-go-related gene (HERG) channel, on gastric cancer cells. Cancer biology & therapy. 2005;4(3):295-301.

Siakotos AN. Analytical separation of nonlipid water soluble substances and gangliosides from other lipids by dextran gel column chromatography. J Am Oil Chem Soc. 1965;42(11):913-9.

Siegel R, Naishadham D, Jemal A. Cancer statistics, 2012. CA Cancer J Clin. 2012;62(1):10-29.

Smith GA, Tsui HW, Newell EW, Jiang X, Zhu XP, Tsui FW, Schlichter LC. Functional up-regulation of HERG K+ channels in neoplastic hematopoietic cells. J Biol Chem. 2002;277(21):18528-34.

Strebe N, Breitling F, Moosmayer D, Brocks B, Dübel S. Cloning of Variable Domains from Mouse Hybridoma by PCR. In: Kontermann R, Dübel S, editors. Antibody Engineering: Springer Berlin Heidelberg; 2010. p. 3-14.

Svennerholm L. Quantitative estimation of sialic acids. II. A colorimetric resorcinol-hydrochloric acid method. Biochim Biophys Acta. 1957;24(3): 604-11.

Takagi J, Petre BM, Walz T, Springer TA. Global conformational rearrangements in integrin extracellular domains in outside-in and inside-out signaling. Cell. 2002;110(5):599-11.

Takahashi T, Suzuki T. Role of sulfatide in normal and pathological cells and tissues. Journal of lipid research. 2012;53(8):1437-50.

Tjandra JJ, Ramadi L, McKenzie IF. Development of human anti-murine antibody (HAMA) response in patients. Immunology and cell biology. 1990;68 (Pt 6):367-76.

Townson K, Greenshields KN, Veitch J, Nicholl D, Eckhardt M, Galanina O, Bovin N, Samain E, Antoine T, Bundle D, Zhang P, Ling CC, Willison HJ. Sulfatide binding properties of murine and human antiganglioside antibodies. Glycobiology. 2007;17(11):1156-66.

Tsuchida T, Saxton RE, Morton DL, Irie RF. Gangliosides of human melanoma. Journal of the National Cancer Institute. 1987;78(1):45-54.

van der Bijl P, Strous GJ, Lopes-Cardozo M, Thomas-Oates J, van Meer G. Synthesis of non-hydroxy-galactosylceramides and galactosyldiglycerides by hydroxy-ceramide galactosyltransferase. The Biochemical journal. 1996;317 (Pt 2):589-97.

Vandenberg JI, Perry MD, Perrin MJ, Mann SA, Ke Y, Hill AP. hERG K(+) channels: structure, function, and clinical significance. Physiological reviews. 2012;92(3):1393-478.

Vernon-Wilson EF, Aurade F, Tian L, Rowe IC, Shipston MJ, Savill J, Brown SB. CD31 delays phagocyte membrane repolarization to promote efficient binding of apoptotic cells. Journal of leukocyte biology. 2007;82(5):1278-88.

Viloria CG, Barros F, Giraldez T, Gomez-Varela D, de la Pena P. Differential effects of amino-terminal distal and proximal domains in the regulation of human erg K(+) channel gating. Biophysical journal. 2000;79(1):231-46.

Völkel T, Korn T, Bach M, Müller R, Kontermann RE. Optimized linker sequences for the expression of monomeric and dimeric bispecific single-chain diabodies. Protein Eng. 2001;14(10):815-23.

Wang Z, Raifu M, Howard M, Smith L, Hansen D, Goldsby R, Ratner D. Universal PCR amplification of mouse immunoglobulin gene variable regions: the design of degenerate primers and an assessment of the effect of DNA polymerase 3' to 5' exonuclease activity. Journal of immunological methods. 2000;233(1-2):167-77.

Wegener KL, Campbell ID. Transmembrane and cytoplasmic domains in integrin activation and protein-protein interactions (review). Molecular membrane biology. 2008;25(5):376-87.

Wegener KL, Partridge AW, Han J, Pickford AR, Liddington RC, Ginsberg MH, Campbell ID. Structural basis of integrin activation by talin. Cell. 2007;128(1): 171-82.

Wei J, Cui L, Liu F, Fan Y, Lang R, Gu F, Guo X, Tang P, Fu L. E-selectin and Sialyl Lewis X expression is associated with lymph node metastasis of invasive micropapillary carcinoma of the breast. International journal of surgical pathology. 2010;18(3):193-200.

Wei JF, Wei L, Zhou X, Lu ZY, Francis K, Hu XY, Liu Y, Xiong WC, Zhang X, Banik NL, Zheng SS, Yu SP. Formation of Kv2.1-FAK complex as a

mechanism of FAK activation, cell polarization and enhanced motility. Journal of cellular physiology. 2008;217(2):544-57.

Xiong JP, Mahalingham B, Alonso JL, Borrelli LA, Rui X, Anand S, Hyman BT, Rysiok T, Muller-Pompalla D, Goodman SL, Arnaout MA. Crystal structure of the complete integrin alphaVbeta3 ectodomain plus an alpha/beta transmembrane fragment. The Journal of cell biology. 2009;186(4):589-600.

Xiong JP, Stehle T, Diefenbach B, Zhang R, Dunker R, Scott DL, Joachimiak A, Goodman SL, Arnaout MA. Crystal structure of the extracellular segment of integrin alpha Vbeta3. Science (New York, NY). 2001;294(5541):339-45.

Yamada N, Chung YS, Takatsuka S, Arimoto Y, Sawada T, Dohi T, Sowa M. Increased sialyl Lewis A expression and fucosyltransferase activity with acquisition of a high metastatic capacity in a colon cancer cell line. British journal of cancer. 1997;76(5):582-7.

Yu RK, Koerner TA, Ando S, Yohe HC, Prestegard JH. High-resolution proton NMR studies of gangliosides. III. Elucidation of the structure of ganglioside GM3 lactone. Journal of biochemistry. 1985;98(5):1367-73.

Zhang M, Liu J, Tseng GN. Gating charges in the activation and inactivation processes of the HERG channel. The Journal of general physiology. 2004;124(6):703-18.

Zhu J, Li YT, Li SC, Cole RB. Structural characterization of gangliosides isolated from mullet milt using electrospray ionization-tandem mass spectrometry. Glycobiology. 1999;9(10):985-93.

Zhu J, Luo BH, Xiao T, Zhang C, Nishida N, Springer TA. Structure of a complete integrin ectodomain in a physiologic resting state and activation and deactivation by applied forces. Molecular cell. 2008;32(6):849-61.

ACKNOWLEDGMENTS

I would like to thank prof. Arcangeli to gave me the opportunity to do my PhD in her lab. I would like to thank Olivia, that during my bachelor and master degree thesis made me discover the love for scientific research, this is the reason I decided to start a PhD. I would like to thank all the people that work and worked in lab Arcangeli in these 3 years. Luca, Angelica, Antonella, Angela, Francesca, Laura, Elena, Massimo, Claudia, Tiziano, Serena, Marika, Olivia, with whom it was a pleasure spend the long working days, and that helped me to overcome the difficulties I encountered in this period. Expecially Angelica, Antonella, Angela e Francesca, besides colleagues I found friends. I would like to thank prof. Becchetti for the precious help in the study of hERG1-β1 complex, and I would like to thank Paolo, Laura and above all Antonella, with whom I shared a part of my work, for the suggestions and experimental help. I would like to thank prof. Mugnai and Antonella Mannini for the suggestions and the precious help in lipid study. I would like to thank Massimo for his patience in FACS analysis and Ilaria for the beautiful immunofluorescence pictures. I would like to thank Claudia, for all the support in these last days. I would like to thank in particular Angelica, with whom I learned all I know, for her precious help and support. I would like to thank my parents, my brother and Giulia, and my friends, Rita, Miriam, Serena, Alessandro, Lorenzo, Irene, Elisabetta, Federica, Francesco, Marta, Sara, Enea and Nicco, for their kindness, their suggestions, and their ability to make me smile. And a very special thanks to Luca, my love, with whom I share all, even this PhD, my english is too bad to describe how important is have you by my side, thank you, for all.

UNIVERSITÀ DEGLI STUDI FIRENZE
DIPARTIMENTO DI SCIENZE BIOMEDICHE SPERIMENTALI E CLINICHE

Dottorato di Ricerca in
SCIENZE BIOMEDICHE
sede amministrativa: Dipartimento di
Scienze Biomediche Sperimentali e Cliniche
coordinatore: Prof. Persio Dello Sbarba

Dottorato di Ricerca in Scienze Biomediche

Presentazione del candidato : Silvia Crescioli
Curriculum: Oncologia Sperimentale e Clinica
Ciclo: XXVI
Titolo della tesi: Antibodies against plasma membrane molecular targets: tools for cancer immunotherapy

A conclusione del corso triennale del XXVI° Ciclo del Dottorato di Ricerca in Scienze Biomediche (*curriculum Oncologia Sperimentale e Clinica*), il Collegio dei Docenti, facendo propria la relazione presentata dalla Prof.ssa Arcangeli, in qualità di *tutor*, circa l'attività di ricerca, l'operosità e l'assiduità del candidato, rilascia con parere unanime il seguente giudizio da presentare alla Commissione Giudicatrice ai fini dell'espletamento dell'esame finale.

La Dr.ssa Silvia Crescioli, nata a Bagno a Ripoli (FI) il 12/04/1984, laureata in Biologia Cellulare e Molecoare il 15/07/2009 discutendo una tesi dal titolo Studio dei meccanismi di regolazione pre e post-trascrizionali dell'espressione del canale del potassio hERG1
con la votazione di 110 e lode, è stata ammessa, a partire dal 01/01/2011, al Dottorato di Ricerca in Scienze Biomediche *curriculum Oncologia Sperimentale e Clinica* (XXVI° Ciclo), svolgendo la propria attività di ricerca presso il Dipartimento di Patologia e Oncologia Sperimentali, sotto il tutoraggio della Prof.ssa Arcangeli

Descrizione dell'attività di ricerca/Risultati ottenuti:

Lo scopo della ricerca svolta nei tre anni di dottorato è stato quello di studiare antigeni tumore associati (tumor associated antigen TAA) esposti sulla membrana di cellule tumorali, e di sviluppare anticorpi contro di essi. Principalmente sono stati studiati due tipi di antigeni tumorali: i glicosfingolipidi GSL (nello specifico GM3 lattone e sulfatidi) e un complesso proteico formato dal canale del potassio voltaggio dipendente hERG1 e dall'integrina β1.
Sempre più evidenze mostrano che i tessuti tumorali possiedono un profilo glicosfingolipidico alterato rispetto alla controparte sana, suggerendo i GSL come validi bersagli per un immunoterapia del cancro. Per questo motivo, in questo lavoro di tesi è stato sviluppato un anticorpo monoclonale utilizzando un antigene sintetico che mima la forma lattonica del GM3. L'anticorpo monoclonale prodotto è stato caratterizzato e ne è stata valutata l'affinità per il GM3 lattone ed altre molecole, in particolare è stata riscontrata una elevata affinità per il sulfatide SM4. In parallelo è stato caratterizzato il contenuto di GM3 lattone e di sulfatide SM4 in varie linee cellulari tumorali, così da trovare dei modelli cellulari su cui testare l'effetto di anticorpi anti GLS.
Nella seconda parte del progetto, lo scopo della ricerca è stato quello di sviluppare un anticorpo bispecifico in grado di legare e inibire la formazione del complesso tra il canale del potassio hERG1 e l'integrina β1. Questo complesso è stato trovato in svariati tipi di tumore, dove regola vari aspetti della progressione tumorale attivando specifiche vie di segnalazione intracellulare. E' stato dunque studiato il meccanismo coinvolto nella formazione del complesso e nel signalling intracellulare ad esso correlato. I risultati ottenuti suggeriscono che le due proteine interagiscono a livello transmembrana o extracellulare e confermano dati già noti da studi precedenti, riguardanti l'importanza del flusso di corrente per la formazione del complesso ed il signalling intracellulare. I risultati suggeriscono quindi che un anticorpo bispecifico in grado di legare il complesso ed inibire il signalling possa essere utile per un'immunoterapia del cancro. Nel nostro laboratorio è stato in precedenza ingegnerizzato un anticorpo monoclonale anti-hERG1, ed è stato prodotto un single chain variable fragment (scFv). In questo lavoro di tesi è stato

progettato un anticorpo bispecifico single chain diabody (scDb) derivante dall'ingegnerizzazione dell'anticorpo monoclonale anti-hERG1 e di un anticorpo monoclonale anti integrina β1. Sono stati dunque assemblati i costrutti per un scFv-anti-β1 e per l'anticorpo bispecifico scDb-hERG1-β1. Questi anticorpi saranno poi prodotti su larga scala in Pichia Pastoris, purificati, e testati su modelli cellulari per valutare l'effetto sulla formazione del complesso e sul signalling ad esso correlato.

Pubblicazioni/Presentazione dati a congressi nazionali e internazionali:

O. Crociani, E. Lastraioli, L. Boni, S. Pillozzi, M. R. Romoli, M. D'Amico, M. Stefanini, S. Crescioli, A. Taddei, L. Bencini, M. Bernini, M. Farsi, S. Beghelli, A. Scarpa, L. Messerini, A. Tomezzoli, C. Vindigni, P. Morgagni, L. Saragoni, F. DiCostanzo, E. Giommoni, F. Roviello, G. DeManzoni, P. Bechi, and A. Arcangeli. hERG1 channels regulate VEGF-A secretion in human gastric cancer: clinicopathologial correlations and therapeutical implications. Clinical Cancer Research, 2014, Jan 21

A. Arcangeli, O.Crociani, S. Crescioli, A. Sette. Caratterizzazione dell'anticorpo monoclonale anti-hERG1 e produzione di un corrispondente scFv - Monoclonal anti- hERG1 characterization and anti-hERG1 scFv production (Brevetto approvato dalla Commissione Brevetti di Unifi (approvato) e di AOUC , brevetto congiunto) e in corso sottomissione al valutatore per l'ottenimento del titolo di brevetto italiano.

ABCD 2013 congress (Ravenna, 12-14 settembre 2013): F. Zanieri, A. Fiore, R. Mercatelli, S. Crescioli, S. Pillozzi, O. Crociani, L. Carraresi, M. D'Amico, L. Gasparoli, P. Defilippi, V. Morello, L. Brizzi, J.M. Mitcheson, F. Quercioli, A. Becchetti, A. Arcangeli. Molecular and functional characterization of the hERG1/β1 integrin complex in tumor cell. (poster)

10th IGCC 2013 (Verona, 19-22): O. Crociani, S. Crescioli, A. Fiore, S. Pillozzi, M. Stefanini, M. D'Amico, E. Lastraioli, L. Gasparoli, A. Arcangeli. hERG1 and VEGF-A in Gastric Cancers cells: expression and functional role. (poster)

PEGS Summit Europe 2012 (Vienna, 6-8 Novembre 2012): A. Sette, S. Crescioli, O. Crociani, E. Lastraioli, M. D'Amico, M. Masselli, A. Arcangeli. A new immune-based strategy to target hERG1 potassium channel. (poster)

Joint National PhD meeting 2011 (Gubbio (PG) 20-22 Ottobre 2011) S. Crescioli, A. Arcangeli. Production of antibodies against molecular targets on the surface of plasma membrane. (poster)

ABCD 2011 congress (Ravenna, 8-10 Settembre 2011): F. Zanieri, A. Sette, S. Crescioli, R. Mercatelli, S. Pillozzi, L. Carraresi, M.F. Brizzi, P. De Filippi, A. Arcangeli. β1integrin/ hERG1 complex as a novel molecular target for antineoplastic therapy. (poster)

Seminari:

Partecipazione all'attività didattica del corso di Immunologia e Tecniche Immunologiche, Corso di Laurea Magistrale in Biotecnologie Molecolari anni 2011-2012, 2012-2013, 2013-2014.
Presentazione dottorato I anno: *Presentazione progetto dottorato*
Presentazione dottorato II anno: *Molecular targets on the surface of plasma membrane: tools for cancer therapy*
Presentazione dottorato III anno: *Plasma membrane molecular targets: tools for cancer immunotherapy*

Durante il corso di dottorato, il candidato ha seguito con il massimo impegno il programma didattico stabilito dal Collegio dei Docenti ed ha portato avanti con entusiasmo e determinazione le sue ricerche, dando prova di grande inventiva ed intraprendenza, nonché di notevole elasticità nella elaborazione dei dati sperimentali. Nel corso del triennio, il candidato ha inoltre maturato una buona cultura di base ed una vasta esperienza diretta in metodiche sperimentali.

Per quanto sopra, il Collegio dei Docenti unanime ritiene che la Dr.ssa Silvia Crescioli possa meritatamente aspirare a conseguire il titolo di Dottore di Ricerca.

Firenze, 14/2/2014 Il Coordinatore del Corso

Prof. Persio Dello Sbarba